

MODELING AND INVESTIGATION OF FAULT RIDE THROUGH
CAPABILITY OF VARIABLE SPEED WIND TURBINES

A THESIS SUBMITTED TO
THE GRADUATE SCHOOL OF NATURAL AND APPLIED SCIENCES
OF
MIDDLE EAST TECHNICAL UNIVERSITY

BY

ERKAN KOÇ

IN PARTIAL FULFILLMENT OF THE REQUIREMENTS
FOR
THE DEGREE OF MASTER OF SCIENCE
IN
ELECTRICAL AND ELECTRONICS ENGINEERING

SEPTEMBER 2010

Approval of the thesis:

**MODELING AND INVESTIGATION OF FAULT RIDE THROUGH
CAPABILITY OF VARIABLE SPEED WIND TURBINES**

submitted by **ERKAN KOÇ** in partial fulfillment of the requirements for the degree
of **Master of Science in Electrical and Electronics Engineering Department,**
Middle East Technical University by,

Prof. Dr. Canan Özgen _____
Dean, Graduate School of **Natural and Applied Sciences**

Prof. Dr. İsmet Erkmn _____
Head of Department, **Electrical and Electronics Engineering**

Prof. Dr. A. Nezh Güven _____
Supervisor, **Electrical and Electronics Engineering Dept., METU**

Examining Committee Members:

Prof. Dr. Nevzat Özay _____
Electrical and Electronics Engineering Dept., METU

Prof. Dr. A. Nezh Güven _____
Electrical and Electronics Engineering Dept., METU

Prof. Dr. Ahmet Rumeli _____
Electrical and Electronics Engineering Dept., METU

Prof. Dr. Işık Çadırcı _____
Electrical and Electronics Engineering Dept., Hacettepe University

Dr. O. Bülent Tör _____
TUBITAK-UZAY

Date: September 17, 2010

I hereby declare that all information in this document has been obtained and presented in accordance with academic rules and ethical conduct. I also declare that, as required by these rules and conduct, I have fully cited and referenced all material and results that are not original to this work.

Name, Last name : Erkan KOÇ

Signature :

ABSTRACT

MODELING AND INVESTIGATION OF FAULT RIDE THROUGH CAPABILITY OF VARIABLE SPEED WIND TURBINES

Koç, Erkan

M.Sc., Department of Electrical and Electronics Engineering

Supervisor : Prof. Dr. A. Nezir Güven

September 2010, 121 pages

Technological improvements on wind energy systems with governmental supports have increased the penetration level of wind power into the grid in recent years. The high level of penetration forces the wind turbines stay connected to the grid during the disturbances in order to enhance system stability. Moreover, power system operators must revise their grid codes in parallel with these developments. This work is devoted to the modeling of variable speed wind turbines and the investigation of fault ride through capability of the wind turbines for grid integration studies.

In the thesis, detailed models of different variable speed wind turbines will be presented. Requirements of grid codes for wind power integration will also be discussed regarding active power control, reactive power control and fault ride through (FRT) capability. Investigation of the wind turbine FRT capability is the main focus of this thesis. Methods to overcome this problem for different types of wind turbines will be also explained in detail. Models of grid-connected wind turbines with doubly-fed induction generator and permanent magnet synchronous generator are implemented in the dedicated power system analysis tool PSCAD/EMTDC. With these models and computer simulations, FRT capabilities of

variable speed wind turbines have been studied and benchmarked and the influences on the grid during the faults are discussed.

Keywords: Variable Speed Wind Turbines, Fault Ride Through Capability, Modeling, Grid Code

ÖZ

DEĞİŞKEN HIZLI RÜZGAR TÜRBİNLERİNİN MODELLENMESİ VE ARIZA SONRASI SİSTEME KATKI YETENEKLERİNİN İNCELENMESİ

Koç, Erkan

Yüksek Lisans, Elektrik ve Elektronik Mühendisliği Bölümü

Tez Yöneticisi : Prof. Dr. A. Nezih Güven

Eylül 2010, 121 sayfa

Son yıllarda rüzgar enerjisi sistemlerindeki teknolojik gelişmeler ve devlet destekleri, rüzgar enerjisinin elektrik şebekesindeki payını artırmaktadır. Bu artan pay sonucunda, sistem kararlılığını artırmak için, oluşan arızalarda rüzgar türbinlerinin sisteme bağlı kalması bir zorunluluk haline gelmiştir. Ayrıca, bu artan pay sebebiyle sistem operatörleri, şebeke yönetmeliklerini tekrar gözden geçirmek zorunda kalmışlardır. Bu tez, rüzgar türbinlerinin elektrik şebekesine entegrasyonu çalışmalarına katkı sağlamak için değişken hızlı rüzgar türbinlerinin modellenmesini ve arıza sonrası sisteme destek verme yeteneklerini inceler.

Bu çalışmada ilk olarak farklı tipte değişken hızlı rüzgar türbinlerinin detaylı modellenmesi anlatılmıştır. Daha sonrasında, rüzgar sistemlerinin şebekeye bağlantısı için gerekli şebeke yönetmeliklerinin aktif/reaktif güç desteği, arıza sonrası sisteme destek verme yetenekleri gibi önemli kısımları incelenmiştir. Rüzgar türbinlerinin arıza sonrası destek verme yeteneklerinin incelenmesi bu tezin ana konusudur. Bu problemin farklı tipteki rüzgar türbinlerinde hangi metotlarla çözümlendiği detaylı bir biçimde anlatılmıştır. Bunun yanında, çift beslemeli asenkron jeneratörler ve sabit mıknatıslı senkron jeneratörlerin kullanıldığı rüzgar türbin modelleri, bir güç sistemi analiz programı olan PSCAD/EMTDC kullanılarak oluşturulmuştur. Oluşturulan bu

modellerde yapılan simülasyon sonuçları kullanılarak rüzgar türbinlerinin arıza sonrası sisteme katkıları, sistemin hata anındaki tepkileri incelenmiş ve karşılaştırılmıştır.

Anahtar Kelimeler: Değişken Hızlı Rüzgar Türbinleri, Arıza Sonrası Sistem Desteği, Modelleme, Şebeke Yönetmeliği

To My Family

ACKNOWLEDGEMENTS

I would like to express my deepest gratitude and sincerest respects to my supervisor Prof. Dr. A. Nezh Güven for his guidance, advice, criticism, encouragements and insight throughout this study.

I would like to show my gratitude also to Müfit Altın for his guidance, advice, criticism, encouragements and insight throughout this work.

I would like to express my special thanks to İlker Yılmaz for his brilliant suggestions, support and contributions. It would be much harder for me to accomplish simulations without his PSCAD/EMTDC background.

The assistance of the valuable staff in Power Electronics Group and Power System Group of TÜBİTAK-UZAY is gratefully acknowledged.

I would like to express my deepest gratitude to Mevlüt Akdeniz, İsa Boğaz, Doğan Gezer, Seda Karatekin, Emine Vardar, Cem Özgür Gerçek, Erkut Cebeci and Hamza Oğuz for their unlimited support throughout my work. I also express my sincerest thanks to Esra Debreli, Sezen Keser, Mustafa Deniz, Oğuz Öztürk, Nazan Aksoy and my housemates for their continuous morale support.

Especially, I would like to thank my mother, father and brother. Life would be difficult without their love and support.

Finally and foremost, I would like to thank my love Şenay for her presence, patience and endless support during this heavy work.

TABLE OF CONTENTS

ABSTRACT.....	iv
ÖZ.....	vi
ACKNOWLEDGMENTS.....	ix
TABLE OF CONTENTS.....	x
LIST OF TABLES.....	xiii
LIST OF FIGURES.....	xiv
CHAPTERS	
1. INTRODUCTION.....	1
1.1 Background.....	1
1.2 Scope of the Thesis.....	5
1.3 Modeling Approach.....	6
1.4 Wind Power Impacts.....	7
1.5 Outline of the Thesis.....	8
2. WIND TURBINE MODELING.....	9
2.1 Introduction.....	9
2.2 Definition of Wind Turbine.....	9
2.2.1 Vertical-axis Wind Turbines.....	10
2.2.2 Horizontal Axis Wind Turbines (HAWT).....	11
2.3 Modeling of Wind Turbines.....	16
2.3.1 Modeling of a Variable Speed Wind Turbine with DFIG.....	17
2.3.1.1 Wind Speed Modeling.....	18
2.3.1.2 Aerodynamic Model.....	20
2.3.1.3 Pitch System.....	25

2.3.1.4	Shaft Modeling	26
2.3.1.5	Generator Modeling.....	27
2.3.1.6	Converter Modeling.....	31
2.3.1.7	Grid-side Converter Controller Modeling	33
2.3.1.8	Rotor-side Converter Controller Modeling	37
2.3.2	Modeling of a Variable Speed Wind Turbine with PMSG.....	42
2.3.2.1	Shaft Modeling	43
2.3.2.2	Converter Modeling.....	43
2.3.2.3	Generator Modeling.....	44
2.3.2.4	Grid-Side Converter Controller Modeling.....	46
2.3.2.5	Generator-Side Converter Controller Modeling.....	47
3.	GRID CODES AND FRT OVERVIEW	49
3.1	Introduction	49
3.2	Grid Codes Overview	49
3.2.1	Active Power Control	50
3.2.2	Reactive Power and Voltage Control	51
3.2.3	Frequency and Voltage Operating Ranges	53
3.2.4	FRT Capability	55
3.3	Turkish Grid Code Review.....	57
3.4	FRT Overview	58
3.4.1	FRT Methods for Fixed Speed Wind Turbines	59
3.4.2	FRT Methods for Variable Speed Wind Turbines.....	63
3.4.2.1	FRT Methods for DFIG Wind Turbines.....	64
3.4.2.2	FRT Methods for Full Scale Wind Turbines	68
4.	SIMULATION RESULTS	73
4.1	Introduction	73

4.2	Model Aggregation.....	73
4.3	Power System Modeling	74
4.4	Wind Farm Model based on Wind Turbines with DFIG.....	77
4.4.1	Performance of DFIG type Wind Turbines under Normal Operating Conditions.....	79
4.4.2	Performance of DFIG type Wind Turbines under Grid Disturbances	81
4.4.3	Suggested Method to Improve FRT Capability of DFIG type Wind Turbine.....	83
4.5	Wind Farm Model based on PMSG Wind Turbines	88
4.5.1	Performance of PMSG type Wind Turbines under Normal Operating Conditions.....	90
4.5.2	Performance of PMSG type Wind Turbines under Grid Disturbances ...	92
4.5.3	Suggested Method to Improve FRT Capability of PMSG type Wind Turbine.....	93
4.6	Comparison of the DFIG and PMSG Type Wind Turbines	98
4.7	An Additional Assessment for Integration of WPPs Connected to the Grid	99
5.	CONCLUSION.....	102
	REFERENCES.....	105
	APPENDICES	
A	CLARKE AND PARK TRANSFORMATION.....	110
B	PSCAD/EMTDC MODEL FOR DFIG.....	112
C	PSCAD/EMTDC MODEL FOR PMSG.....	117

LIST OF TABLES

TABLES

Table 1.1 Wind Power Installed in European Countries by the End of 2009	2
Table 4.1 154 kV Line Parameters of the Equivalent Circuit	75
Table 4.2 DFIG parameters used in PSCAD/EMTDC model	77
Table 4.3 Other Parameters Used in Wind turbine with DFIG Model	77
Table 4.4 PMSG parameters used in PSCAD/EMTDC model.....	89
Table 4.5 Other Parameters Used in Wind turbine with PMSG Model.....	89
Table B.1 DFIG Type WPP Parameters.....	114
Table C.1 PMSG Type WPP Parameters.....	119

LIST OF FIGURES

FIGURES

Figure 1.1 Global Installed Wind Capacity [1].....	2
Figure 1.2 Turkey Wind Resource Map at 50 m [3].....	3
Figure 2.1 Wind Turbines Types with respect to Orientation of Spin Axis	10
Figure 2.2 Inside a Wind Turbine [10]	11
Figure 2.3 Wind Turbine Configurations [4].....	15
Figure 2.4 Block Diagram of DFIG Type VSWT	17
Figure 2.5 C_p as a Function of λ and β	22
Figure 2.6 Maximum Power Curve for Different Wind Speeds [15]	24
Figure 2.7 Wind Speed versus Wind Turbine Power Curve of DFIG Type VSWTs	24
Figure 2.8 Pitch Angle Set-points With Respect to Wind Speed.....	25
Figure 2.9 Generic Control Scheme of Pitch Angle	26
Figure 2.10 Representation of Shaft Models	27
Figure 2.11 Steady State Equivalent Circuit of the DFIG	28
Figure 2.12 D-Q Equivalent Circuit Model of DFIG.....	29
Figure 2.13 Converter Models of DFIG Type Wind Turbine.....	32
Figure 2.14 Connection Diagram of Grid-Side Converter to the Grid	33
Figure 2.15 Voltage Vector Orientation of Grid-Side Converter	34
Figure 2.16 Vector Control Diagram of Grid-Side Converter	37
Figure 2.17 Connection Diagram of Rotor-Side Converter to the Generator	38
Figure 2.18 Stator Flux Vector Orientation of Rotor-Side Converter	38
Figure 2.19 Vector Control Diagram of Rotor-side Converter	41
Figure 2.20 Block Diagram of PMSG Type Wind Turbine.....	42
Figure 2.21 Converter Models of PMSG Type Wind Turbines.....	44
Figure 2.22 D-Q Equivalent Circuit of PMSG	45
Figure 2.23 Connection Diagram of Generator Side Converter	47

Figure 2.24 Vector Control Diagram of Generator Side Converter of the PMSG type Wind Turbines.....	48
Figure 3.1 Active Power Control Requirements.....	51
Figure 3.2 P-Q Dependencies of Three Variants [6]	52
Figure 3.3 V-Q Dependency [9]	53
Figure 3.4 Voltage/Frequency Operating Ranges.....	54
Figure 3.5 Comparison of the Operating Frequency Limits in European Countries .	54
Figure 3.6 Limiting Voltage Curves at PCC.....	56
Figure 3.7 Principle of Voltage Support During a Grid Fault [6].....	57
Figure 3.8 Connection of STATCOM at PCC.....	60
Figure 3.9 Schematic Arrangement of Braking Resistor [32].....	61
Figure 3.10 Basic Configuration of Superconducting Magnetic Energy Storage System [30]	62
Figure 3.11 Overall Comparison of Fixed Speed Wind Turbines FRT Methods [30]	63
Figure 3.12 Schematic of a Crowbar System.....	65
Figure 3.13 Schematic of Anti-parallel Thyristor System	66
Figure 3.14 Schematic of Transient Control Mode System [34]	67
Figure 3.15 Control Strategies for PMSG Type Wind Turbines [38].....	71
Figure 3.16 Positioning of Braking Resistor in PMSG Type Wind Turbines	72
Figure 4.1 Single Line Diagram of the Studied Region.....	76
Figure 4.2 Power System Model.....	76
Figure 4.3 Performance of DFIG type Wind Turbine under Normal Operating Condition with Varying Wind Speed.....	80
Figure 4.4 Simulation Results of DFIG Type Wind Turbine for a 3-Phase to Ground Fault at PCC for Duration of 150 ms	82
Figure 4.5 Simulation Results of DFIG Type Wind Turbine with Suggested FRT Method for a 3-Phase to Ground Fault at PCC for Duration of 150 ms	85
Figure 4.6 Simulation Results of DFIG Type Wind Turbine with Suggested FRT Method for a 3-Phase to Ground Fault at Fault Position-1 for Duration of 150 ms ..	86

Figure 4.7 Simulation Results of DFIG Type Wind Turbine with Suggested FRT Method for a 3-Phase to Ground Fault at Fault Position-2 for Duration of 150 ms ..	87
Figure 4.8 Simulation Results of DFIG Type Wind Turbine for a 3-Phase to Ground Fault at Fault Position-2 for Duration of 150 ms and the Faulted Line is opened.....	88
Figure 4.9 Performance of PMSG Type Wind Turbine under Normal Operating Condition with Varying Wind Speed.....	91
Figure 4.10 DC-link Voltage of PMSG Type Wind Turbine under Grid Fault for Duration of 150 ms	92
Figure 4.11 DC-link Voltage of PMSG Type Wind Turbine under Grid Fault for Duration of 150 ms with Suggested FRT Method	94
Figure 4.12 Simulation Results of PMSG Type Wind Turbine with Suggested FRT Method for a 3-Phase to Ground Fault at PCC for Duration of 150 ms	95
Figure 4.13 Function Diagram of DC-Link Block with Protection Signal.....	96
Figure 4.14 Simulation Results of PMSG Type Wind Turbine with Suggested FRT Method for a 3-Phase to Ground Fault at Fault Position-1 for Duration of 150 ms ..	97
Figure 4.15 Simulation Results of PMSG Type Wind Turbine for a 3-Phase to Ground Fault at Fault Position-1 for Duration of 150 ms and the Faulted Line is opened	98
Figure A.1 Phasor Diagrams Used in Deriving Transformation Matrices.....	111
Figure B.1 General Block Diagram of DFIG Type WPP Model.....	112
Figure B.2 Block Diagram of Turbine and Wind Speed Model.....	113
Figure B.3 Diagram of the DFIG.....	114
Figure B.4 Block Diagram of Converters.....	115
Figure B.5 Block Diagram of the Converter Controllers.....	116
Figure C.1 General Block Diagram of PMSG Type WPP Model.....	117
Figure C.2 Block Diagram of Turbine and Wind Speed Model.....	118
Figure C.3 Diagram of the PMSG.....	119
Figure C.4 Block Diagram of Converters.....	120
Figure C.5 Block Diagram of the Converter Controllers.....	121

CHAPTER 1

INTRODUCTION

1.1 Background

As the price of the fossil fuels is increasing and their availability is dwindling; and moreover the change of climate has almost reached an irreversible point, renewable energy is becoming more and more important. One of the leading alternatives among these renewable sources (biomass, solar, geothermal, ocean, small hydro) is wind energy. Technological improvements on wind energy systems with governmental supports have increased the penetration level of wind power into the grid in recent years. The rapid growth of wind power brings lots of study and research for integration of wind energy into conventional power systems. In addition to this, governments have granted funds for research and support in renewable energy sources. The advantages of using wind energy are reduced CO₂ emission, reduced operational cost (as no fuel is required) and added capacity value to a power system (ability to contribute to peak demands). In Figure 1.1, the increase of the wind power installation can be easily seen worldwide through years 1996 to 2009 [1]. As seen, global annual installed wind capacity is exponentially increased recent years.

When looking into the installed wind power in Europe in Table 1.1, Germany has the lead with respect to the installed capacity and Spain follows Germany in the second place. Denmark has also the largest wind penetration level (20%) and expects to reach 50% level by the help of strong connections both to the ENTSO-E, Norway and Sweden [2].

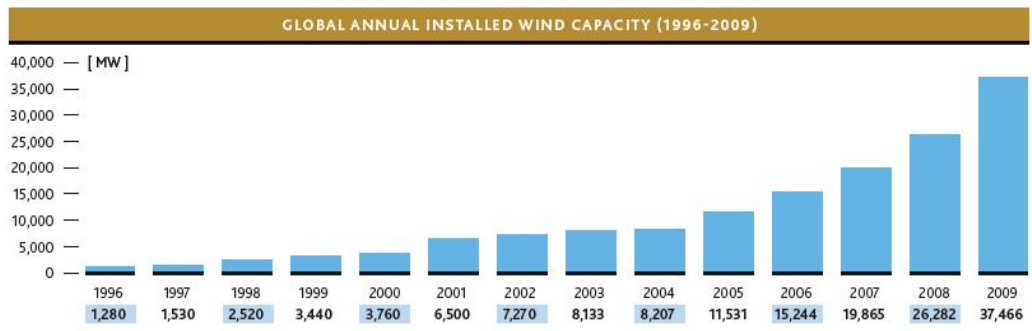
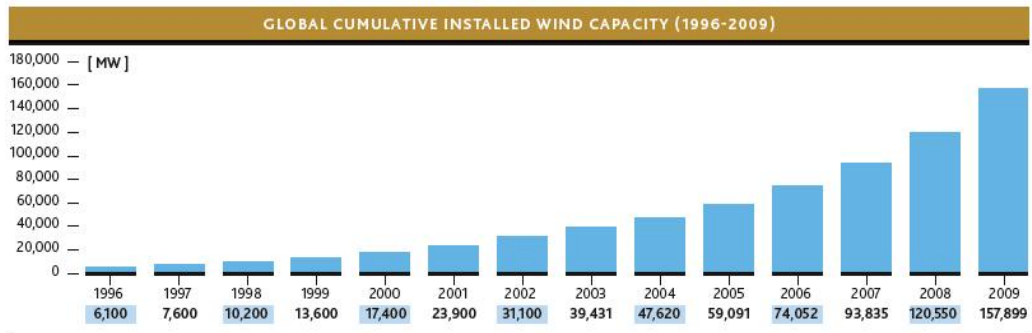


Figure 1.1 Global Installed Wind Capacity [1]

Table 1.1 Wind Power Installed in European Countries by the End of 2009

Germany	25777 MW
Spain	19149 MW
Italy	4850 MW
France	4492 MW
United Kingdom	4051 MW
Portugal	3535 MW
Denmark	3465 MW
Netherlands	2229 MW
Sweden	1560 MW
Ireland	1260 MW
Greece	1087 MW
Austria	995 MW
Turkey	801 MW

As seen from Table 1.1, Turkey is in the early stages of these developments; however, the potential of wind power is very well known as shown in Figure 1.2 and future projections are expected up to 20% penetration level of the overall installed generation capacity. This high level of penetrations forces the power system operators to revise their grid codes and investigate the compatibility of the wind turbines to the grid. The integration studies are performed by the Turkish Electricity Transmission Company (TEIAS) and Energy Market Regulatory Authority (EMRA), as planned the impacts of the wind power will be smoothed according to the regulations and grid codes.

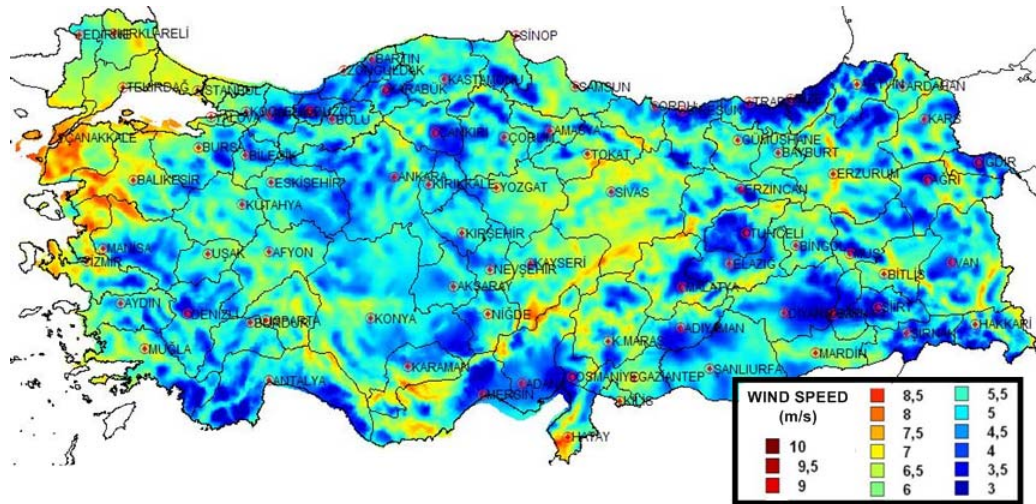


Figure 1.2 Turkey Wind Resource Map at 50 m [3]

The previously mentioned progress of wind power has changed the conventional power system operation. The advantages and the future growth of the wind power are therefore available only when wind farms operate according to the regulations that are prescribed by power system operators for the stability and reliability of the system. Before the rapid increase of the wind power generation, wind turbines had been considered as distributed energy sources in medium and low voltage

distribution systems. The wind turbine technology was not adequate to participate in power system control in response to voltage or frequency disturbances [4]. Common practice during a system disturbance was to disconnect the wind turbines and reconnect them after the fault clearance. However, high wind power penetration together with the recent developments in wind turbine technology has changed this picture. Meanwhile, Transmission System Operators (TSOs), wind turbine manufacturers and Wind Power Plant (WPP) developers would work in a cooperative way to integrate future wind installations and stable power system operation.

The wind integration studies can be summarized under the following categories:

- Grid code revisions carried out by power system operators together with WPP developers to define the WPP connection, planning and operation.
- Wind turbine technology developments performed by wind turbine manufacturers.
- WPP connection studies regarding the WPP infrastructure and controller, conducted by the WPP developers to satisfy the grid code requirements or technical regulations.

As the conventional power plants largely composed of synchronous generators, they are able to support the power system by providing inertia response, re-synchronizing torque, oscillation damping, short circuit capability and voltage recovery during faults. These features allow the conventional power plants comply with the grid codes, thus today power system operators have a quite stable and reliable grid operation worldwide. On the other hand, WPPs have completely different aspects which bring additional considerations to the control system. The control structure is not straightforward as in the conventional power plant case mentioned above. The characteristic aspects of the WPPs can be summarized as follows [5]:

- WPPs have wind turbines with converter-based grid interface technology (permanent magnet synchronous generators with full-scale converters or doubly-fed induction generators with partial scale converters).
- The generator speed of the wind turbines is varying and fluctuates due to the wind speed (variable wind speed turbines). In other words, wind turbines rotor speed is eventually decoupled from the frequency of the transmission system because of the usage of full-scale converters.
- The typical size of the wind turbines is much smaller with respect to conventional units (from hundreds kW to 7 MW).
- WPPs are not simply collections of individual wind turbines; they have collector systems and other devices (energy storage, FACTS devices, etc.) with controllers. This means each individual wind turbine terminals face different operating conditions from the point of connection during the steady-state and the transient situations.
- Each individual wind turbine has its own electrical and mechanical control systems (wind turbine control level).
- Active and reactive power controls are decoupled in the converter-based wind turbines.

1.2 Scope of the Thesis

Related to mentioned integration studies above, this thesis mainly deals with the wind turbine technology while taking into account the inherent differences of the wind turbine stated before. The main focus is the transient voltage stability related to the three-phase short circuit faults occurring in the transmission system with large amount of connected wind power.

The content of this work could be separated into three parts:

1. Composure (development) of dynamic wind turbine models. This aims to build a set of existing wind turbine models for the power system analysis.
2. Overview of the general grid code requirements for the wind turbine integration studies.
3. Implementation of the turbine modeling into one of the existing simulation toolboxes to analyze the transient voltage stability. Simulations of the models are performed and the results are presented according to grid codes and different wind turbine technologies in a comparative way.

1.3 Modeling Approach

Before connecting wind turbines to the transmission system, wind turbine models are necessary for grid operation both in steady-state and transient conditions and also for planning and market issues. The simulation model complexity depends on the target of the investigation and simulation tool capability. In this work, PSCAD/EMTDC is used for the transient voltage stability analyses. The models that are used in the analyses are described briefly as follows:

1. The wind speed model represents the whole field of wind speeds in the rotor plane of the wind turbine and can be constituted of the following four parts:
 - The average value,
 - The ramp component,
 - The gust component,
 - The turbulence component.
2. The aerodynamic model of the wind blade takes equivalent wind speed as input and extracts some of wind kinetic energy to the shaft model as output.
3. The shaft model converts the kinetic energy extracted by aerodynamic model into rotational energy, and then delivers this energy via a drive train (gearbox) to the generator.

4. A number of generator configurations are used in conversion of mechanical power into electrical power and these are summarized in wind turbine concepts part. In this thesis for generator modeling, PSCAD/EMTDC software library provides dedicated models for variable speed generators.
5. Voltage source converters are used for controlling variable speed generators.

1.4 Wind Power Impacts

TSOs are responsible for network operations in steady-state and transient conditions. According to TSOs perspective, it must be proven for the power plants connected to transmission network that the reliability and stability of the network should not be adversely affected. Thus the grid code requirements must clearly define the connection criteria of the WPPs into the transmission network. So far the countries experiencing high wind penetration have revised their grid code. As described before, the grid code revisions are one side of the wind integration studies.

According to the grid codes, common requirements can be defined as follows:

- Active power control,
- Reactive power control,
- Frequency control,
- Inertia emulation,
- Fault Ride Through (FRT) Capability.

The transient voltage stability corresponds to the FRT capability in the grid codes. During grid disturbances, voltage dips can typically lead to WPP disconnections that will cause instability and yield to blackouts. To avoid these problems, the grid codes require WPPs to continue operation even if the voltage dip reaches very low levels, support the voltage recovery by injecting reactive current and restore active power

after the fault clearance with a limited ramp values. These FRT specifications are clearly defined in the grid codes [6], [7], [8] and [9].

1.5 Outline of the Thesis

In this thesis, the main objective is to develop and investigate the Variable Speed Wind Turbine (VSWT) models for the grid operation performance of the wind turbines in steady-state and especially during fault conditions by using a power system transient analysis program, namely PSCAD/EMTDC. The wind turbine models are developed with the focus on simulation of the wind turbines during grid faults (3-phase short circuit faults) and satisfying the grid code requirements such as FRT capability.

Chapter 2 describes wind turbines and wind turbine classifications according to the orientation of spin axis, number of blades and rotor speeds. Also detailed models of a VSWT equipped with voltage-sourced converters including the wind speed model, the aerodynamic model, the shaft model and the generator model will be explained. The differences between the models of VSWT are expressed in detailed. In chapter 3, the grid code requirements for the grid integration of the wind turbines will be explained particularly. The FRT methods of different wind turbine types are also explained in this chapter. In chapter 4, the transient responses of the variable-speed wind turbines during a 3-phase short circuit fault in the grid are analyzed and compared in detail. The simulation results will be presented and annotated in this chapter. Chapter 5 concludes and summarizes the results obtained in the thesis. Additionally, discussions for the FRT requirements based on the comparison of the wind turbine technologies and the integration of future wind installations are also given in Chapter 5.

CHAPTER 2

WIND TURBINE MODELING

2.1 Introduction

This chapter presents a comprehensive tutorial on wind turbine concept and modeling in power systems. The need for the wind turbine models has arisen in the last decades because of the fast emergence of the wind power into the power system. Although the wind turbine is composed of aerodynamic, mechanical and electrical components, it should be considered as one electro-mechanical component and modeled similar to the conventional generating units in the transmission system in terms of time constants and complexity.

The chapter starts with the definition and classifications of a wind turbine. Then the components that comprise the turbine and wind turbine technologies will be explained briefly. Afterwards, modeling of VSWT with partial scale frequency converter will be explained including wind model, aerodynamic model, shaft model, generator model and converter model. Finally, the state of the art turbine model, VSWT with full-scale frequency converter, will be explained.

2.2 Definition of Wind Turbine

Wind turbines are rotary machines that use moving air in the wind to generate electricity by using the turbine blades. As the need for the wind turbines are growing, studies on this topic are also increasing. As a result of these studies, the energy market has several types of wind turbines and these turbines can be divided into

classifications according to their orientation of the spin axis, structure or speed of the rotor. The distinctive classification in the market is according to the orientation of the spin axis and wind turbines can be divided into two: vertical axis and horizontal axis wind turbines.

2.2.1 Vertical-axis Wind Turbines

Vertical-axis wind turbine (VAWT) which is also known as Darrieus turbine is a type of wind turbine where the main rotor shaft runs vertically as in Figure 2.1. VAWTs have the advantage that they do not need to be pointed into the wind to be effective; this is especially important where the wind direction is highly variable. The gearbox and generator can be placed at ground level so the tower structure is less massive and can be easily accessible for maintenance. On the other side there are some disadvantages like no self-starting capability, high torque fluctuations and speed regulation difficulties in high winds. Besides, lower amount of energy will be extracted because of the decrease in wind speed in lower heights.



Figure 2.1 Wind Turbines Types with respect to Orientation of Spin Axis

2.2.2 Horizontal Axis Wind Turbines (HAWT)

Figure 2.1 reveals HAWTs, which have the blades, hub, rotor shaft and generator at the top of a tower. Since HAWTs are equipped with tall towers, they can access strong winds which mean more power output. Besides, their blades always move perpendicularly to the wind by the yaw control, they can receive power through the whole rotation. Also having a pitch system, HAWTs can extract optimum amount of energy from the wind. However, settling the gearbox and generator over the nacelle made turbines' design more expensive and complicated. Requiring an additional yaw control mechanism and installation difficulties are other disadvantages of HAWTs. Figure 2.2 illustrates the basic components of HAWT system.

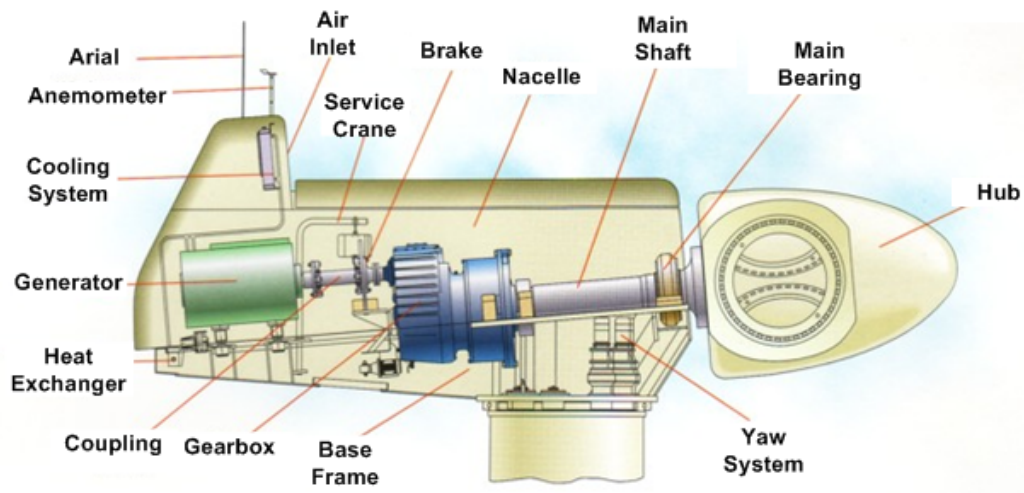


Figure 2.2 Inside a Wind Turbine [10]

These components can be defined as;

- **Anemometer**
Measures the wind speed and transmits it to the controller.
- **Blades**

Cause the rotation of rotor by the blow of wind through them.

- **Brake**
A brake system which can be a mechanical, electrical or hydraulic is used for stopping the rotor in emergency or maintenance conditions.
- **Drive-train**
Drive-train is the combination of mechanical parts including rotor hub, rotor shaft, gearbox and generator shaft which converts the rotors mechanical rotation into electrical energy.
- **Cooling system**
Cooling system is used to cool the generator. There are two types of cooling system which are air cooled and water cooled systems.
- **Controller**
Manages the turbine by taking all required signals from measurements and sending required commands to the devices.
- **Gear box**
Gears increase the generator speed by connecting the low-speed shaft to the high-speed one.
- **Generator**
The wind turbine generators (Induction or synchronous machines) convert mechanical energy to electrical energy.
- **High-speed shaft**
Shaft of the generator.
- **Low-speed shaft**
Shaft of the turbine.
- **Nacelle**
The nacelle is a housing that placed on top of the tower and contains the gear box, shafts, controllers, generator and yaw system.
- **Pitch system**
Pitch system controls the blades in proportion to the wind speed for extracting maximum energy from the wind.

- **Rotor**
The rotor receives the kinetic energy from the wind stream by blades and transforms it into mechanical energy. It consists of blades, hub, shaft, bearings and other internals.
- **Tower**
Towers are made from concrete or steel lattice that support nacelle, and lift the nacelle to a higher height where blades can safely clear the ground.
- **Wind vane**
Measures wind direction and communicate with the yaw system to orient the turbine perpendicularly with respect to the wind.
- **Yaw mechanism**
The wind turbine yaw system is used to turn the nacelle against the wind.

HAWTs can be classified according to number of blades as single bladed, two bladed, three bladed and multi bladed or they can be further classified as upwind and downwind turbines with respect to direction of receiving wind [11]. Besides, according to the rotor speed, they can be classified as fixed speed and variable speed wind turbines. Moreover, there are four major wind turbine configurations in the literature [4];

1. The early and simple configuration represents the turbines that are directly connected to the grid and equipped with an asynchronous squirrel cage induction generator (SCIG). This configuration needs capacitor banks for reactive power compensation. Further improvements are realized by adding blade-angle control (pitch control) to the wind turbine.
2. Another configuration corresponds to wound rotor induction generator (WRIG) equipped with variable rotor resistor circuit. The mechanical construction is similar to the SCIG concept; however there is an additional rotor circuit in order to control the active power and speed of the rotor by

changing the rotor resistance. The capacitor banks are used for the reactive power compensation.

3. VSWTs with partial scale frequency converter configuration which is known as the doubly fed induction generator (DFIG) concept, implies a WRIG with converter circuit in the rotor. The converter which is about %30 of rated generator power performs the reactive power compensation and the smoother grid connection.
4. By the latest developments and requirements, VSWTs are connected to the power system through full-scale frequency converter. Similar to the partial converter concept, full scale converter performs decoupled active and reactive power control with much smoother grid connection and operation. There are two types of generator used in this configuration which are wound rotor synchronous generators (excited electrically) and the Permanent Magnet Synchronous Generators (PMSG).

The concepts mentioned above are illustrated in Figure 2.3. As a result of these classifications, there are many combinations of wind turbines available in the market. However, the scope of this thesis will be limited to the VSWTs with partial and full scale converter concepts as they are the state of the art turbine technologies.

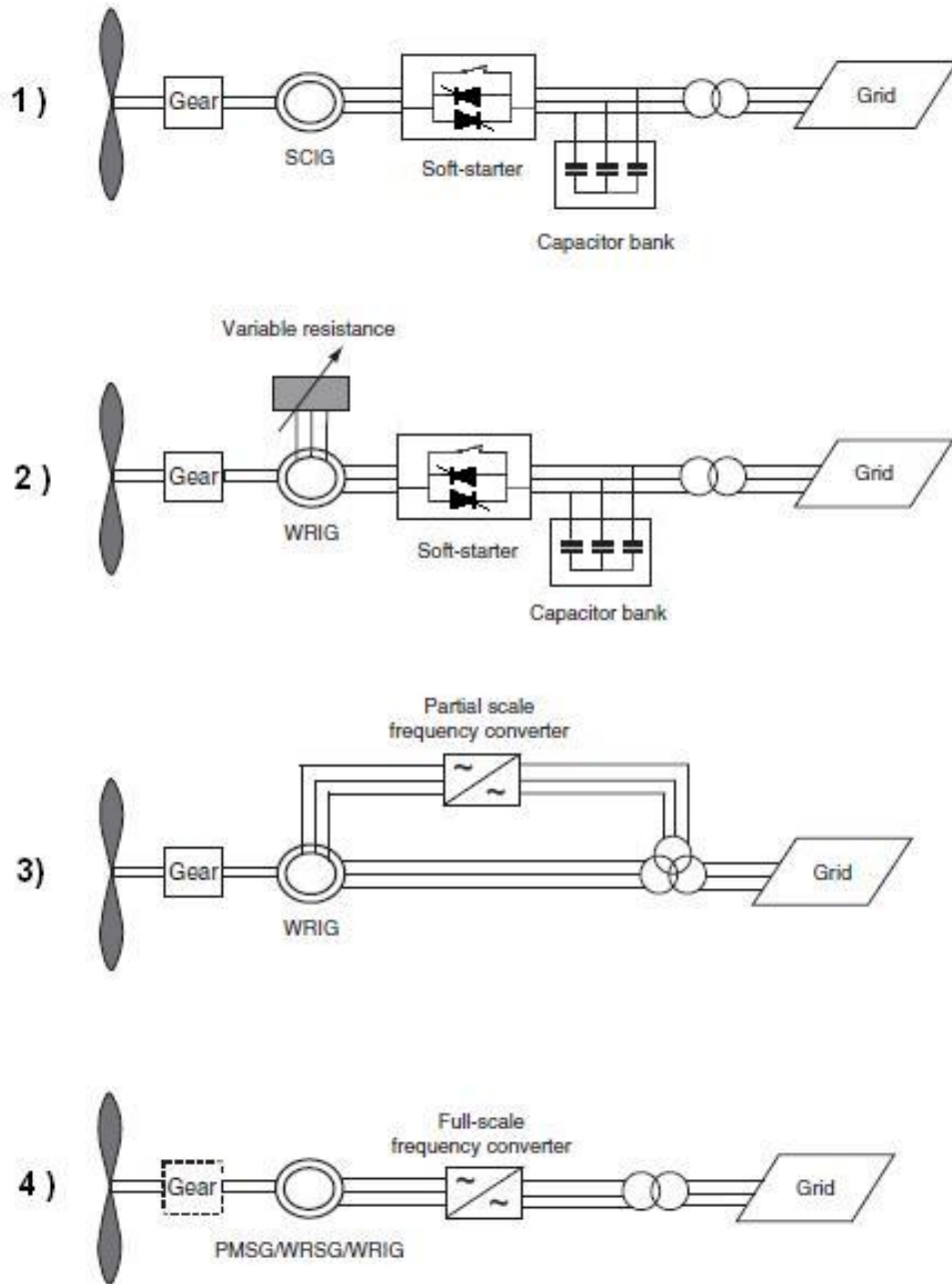


Figure 2.3 Wind Turbine Configurations [4]

2.3 Modeling of Wind Turbines

As described in Section 2.2, there are two major wind turbine categories according to their speed which are fixed speed wind turbines (SCIG and WRIG) and variable speed wind turbines (DFIG and PMSG). The fixed speed wind turbines were widely used in the early 1990s and had the highest number of installations due to their simple solution, where the generator is directly connected to the grid. Since the generator, which is a SCIG, is directly coupled to the grid, the rotor has to rotate almost same with the constant frequency of grid. This type of wind turbine was attractive because of its advantages like being simple, cost effective, robust, reliable and well-proven. However it is not preferred nowadays and is not in the scope of this thesis, since direct coupling of generator with grid results in high fluctuations in the grid and the energy capture of these turbines are not as efficient as in variable speed systems.

In recent years, the use of VSWT has become worldwide. This type of wind turbine has designed to increase the aerodynamic efficiency in various ranges of wind speeds. Their electrical system is more complex than the fixed-speed wind turbines. Better power quality, higher amount of energy extraction and less mechanical stress on the turbines are considered as the major advantages of VSWTs. However, the disadvantages of these wind turbines are semi-conductor losses, utilization of more components and the increased cost due to the power electronics [4].

As mentioned in Section 2.2, the scope of this thesis will be limited to the VSWTs with partial (DFIG) and full scale converter (PMSG) concepts as they are the state of the art turbine technologies. The rest of this chapter will describe the modeling of VSWTs.

2.3.1 Modeling of a Variable Speed Wind Turbine with DFIG

In the DFIG type wind turbine, the rotor of induction generator is wound and has slip ring. This wound rotor is connected to the grid through two back-to-back converters via slip ring, whereas stator is directly coupled to grid. Power output of the turbine is controlled by using the pitch system and also by controlling two back-to-back converters. This type is widely used today since it provides high efficiency with its variable speed operation, interference with grid is reduced since the rotor is decoupled from the grid, and is more cost-effective, since its back-to-back converters have partial (about 30%) rating of wind turbine rated power.

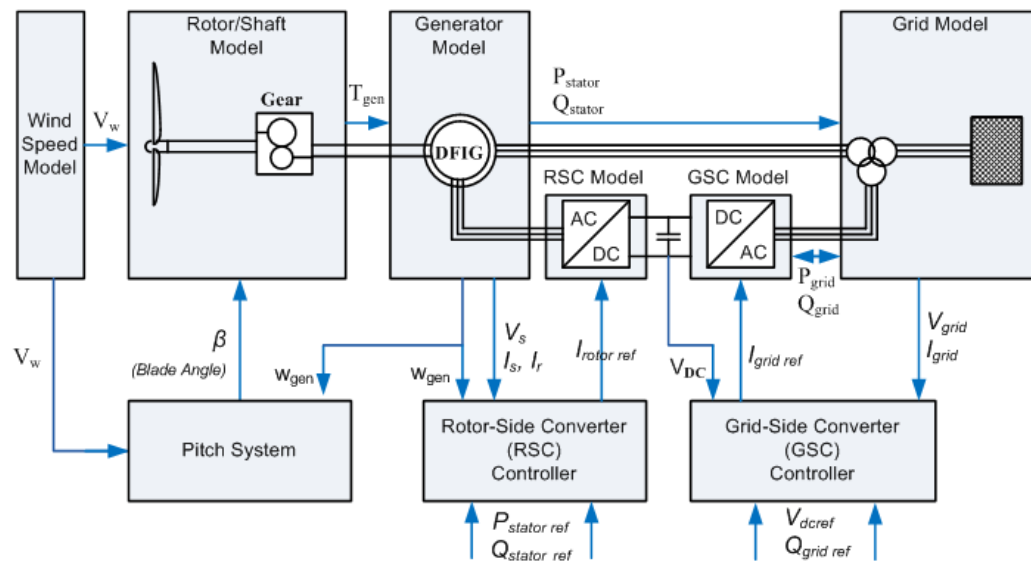


Figure 2.4 Block Diagram of DFIG Type VSWT

In Figure 2.4, general structure of a VSWT with DFIG is represented. As seen, this type of turbine model is comprised of a wind speed model, a rotor (aerodynamic) model, a pitch model, a shaft model, a generator model, a converter model and a controller model.

2.3.1.1 Wind Speed Modeling

There are two approaches for modeling wind speed in simulations which use the measured data or formulate the wind speed according to empirical data. The first approach has the advantage of using the real wind data while simulating the performance of the turbine. But, the simulations can use only wind speed sequences that have already been measured. In the second approach, wind speed model can generate desired wind speed sequences to be chosen by the user. Thus, setting the value of the required parameters to an appropriate value, the effects of the wind speed to the wind farm can be properly simulated. In this thesis, the wind speed model has been used as a formulation that is similar to that proposed in [12] and consists of the following four components;

- Base wind velocity, V_{WB} (m/s)
- Gust wind component, V_{WG} (m/s)
- Ramp wind component, V_{WR} (m/s)
- Noise wind component, V_{WN} (m/s)

The wind speed, V_W in m/s , is independent from the characteristics of the wind turbine therefore, it can be written as the combination of the above-mentioned four components as in (2.1).

$$V_W = V_{WB} + V_{WG} + V_{WR} + V_{WN} \quad (2.1)$$

The base wind velocity is constant value that is always assumed to be present in studies where the wind turbine is required to be in operation. It can be calculated from the power generated in the load-flow combined with the nominal power of the turbine [4].

The gust wind component is formulated in (2.2) where T_{sg} is the starting time of the wind speed gust in *second*, T_{eg} is the end time of the wind speed gust in *second* and A_g is the amplitude of the wind speed gust in *m/s* [12];

$$\begin{aligned}
 t < T_{sg} &\rightarrow V_{WG} = 0 \\
 T_{sg} \leq t \leq T_{eg} &\rightarrow V_{WG} = A_g \left\{ 1 - \cos \left[2\pi \left(\frac{t - T_{sg}}{T_{eg} - T_{sg}} \right) \right] \right\} \\
 T_{eg} > t &\rightarrow V_{WG} = 0
 \end{aligned} \tag{2.2}$$

The ramp wind component is formulated in (2.3) where T_{sr} is the starting time of the wind speed ramp in *second*, T_{er} is the end time of the wind speed ramp in *second* and A_r is the amplitude of the wind speed ramp in *m/s* [12];

$$\begin{aligned}
 t < T_{sr} &\rightarrow V_{WR} = 0 \\
 T_{sr} \leq t \leq T_{er} &\rightarrow V_{WR} = A_r \left(\frac{t - T_{sr}}{T_{er} - T_{sr}} \right) \\
 T_{er} > t &\rightarrow V_{WR} = 0
 \end{aligned} \tag{2.3}$$

Finally, the noise wind component is the random noise component and is formulated in (2.4) where $w_i = (i-1/2)\Delta w$, ϕ_i is variable with uniform probability density and $S_V(w_i)$ is the spectral density function [12].

$$V_{WN} = 2 \sum_{i=1}^N [S_V(w_i) \Delta w]^{1/2} \cos(w_i t + \phi_i) \tag{2.4}$$

Since the transient stability analyses are performed for short periods: gust, ramp and noise wind components do not influence the simulation results in this thesis. Thus, base wind velocity is the main component used in the analysis.

2.3.1.2 Aerodynamic Model

The power production of wind turbine depends on the interaction between the wind and the turbine rotor. Turbine rotor blades extract some kinetic energy from the flow air in the wind and transform this energy into mechanical rotational energy. In order to obtain the amount of mechanical energy transformed by turbine blades, firstly the kinetic energy of a moving object in the air should be found as in (2.5) where E is the kinetic energy in *joules*, m is the mass in *kg* and V is the speed of the object in *m/s*.

$$E = \frac{1}{2} m V^2 \quad (2.5)$$

Power of the moving air, P , can be found by taking the derivative of (2.5);

$$P = \frac{dE}{dt} = \frac{d}{dt} \left(\frac{1}{2} m V^2 \right) = \frac{1}{2} V^2 \left(\frac{dm}{dt} \right) \quad (2.6)$$

Mass flow rate, dm/dt , could be expressed as in (2.7) where ρ is the air density in *kg/m³* and A is the flow area in *m²*.

$$\frac{dm}{dt} = \rho A V \quad (2.7)$$

Inserting (2.7) into (2.6), the power of the moving air passing across an area could be found as in (2.8);

$$P = \frac{1}{2} \rho A V^3 \quad (2.8)$$

From equation (2.8), power of the wind can be expressed as in (2.9);

$$P_{wind} = \frac{1}{2} \rho A V_{wind}^3 \quad (2.9)$$

After calculating the power of the wind, the power that is extracted by wind turbine can be calculated. Since the air flow must be continuous behind the blades to extract power, only a fraction of the kinetic can be absorbed by the blades of the wind turbine. The ratio of the power absorbed by the blades to the total wind power is called the power coefficient, c_p , and has a theoretical maximum value of 0,599. This theoretical maximum value is called Betz Limit and explained in [13] in detail. C_p is determined by the aerodynamic structure of the blades and the harmony between blades and blowing wind. Thus, c_p is a function of two parameters which are the blade pitch angle, β , and tip speed ratio, λ . The tip speed ratio is the ratio of the turbine tip speed and wind speed as in (2.10) where ω is the rotor rotational speed in *rad/s* and R is the radius of the blade in *m*.

$$\lambda = \frac{\omega R}{V} \quad (2.10)$$

Besides, structure of the rotor can be changed by changing the pitch angle of the blades. Hence c_p changes with changing pitch angle of the blades. As a result, extracted power output of the turbine can be calculated as in (2.11);

$$P_{mechanical} = \frac{1}{2} \rho A V_{wind}^3 c_p(\lambda, \beta) \quad (2.11)$$

By using the rotational speed of the rotor, torque on the rotor shaft can be calculated as in (2.12).

$$T_{mechanical} = \frac{P_{mechanical}}{\omega_{rotor}} \quad (2.12)$$

The power coefficient versus tip speed ratio curves with respect to different pitch angles are generally given by wind turbine manufacturers as shown in Figure 2.5 and it is seen that wind turbine has different power-speed characteristics for every wind speed and pitch angle.

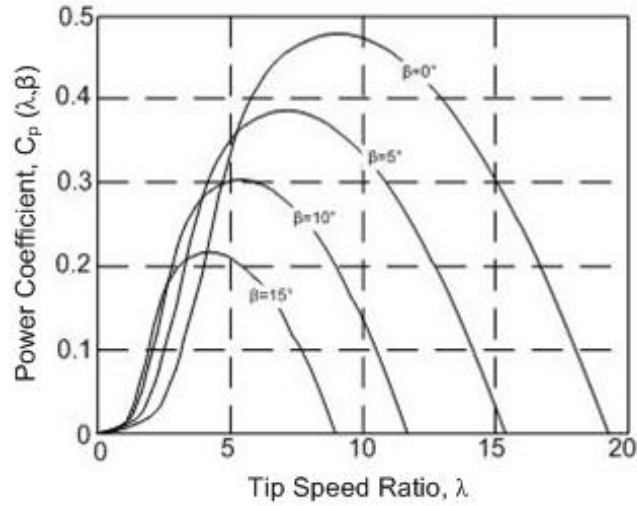


Figure 2.5 C_p as a Function of λ and β

These curves of different wind turbines are similar and can be calculated from measurements, approximate equations or numerical methods. By applying approximate equation method, it is possible to represent c_p by a normalized formula, (2.13), as described in [14] and [15].

$$c_p(\lambda, \beta) = c_1 \left(\frac{c_2}{\lambda_i} - c_3 \beta - c_4 \beta^{c_5} - c_6 \right) e^{-c_7/\lambda_i} \quad (2.13)$$

where constants $c_1, c_2, c_3, c_4, c_5, c_6, c_7, c_8$ and c_9 are given by wind turbine manufacturers and λ_i is described in (2.14).

$$\lambda_i = \frac{1}{\frac{1}{\lambda + c_8 \beta} + \frac{c_9}{\beta^3 + 1}} \quad (2.14)$$

The extracted power can be maximized with largest c_p value, which is obtained for optimum pitch angle and optimum tip speed ratio. Pitch angle is optimum for 0° ,

except for the high wind speeds and transient conditions. Optimum tip speed ratio, λ_{opt} , means that; for every wind speed there is a rotor speed, which is proportional to the wind speed giving the largest c_p value. Then, optimum rotor speed can be written as in (2.15);

$$W_{rotor_opt} = \frac{\lambda_{opt} V_{wind}}{R} \quad (2.15)$$

In Figure 2.6, wind power is drawn with respect to rotor speed for different wind speed values for optimum pitch angle, which is assumed as 0° here. Each curve represents $c_p(\lambda, \beta)$ curves, where the maximum points refer to the rotor speeds giving optimum tip speed ratios. When rotor is operated to rotate at these optimum points, then maximum power is obtained by rotor.

The rotor radius, maximum rotor speed and the hardware rating of the wind turbine are design parameters which depend on the application. If the wind speed exceeds rated value, the power of the wind turbine is limited by the control algorithm (using the pitch system). For very high wind speeds (cut-off speed), the wind turbine is stopped considering mechanical reliability. Also there exists a minimum wind speed (cut-in speed), below which the wind turbine is not enabled considering the power of the wind and power loss of wind turbine. As a result, Figure 2.7 is obtained, which shows the maximum power values versus wind speed at steady-state conditions.

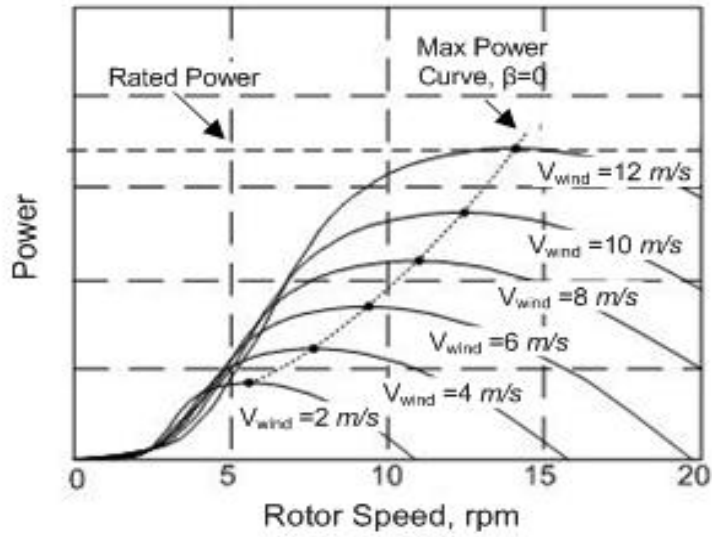


Figure 2.6 Maximum Power Curve for Different Wind Speeds [15]

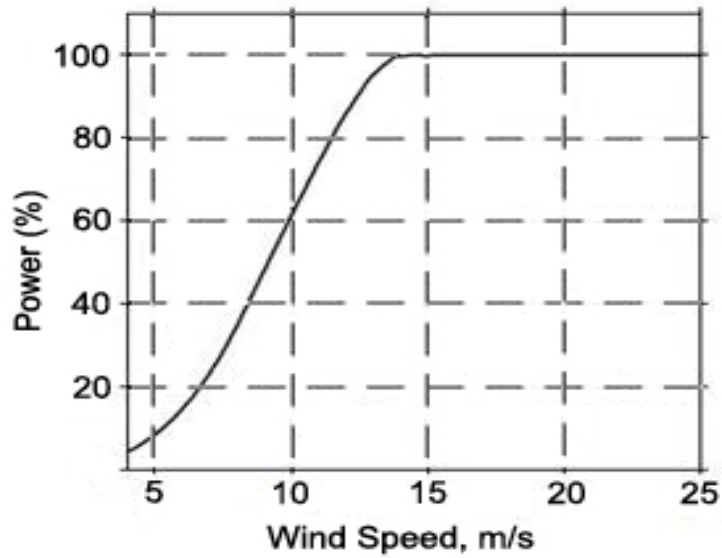


Figure 2.7 Wind Speed versus Wind Turbine Power Curve of DFIG Type VSWTs

2.3.1.3 Pitch System

Pitch system is utilized for reduction of the power extraction from the wind in order to maintain the rotor speed in the set value or limit the power to a pre-specified value. As described in 2.3.1.2, blade pitch angle is generally kept constant at 0° for extracting maximum power from the wind turbine. However, because of the hardware strength limits of the wind turbine, pitch angle must be controlled in high wind speeds and transient conditions. By regulating it, speed of the rotor and power output of the turbine can be controlled in wind turbine operating limits. In Figure 2.8, pitch angle variation with respect to wind speed in steady state operation is represented.

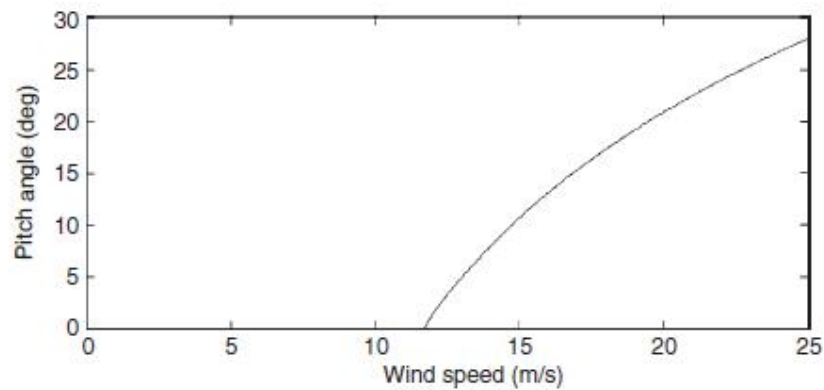


Figure 2.8 Pitch Angle Set-points With Respect to Wind Speed

The block diagram of the pitch angle control scheme, including dynamics is shown in Figure 2.9. Tracking error of power will give an appropriate blade angle which will be compared with measured β and inserted into the pitch control system; therefore errors in the position of the blade could be corrected.

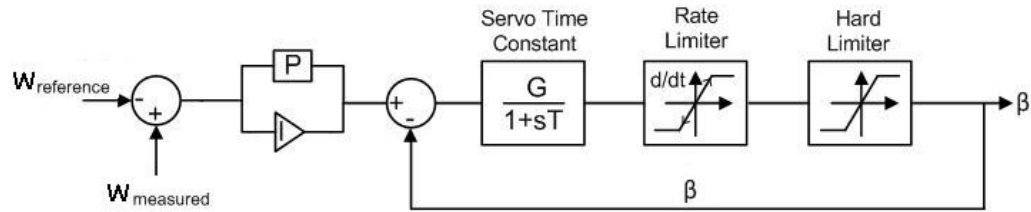


Figure 2.9 Generic Control Scheme of Pitch Angle

Because of the mechanical limitations, there is a hard limiter and a rate limiter in the control scheme. Hard limiter is used for determining the endpoints of the pitch angles whereas the rate limiter determines the maximum rate of pitch angle change which is different for steady state and transient conditions. Generally rate limit is $10^\circ/\text{sec}$ for steady state and $15^\circ/\text{sec}$ for transient conditions.

2.3.1.4 Shaft Modeling

The shaft system includes gearbox, turbine and generator rotors, low-speed and high-speed shafts. It is obvious that, accurate results can be obtained by including all these parts of the turbine in the model. Considering the drive train, which has the most important effect on the output power, shaft system can be modeled as a two-mass system as shown in Figure 2.10. The approach adapted to drive train system is that the wind turbine and generator rotor can be modeled as masses, while the turbine shaft can be modeled as spring element. However, VSWTs are equipped with generators controlled by the converters that minimize any effects from shaft to the grid. Since the aim of these controllers is to minimize the impact of the shaft, the shaft system has no significant effects to the grid and may be neglected or may be modeled as a single lumped mass model in which all of the components in drive train are lumped together.

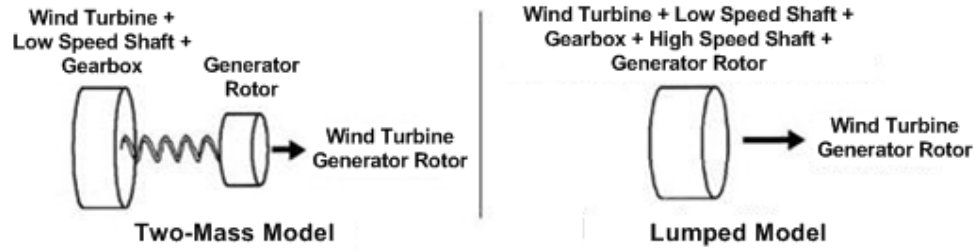


Figure 2.10 Representation of Shaft Models

The dynamic behavior of such single lumped mass system can be described in (2.16) where J_{WG} is the total of wind turbine mechanical inertia and generator mechanical inertia in $kg\cdot m^2$, w is the rotor speed in rad/s , T_W is the wind turbine aerodynamic torque in Nm , T_G is the generator electromagnetic torque in Nm and D is a friction coefficient in Nm/rad [17].

$$J_{WG} \frac{dw}{dt} = T_W - T_G - D \quad (2.16)$$

2.3.1.5 Generator Modeling

A WRIG with power electronic converters connected to rotor, fed on both rotor and stator is called doubly-fed induction generator. In DFIG, the rotor is connected to the grid through two back-to-back converters via a slip ring, where stator is directly coupled to grid. The main objective of DFIG used in wind turbine systems is to control the rotor speed where it can extract maximum power from the wind. However, being polyphase electromagnetic systems, induction machines have a nonlinear and highly interactive multivariable control structure which lead to control difficulties. Field oriented control (vector control) method can be used to handle these difficulties, which transforms the dynamic structure of the induction generator

into separately excited decoupled control structure with independent control of flux and torque [18].

Figure 2.11 shows the schematic of the steady state equivalent circuit of the DFIG, where the quantities on the rotor side are referred to the stator side.

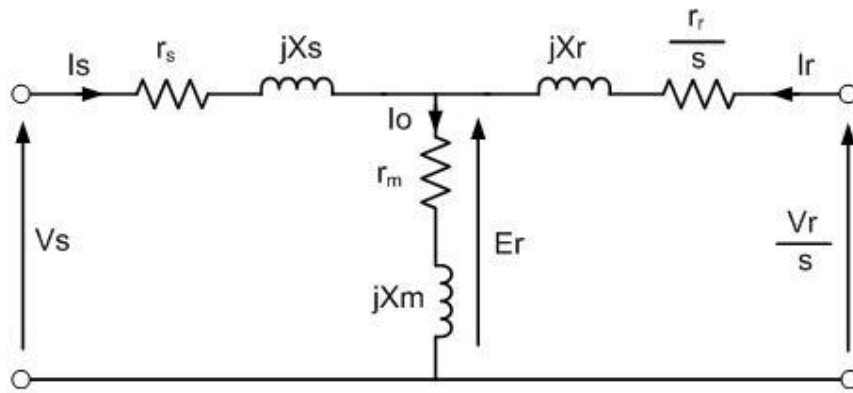


Figure 2.11 Steady State Equivalent Circuit of the DFIG

In Figure 2.11, V_s and V_r are the stator phase voltage and rotor phase voltage applied to the induction machine respectively in V , E_r is the electric motive force in V , I_s is the stator current in A , I_r is the rotor current in A and I_0 is the no-load current in A . This steady state equivalent circuit, based on calculations with rms-values of voltages and currents, can only be applied to steady state analysis of the DFIG. So the DFIG model must be built according to used vector control method for convenience. In order to apply vector control to a DFIG, this steady state equivalent circuit will be transformed into the d-q equivalent circuit as shown in Figure 2.12. While doing the transformation some assumptions and simplifications are made [19];

- The stator and rotor windings of the DFIG are assumed symmetric.
- The windings sinusoidally distributed around the circumference of the DFIG.

- The air gap is constant.
- Saturation is neglected.
- Iron losses are neglected.

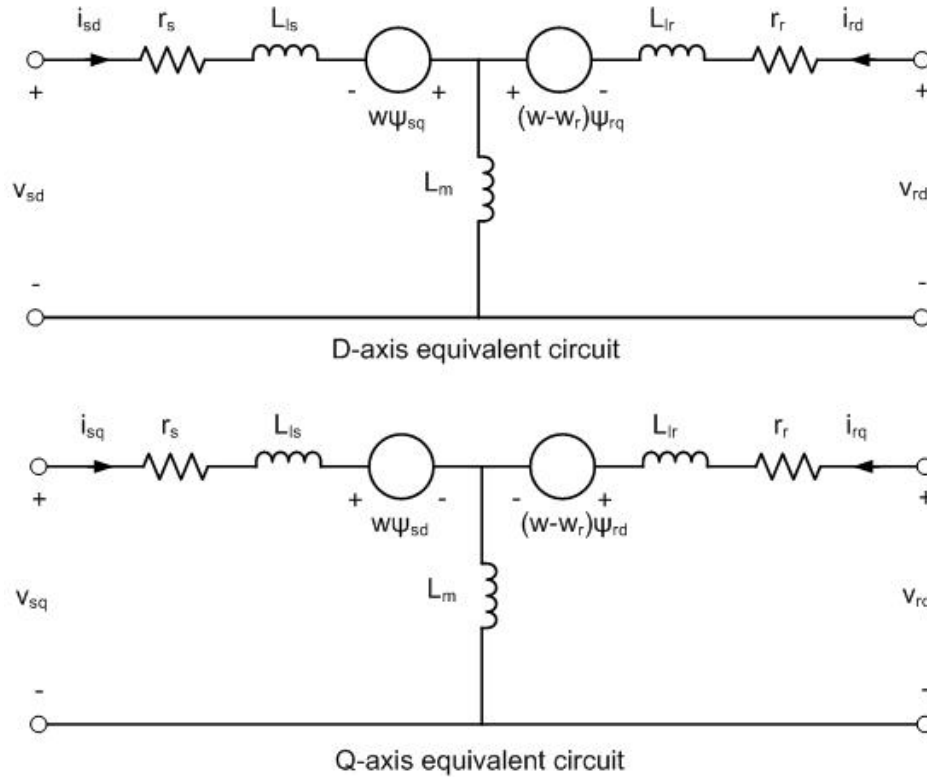


Figure 2.12 D-Q Equivalent Circuit Model of DFIG

The transformation is made in two steps; firstly, the stationary 3-phase variables (a-b-c frame) are transformed into stationary 2-phase (alpha-beta frame) variables, and then transformed to rotating 2-phase variables (d-q frame) by using Clark and Park Transformations expressed in Appendix A. The reduction from three to two-phase reference frame has the advantage that the fluxes in the two phases do not interact with each other. This brings the advantage that time varying signals of the three-phase system becomes constant when referred to the two-phase system.

The voltage equations of an induction generator in the d-q reference frame can be found in the Literature in [18] and [20] and are as follows;

$$\begin{aligned}
v_{ds} &= R_s i_{ds} + \frac{d\psi_{ds}}{dt} - w\psi_{qs} \\
v_{qs} &= R_s i_{qs} + \frac{d\psi_{qs}}{dt} - w\psi_{ds} \\
v_{dr} &= R_r i_{dr} + \frac{d\psi_{dr}}{dt} - (w - w_r)\psi_{qr} \\
v_{qr} &= R_r i_{qr} + \frac{d\psi_{qr}}{dt} - (w - w_r)\psi_{dr}
\end{aligned} \tag{2.17}$$

where v_{ds} , v_{qs} , v_{dr} , v_{qr} , i_{ds} , i_{qs} , i_{dr} , i_{qr} and ψ_{ds} , ψ_{qs} , ψ_{dr} , ψ_{qr} are voltage, current and flux linkages of the stator and rotor d-q axes, R_s and R_r are the resistance of stator and rotor windings, w is the speed of the reference frame, and w_r is the electrical angular velocity of the generator rotor. Flux linkage used in (2.17) can be obtained as;

$$\begin{aligned}
\psi_{ds} &= L_s i_{ds} + L_m i_{dr} \\
\psi_{qs} &= L_s i_{qs} + L_m i_{qr} \\
\psi_{dr} &= L_r i_{dr} + L_m i_{ds} \\
\psi_{qr} &= L_r i_{qr} + L_m i_{qs}
\end{aligned} \tag{2.18}$$

where L_m , L_s and L_r are the stator, rotor and mutual inductances and L_s and L_r can be defined as;

$$\begin{aligned}
L_s &= L_{ls} + L_m \\
L_r &= L_{lr} + L_m
\end{aligned} \tag{2.19}$$

where L_{ls} , and L_{lr} are the stator and rotor leakage inductances.

Stator-side and rotor-side active and reactive powers generated or consumed by DFIG can be calculated by the following equations (2.20):

$$\begin{aligned}
 P_s &= \frac{3}{2}(v_{ds}i_{ds} + v_{qs}i_{qs}) \\
 P_r &= \frac{3}{2}(v_{dr}i_{dr} + v_{qr}i_{qr}) \\
 Q_s &= \frac{3}{2}(v_{qs}i_{ds} - v_{ds}i_{qs}) \\
 Q_r &= \frac{3}{2}(v_{qr}i_{dr} - v_{dr}i_{qr})
 \end{aligned} \tag{2.20}$$

where P_s , P_r , Q_s and Q_r are active and reactive powers of the stator and rotor calculated from d-q axes voltages and currents. The electrical torque generated in the machine can be calculated using following equation where p is the number of poles and T_g is the electrical torque.

$$T_g = \frac{3}{2}pL_m(i_{qs}i_{dr} + i_{ds}i_{dr}) \tag{2.21}$$

By neglecting the stator dynamics (stator $d\psi/dt$ terms) in above equations, a reduced order model can be used in transient stability analysis.

2.3.1.6 Converter Modeling

DFIG can operate in the wide speed range with the help of converters connected to its rotor. These converters can be cyclo-converters, naturally or line-commutated converters or low-frequency forced commutated thyristor converters as described in [18]. Moreover, PWM voltage sourced converters are generally used in DFIG since they can produce a sinusoidal AC output voltage whose frequency and magnitude can be both controlled [19]. These converters can be modeled in detail as a voltage sourced converter with switching elements and pulse modulators. However the scope

of this thesis is neither concentrated on the switches of the PWM voltage source converter nor switching of the power electronic devices. Besides, if switching devices are used, simulation speed will be very slow because of the small simulation time steps for high frequency switching. Therefore, converters can be modeled as controlled voltage sources.

In Figure 2.13-a, DFIG with two back-to-back connected voltage sourced converters is shown whereas in Figure 2.13-b, DFIG with controlled voltage source is shown.

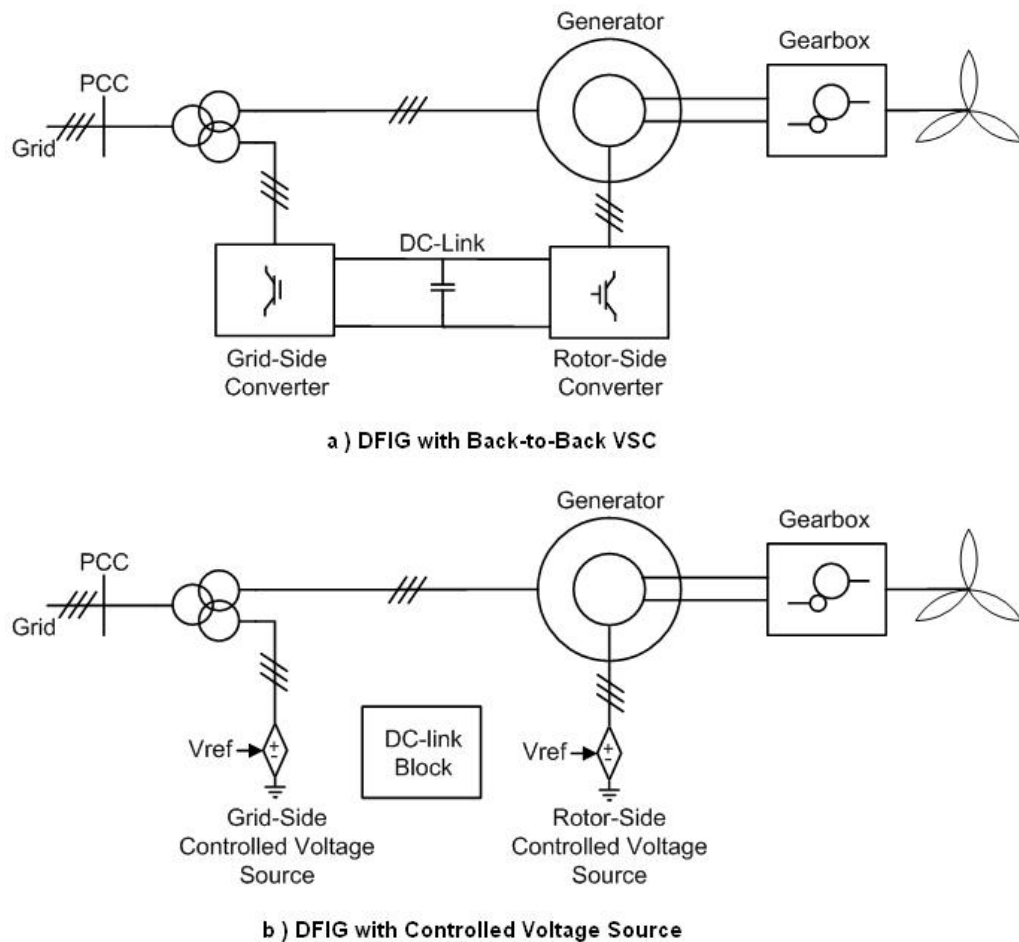


Figure 2.13 Converter Models of DFIG Type Wind Turbine

These converters should work as a rectifier and as an inverter to be able to transfer energy in both directions i.e. to provide a path for power flow from rotor side converter to the grid in super-synchronous speed (rotor speed is greater than synchronous speed) and from the grid to rotor side converter in sub-synchronous speeds (rotor speed is slower than synchronous speed). The rotor side converter is responsible for controlling the generator active and reactive power and work in slip frequency. On the other hand, the grid-side converter is responsible for controlling the DC-link voltage, regardless of the magnitude and direction of rotor power.

2.3.1.7 Grid-side Converter Controller Modeling

As mentioned in converter modeling, the main objectives of the grid-side converter are providing unity power factor at grid side and controlling the dc-link voltage. To do these, grid-side converter permits bidirectional power flow. Before explaining the control structure, the connection diagram of grid-side converter to the grid is shown in Figure 2.14, where R and L are line resistance and inductance, respectively. Since dc-link is operated at lower voltages because of the low rotor voltages, the converter is connected to the grid over a transformer.

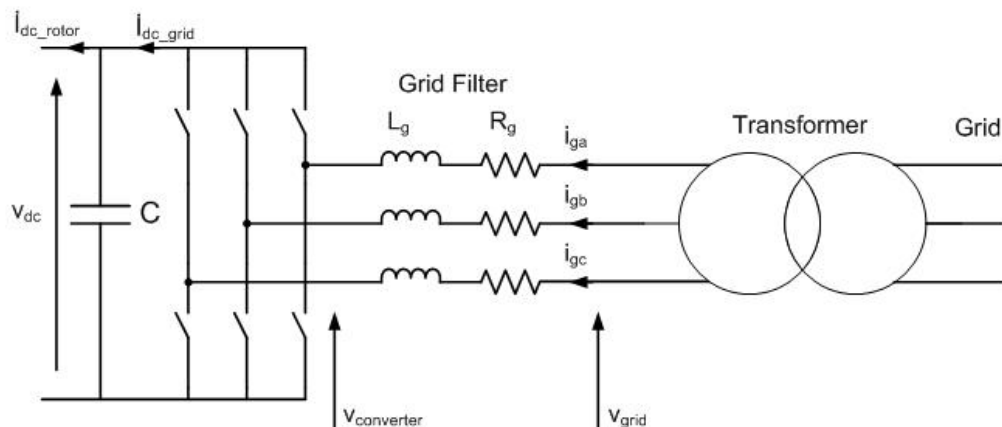


Figure 2.14 Connection Diagram of Grid-Side Converter to the Grid

The stator voltage oriented vector control is used for decoupled control of the dc-link voltage and reactive power. The voltage is oriented along d-axis as shown in Figure 2.15.

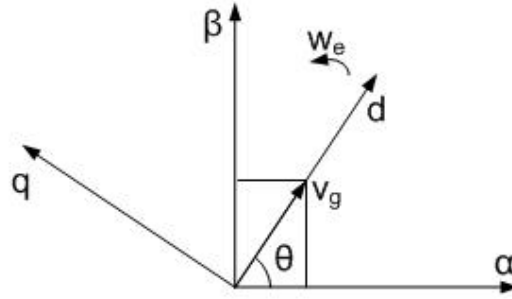


Figure 2.15 Voltage Vector Orientation of Grid-Side Converter

The voltage balance equations in Figure 2.14 across the inductors and resistors are;

$$\begin{bmatrix} v_{ga} \\ v_{gb} \\ v_{gc} \end{bmatrix} = R_g \begin{bmatrix} i_{ga} \\ i_{gb} \\ i_{gc} \end{bmatrix} + L_g \frac{d}{dt} \begin{bmatrix} i_{ga} \\ i_{gb} \\ i_{gc} \end{bmatrix} + \begin{bmatrix} v_{gca} \\ v_{gcb} \\ v_{gcc} \end{bmatrix} \quad (2.22)$$

By using abc to dq transformation, (2.23) is obtained where w_e is the angular speed of the grid voltage, v_{gd} and v_{gq} are grid voltages in d and q axes, v_{gcd} and v_{gcq} are grid-side converter voltages in d and q axes, and i_{gd} and i_{gq} are grid-side converter currents in d and q axes.

$$\begin{aligned} v_{gd} &= R_g i_{gd} + L_g \frac{di_{gd}}{dt} - w_e L_g i_{gq} + v_{gcd} \\ v_{gq} &= R_g i_{gq} + L_g \frac{di_{gq}}{dt} + w_e L_g i_{gd} + v_{gcq} \end{aligned} \quad (2.23)$$

The angular position θ of the grid voltage can be calculated as in (2.24) where $v_{g\alpha}$ and $v_{g\beta}$ are the α - β axes grid voltage components.

$$\theta_e = \int \omega_e dt = \tan^{-1} \frac{v_{g\beta}}{v_{g\alpha}} \quad (2.24)$$

Since the d-axis of the reference frame is aligning with the grid voltage vector as in Figure 2.15, the q component of the grid voltage is zero. Hence the active and reactive power flow between the grid and the grid side converter will be proportional to i_d and i_q , respectively as in (2.25);

$$\begin{aligned} P_g &= \frac{3}{2} v_{gd} i_{gd} \\ Q_g &= -\frac{3}{2} v_{gd} i_{gq} \end{aligned} \quad (2.25)$$

Grid side converter controls the DC-link voltage based on the energy conservation principle. Neglecting power losses in the converter, the instantaneous power must be same on both sides of the converter as in (2.26) where v_{dc} and i_{dc} are the DC-link voltage and current, v_a, v_b, v_c and i_a, i_b, i_c are the AC-side voltages and currents respectively.

$$v_{dc} i_{dc} = v_a i_a + v_b i_b + v_c i_c \quad (2.26)$$

Beside these, power flow over both converters must be same instantaneously as the DC-link voltage can be kept stable. As can be concluded from (2.27), DC current differences between converters will increase or decrease the DC-link voltage.

$$C \frac{dv_{dc}}{dt} = i_{dcg} - i_{dcr} \quad (2.27)$$

It can be concluded from above equations that dc-link voltage can be controlled by d-axis current and reactive power output of the converter can be controlled by q-axis current. Then, the equations above can be rewritten as [18];

$$\begin{aligned} v_{gcd} &= -\left(R_g i_{gd} + L_g \frac{di_{gd}}{dt}\right) + \omega_e L_g i_{gq} + v_{gd} \\ v_{gcq} &= -\left(R_g i_{gq} + L_g \frac{di_{gq}}{dt}\right) - \omega_e L_g i_{gd} \end{aligned} \quad (2.28)$$

Then, the grid side converter control equations can be rewritten as in [18] where v_{gcd}^* and v_{gcq}^* are the reference voltage values for the converter, k_{pd} and k_{id} are the PI block gains of d-axis and k_{pq} and k_{iq} are the PI block gains of q-axis.

$$\begin{aligned} v_{gcd}^* &= -\left(k_{pd} + k_{id} \int \right) (i_{gd}^* - i_{gd}) + \omega_e L_g i_{gq} + v_{gd} \\ v_{gcq}^* &= -\left(k_{pq} + k_{iq} \int \right) (i_{gq}^* - i_{gq}) + \omega_e L_g i_{gd} \end{aligned} \quad (2.29)$$

As seen in Figure 2.16, two types of current control loops are included in the control scheme of the grid-side converter. The slower loop which is named as “outer” is used to control the dc-link voltage; and the fast one which was called as “inner” is made use of controlling the current through the grid filter. Cross-coupling terms which are shown at the right hand side of the equation provide proper decoupling between axes and improve the transient response of the converter. These terms are added to the inner control loop outputs and the sum is transformed to *a-b-c* frame to generate the voltage reference to the converter model.

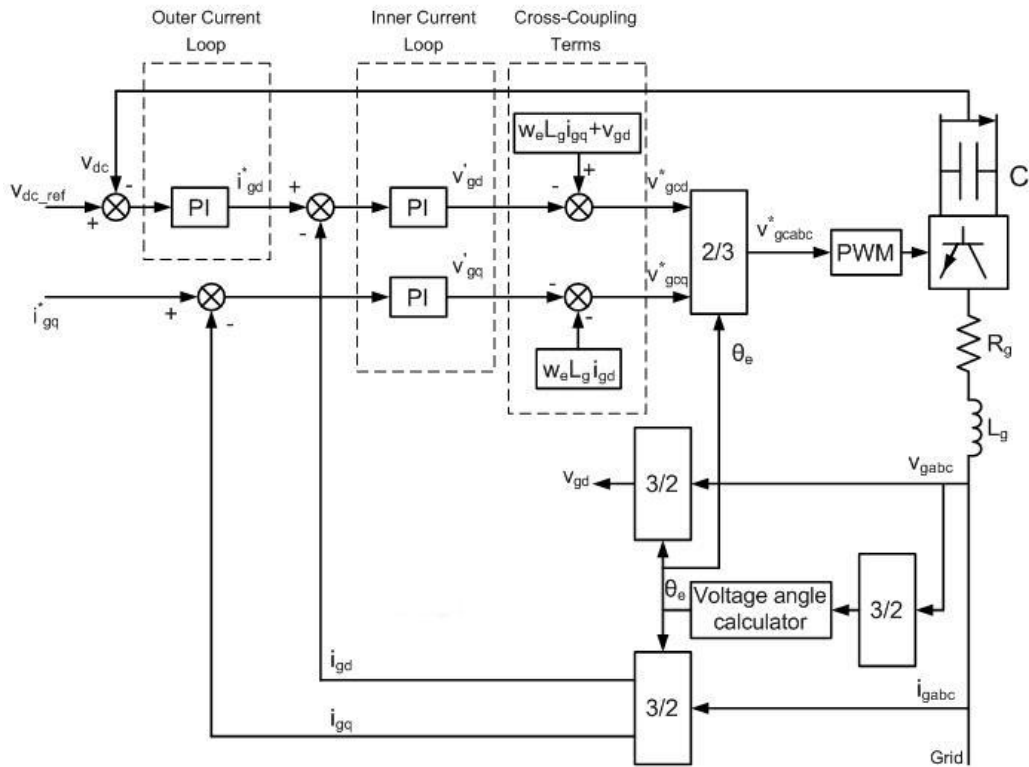


Figure 2.16 Vector Control Diagram of Grid-Side Converter

2.3.1.8 Rotor-side Converter Controller Modeling

As mentioned 2.3.1.6, the main objectives of the rotor-side converter are controlling the generator active and reactive power and work in slip frequency. Before explaining the control structure, the connection diagram of rotor-side converter to the generator is shown in Figure 2.17.

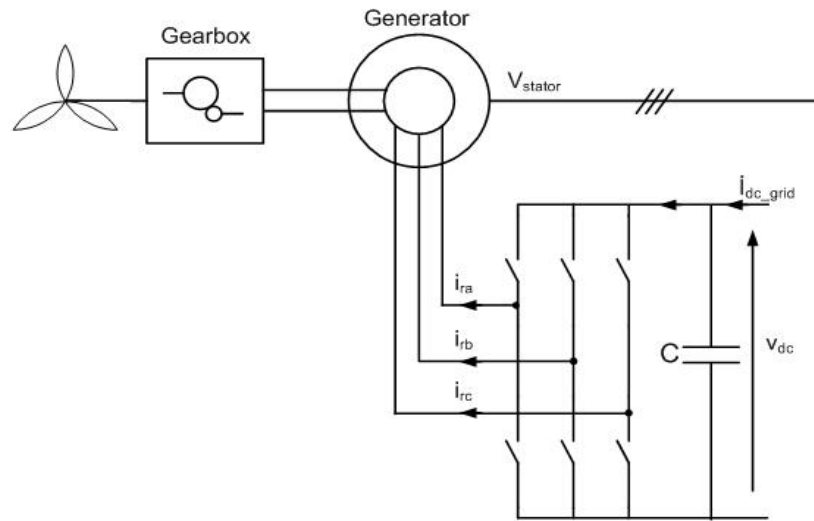


Figure 2.17 Connection Diagram of Rotor-Side Converter to the Generator

The control scheme presented to control the rotor-side converter is stator flux oriented vector control. This method is achieved by online estimation of stator flux vector position where it is less sensitive to machine parameters and only dependent to stator resistance [18]. The stator flux is oriented along d-axis as shown in Figure 2.18 . Since vector orientation is along d axis, the q axis component of the stator flux is zero.

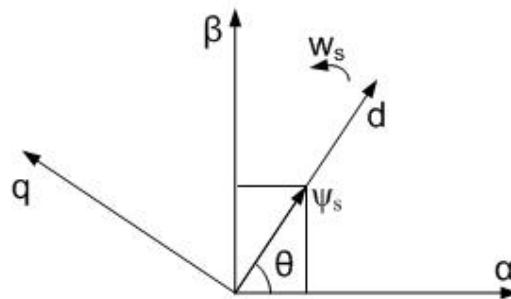


Figure 2.18 Stator Flux Vector Orientation of Rotor-Side Converter

From stator voltage and currents, magnitude and phase of the stator flux vector can be calculated;

$$\begin{aligned}
\psi_{\alpha s} &= \int (v_{\alpha s} - r_s i_{\alpha s}) dt \\
\psi_{\beta s} &= \int (v_{\beta s} - r_s i_{\beta s}) dt \\
\theta &= \int \omega_s dt = \tan^{-1} \frac{\psi_{\beta s}}{\psi_{\alpha s}}
\end{aligned} \tag{2.30}$$

where $\psi_{\alpha s}$, $\psi_{\beta s}$, $v_{\alpha s}$, $v_{\beta s}$ and $i_{\alpha s}$, $i_{\beta s}$ are the α - β axis stator flux, voltages and currents, and ω_s is the angular velocity of the stator flux. Since the stator resistance voltage drop is small and stator is directly connected to grid, the stator flux can be considered constant and it lags the stator voltage vector by 90° . Then DFIG model may be rewritten as in (2.31) [19]:

$$\begin{aligned}
v_{sd} &= 0 \\
v_s &= v_{sq} = \omega_s \psi_{sd} \\
v_{rd} &= r_r i_{rd} + \sigma L_r \frac{di_{rd}}{dt} - \omega_{slip} \sigma L_r i_{rq} \\
v_{rq} &= r_r i_{rq} + \sigma L_r \frac{di_{rq}}{dt} - \omega_{slip} (L_{mm} i_{ms} + \sigma L_r i_{rd}) \\
\psi_s &= \psi_{sd} = L_m i_{ms} = L_s i_{sd} + L_m i_{rd} \\
\psi_{rd} &= \frac{L_m^2}{L_s} i_{ms} + \sigma L_r i_{rd} \\
\psi_{rq} &= \sigma L_r i_{rq}
\end{aligned} \tag{2.31}$$

where

$$\begin{aligned}
w_s &= w_e \\
w_{slip} &= w_s - w_r \\
\sigma &= 1 - \frac{L_m^2}{L_s L_r} \\
L_{mm} &= \frac{L_m^2}{L_s}
\end{aligned}$$

In (2.31), v_s is the magnitude of the stator phase voltage, w_e is the electrical angular velocity of the stator voltage, ψ_s is the magnitude of the stator flux linkage, and i_{ms} is the magnetizing current of the generator. Moreover, active and reactive power of the stator can be written as:

$$\begin{aligned}
P_s &= \frac{3}{2} (v_{sd} i_{sd} + v_{sq} i_{sq}) \\
Q_s &= \frac{3}{2} (v_{sq} i_{sd} - v_{sd} i_{sq})
\end{aligned} \tag{2.32}$$

Since the d component of stator voltage is zero, active and reactive powers of the stator are controlled by i_{rq} and i_{rd} respectively. From here, by controlling v_{rq} and v_{rd} , rotor currents can be controlled i.e., active and reactive powers of the stator can be controlled. From (2.31) and [18], rotor-side converter control equations can be rewritten as (2.33) where v_{rd}^* and v_{rq}^* are the reference voltage values for the converter, k_{pd} and k_{id} are the PI block gains of d-axis and k_{pq} and k_{iq} are the PI block gains of q-axis.

$$\begin{aligned}
v_{rd}^* &= \left(k_{pd} + k_{id} \int \right) (i_{rd}^* - i_{rd}) - (w_e - w_r) \sigma L_r i_{rq} \\
v_{rq}^* &= \left(k_{pq} + k_{iq} \int \right) (i_{rq}^* - i_{rq}) + (w_e - w_r) \sigma L_r i_{rd} + (w_e - w_r) \frac{L_m}{L_s} \psi_{sd}
\end{aligned} \tag{2.33}$$

As seen in Figure 2.19, the control scheme of the rotor-side converter consists of a fast inner current control loop, which controls the d- and q-axis rotor currents, and an outer slower control loop that controls the active and reactive power on the stator. Cross-coupling terms which shown at the right hand side of the equation provide decoupling between axes and improves the transient response of the converter. These

terms are added to the inner control loop outputs and summation is transformed to a - b - c frame to generate the voltage reference to the converter model.

In Figure 2.19, the active power reference, P_{s_ref} , is obtained via lookup table from a measured generator speed, which satisfies the optimal power tracking for maximum energy capture from the wind [19]. The reactive power reference, Q_{s_ref} , generally set to zero. However if needed (set by TSO or FRT conditions), Q_{ref} can be adjusted by using a lookup table or a control block.

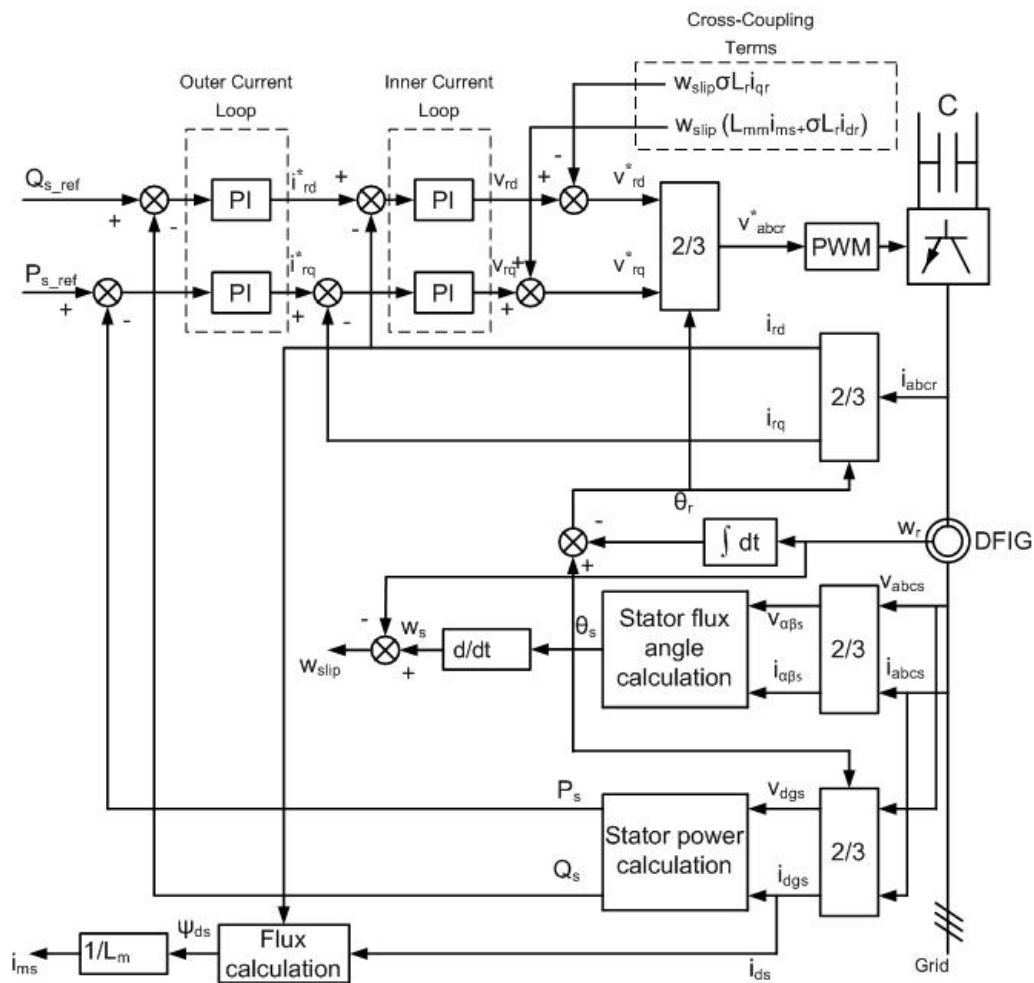


Figure 2.19 Vector Control Diagram of Rotor-side Converter

2.3.2 Modeling of a Variable Speed Wind Turbine with PMSG

Full Scale Wind Turbines (FSWT) are the state-of-the-art type wind turbines that the generator is completely decoupled from the grid with two back-to-back converters and whole power is transferred through these controlled converters. One converter is used on the generator side and the other one is used on the grid side. FSWTs can employ both induction (asynchronous) and synchronous type generators, where synchronous generators can be separately excited (conventional) or permanent magnet type. Generally multi-pole permanent magnet synchronous generators are employed, which removes the need for a gearbox between wind turbine rotor and generator. Since this type of wind turbines has many advantages like mechanical reliability, better efficiency, reduced risk of possible drive-train oscillations, this thesis will deal with PMSG type FSWTs.

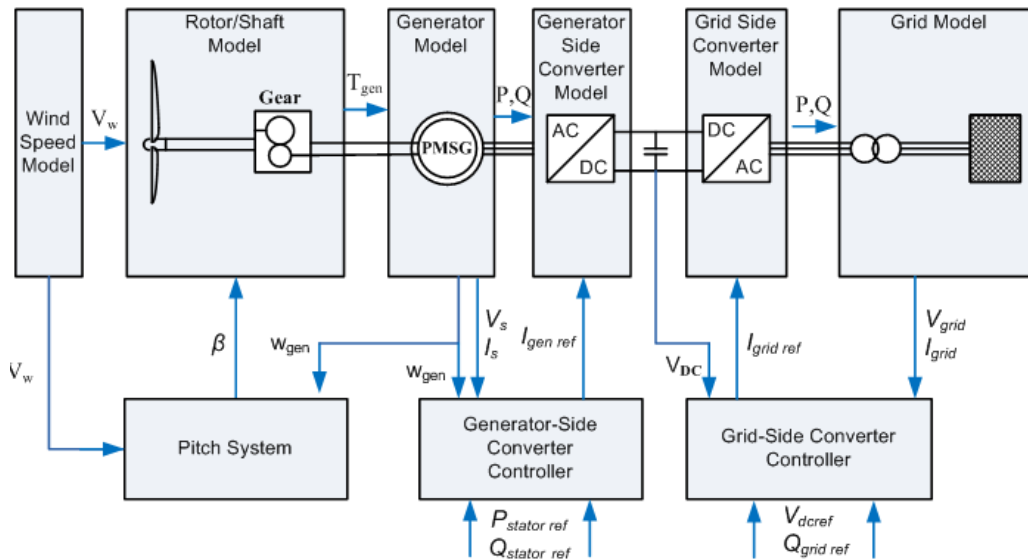


Figure 2.20 Block Diagram of PMSG Type Wind Turbine

Figure 2.20 depicts the general block diagram of a VSWT with PMSG. As seen, the model of a VSWT equipped with PMSG is very similar to that of a VSWT with a DFIG. Wind speed model, rotor (aerodynamic) model and pitch model are identical to those in DFIG type wind turbine model.

2.3.2.1 Shaft Modeling

Directly connecting rotor to the generator and connecting the rotor to the generator over a gearbox are the two options for shaft system. The former method, known as direct-drive, has the advantages of being simple, mechanically reliable, efficient and having a lower risk of possible drive-train oscillations, and hence it is the state-of-the-art technology for PMSG type turbines. For direct-drive systems, shaft model is not required and for the connections with gearbox, the shaft model explained in DFIG section can be used.

2.3.2.2 Converter Modeling

Although there are several options for converters to connect the generator to the grid [21][22], the converter model used in PMSG type wind turbines is very similar to the one in DFIG type turbines. The difference is, since generator is completely decoupled from the grid with two back-to-back converters, whole power is transferred through those controlled converters. Hence, the converter ratings must be equal to ratings of the generator and the converter must be able to work as a rectifier and as an inverter to allow transfer energy in both directions. Similar to DFIG converter model, the generator-side converter is responsible for controlling the generator active and reactive power. On the other hand, the grid-side converter is responsible for controlling the DC-link voltage and reactive power output of the converter. Therefore, as in DFIG, converters can be modeled as controlled voltage sources as shown in Figure 2.21.

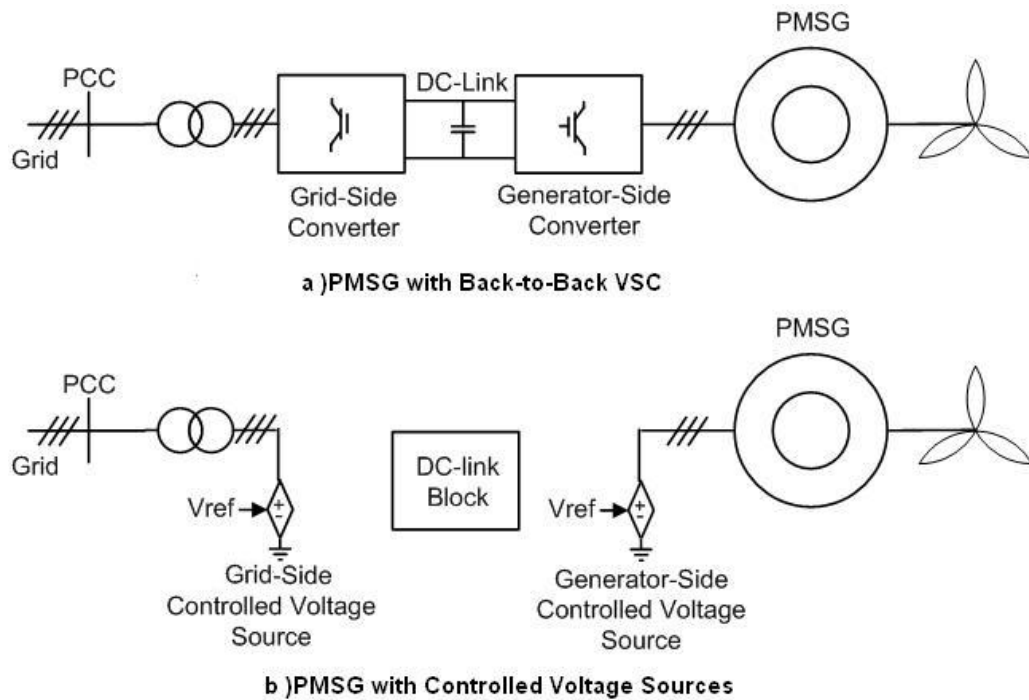


Figure 2.21 Converter Models of PMSG Type Wind Turbines

2.3.2.3 Generator Modeling

PMSG is a special type of synchronous machine with constant field. Since detailed explanation of synchronous machine equivalent circuit and equations are present in [20], the PMSG model is not investigated in detail. Thus a model of PMSG similar to the synchronous machine model explained in [20] will be constructed based on the following assumptions:

- Distributions of stator windings are sinusoidal,
- Magnetic hysteresis and saturation effects are negligible,
- Stator winding is symmetrical,
- Damping windings are not considered,
- Resistances are constant.

In order to apply vector control to a PMSG, according to above assumptions, the steady state equivalent circuit will be transformed into rotor (flux) oriented d - q equivalent circuit as shown in Figure 2.22.

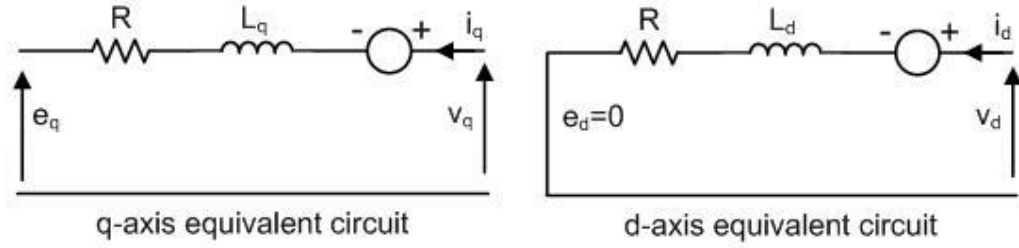


Figure 2.22 D-Q Equivalent Circuit of PMSG

The voltage equations of a synchronous machine in [20] can be transformed into d - q frame by using the rotor oriented reference frame and formulas in Appendix A as follows;

$$\begin{aligned} v_{sd} &= R_s i_{sd} - w \psi_{sq} + \frac{d\psi_{sd}}{dt} \\ v_{sq} &= R_s i_{sq} + w \psi_{sd} + \frac{d\psi_{sq}}{dt} \end{aligned} \quad (2.34)$$

The terms $w\psi_{ds}$ and $w\psi_{qs}$ are speed-voltage terms which appear as a result of the rotating reference frame rotating at angular velocity w [23]. The stator flux components are expressed in (2.35) where L_d and L_q are the stator inductances in the d - q reference frame.

$$\begin{aligned} \psi_{sd} &= L_d i_{sd} + \psi_{PM} \\ \psi_{sq} &= L_q i_{sq} \end{aligned} \quad (2.35)$$

Putting (2.35) into (2.34);

$$\begin{aligned} v_{sd} &= R_s i_{sd} + \frac{d\psi_{sd}}{dt} - \omega L_q i_{sq} \\ v_{sq} &= R_s i_{sq} + \frac{d\psi_{sq}}{dt} + \omega L_d i_{sd} + \psi_{PM} \end{aligned} \quad (2.36)$$

As the PMSG is assumed to be a round rotor machine, the electromagnetic torque can be expressed as:

$$T_e = \frac{3}{2} p \psi_{PM} i_{sq} \quad (2.37)$$

Then active and reactive power can be given by equation (2.38).

$$\begin{aligned} P_s &= \frac{3}{2} (v_{sd} i_{sd} + v_{sq} i_{sq}) \\ Q_s &= \frac{3}{2} (v_{sq} i_{sd} - v_{sd} i_{sq}) \end{aligned} \quad (2.38)$$

Different from DFIG, PMSG exchanges reactive power with the converter, as it is fully decoupled from the grid.

2.3.2.4 Grid-Side Converter Controller Modeling

As in DFIG, grid-side converter of PMSG is responsible for injection of reactive power to the grid and regulation of DC-link voltage. Since the converter model and the connection diagram of converter are same with DFIG, controller model of grid-side converter is same as DFIG grid-side converter. Then Figure 2.16 can be used for the vector control scheme [21].

2.3.2.5 Generator-Side Converter Controller Modeling

Similar to DFIG rotor-side converter, the main objective of the generator-side converter of PMSG is controlling the generator active and reactive power. However, generator-side converter is directly connected to the stator of the generator as in Figure 2.23 unlike DFIG.

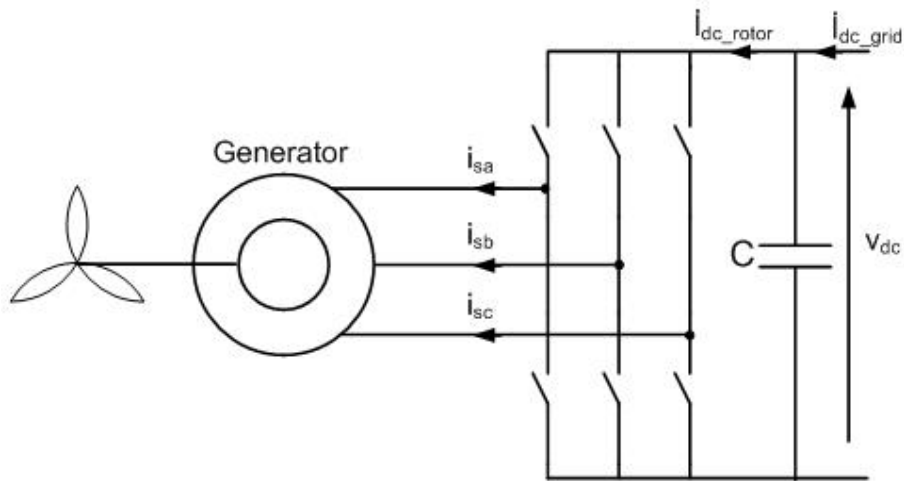


Figure 2.23 Connection Diagram of Generator Side Converter

Since the converter model is same with DFIG rotor side converter and Stator Flux Vector Orientation method is used, the control structure of the converter is similar to DFIG as given in (2.36). The control diagram of the generator-side converter is shown in Figure 2.24 [21]:

CHAPTER 3

GRID CODES AND FRT OVERVIEW

3.1 Introduction

In the introduction chapter, the importance of grid codes and grid connection issues of wind power were briefly introduced with the high wind power penetration in power system. Additionally, wind turbine technologies and wind power impacts on power system have also been described. In this chapter, the grid code requirements of the system and fault ride-through capabilities of different wind turbine technologies will be explained in detail.

3.2 Grid Codes Overview

Grid codes define the connection and operational requirements for all parties such as power plant owners, large consumers and ancillary service providers, connected to the transmission system. Original grid codes for the power plants were specified considering synchronous machines. However, wind turbines are based on different technologies which have significant impacts on the conventional transmission system [24]. TSOs have revised their grid codes to sustain reliable and stable power generation to the loads while enabling the large scale of wind power generation [6][7][8][9]. Although the requirements depend on the inherent characteristics of each transmission system, structural harmonization study of the grid codes has been intended to establish a generic common grid code format where the general layout and specifications, not the values, are fixed and agreed upon by all the TSOs, WPP developers, and wind turbine manufacturers [25]. Taking this line of thinking, WPPs,

regardless of any specific grid codes, must satisfy the common requirements. The most common requirements comprise:

- Active power control,
- Reactive power and voltage control,
- Frequency and voltage operating ranges,
- Fault ride through capability.

The given requirements and more detailed discussions have already been made in the literature [2][24][25] and [26]. Here, a brief review of the mentioned common requirements is included for the investigations performed in this thesis.

3.2.1 Active Power Control

Wind turbines have to participate dynamically in the grid operation control by regulating their active power output. Active power regulation in the grid codes include active power control modes, which limit the maximum active power, balance the active power output, and define the ramp rates in the upward or downward direction. Some examples of these control modes are given in Figure 3.1.

The control modes provide TSOs to manage wind turbines in a predictable way reducing the uncertainties caused by the wind. They would also be the supervisory tools to integrate wind turbines into existing transmission planning and market operations. Additionally, reserve power can be maintained through using these modes for the frequency control. Active power reference (from TSOs) update rate, start-up ramp rate, shut down ramp rate, and system protection functions are the additional requirements specified under the active power control title in the grid codes.

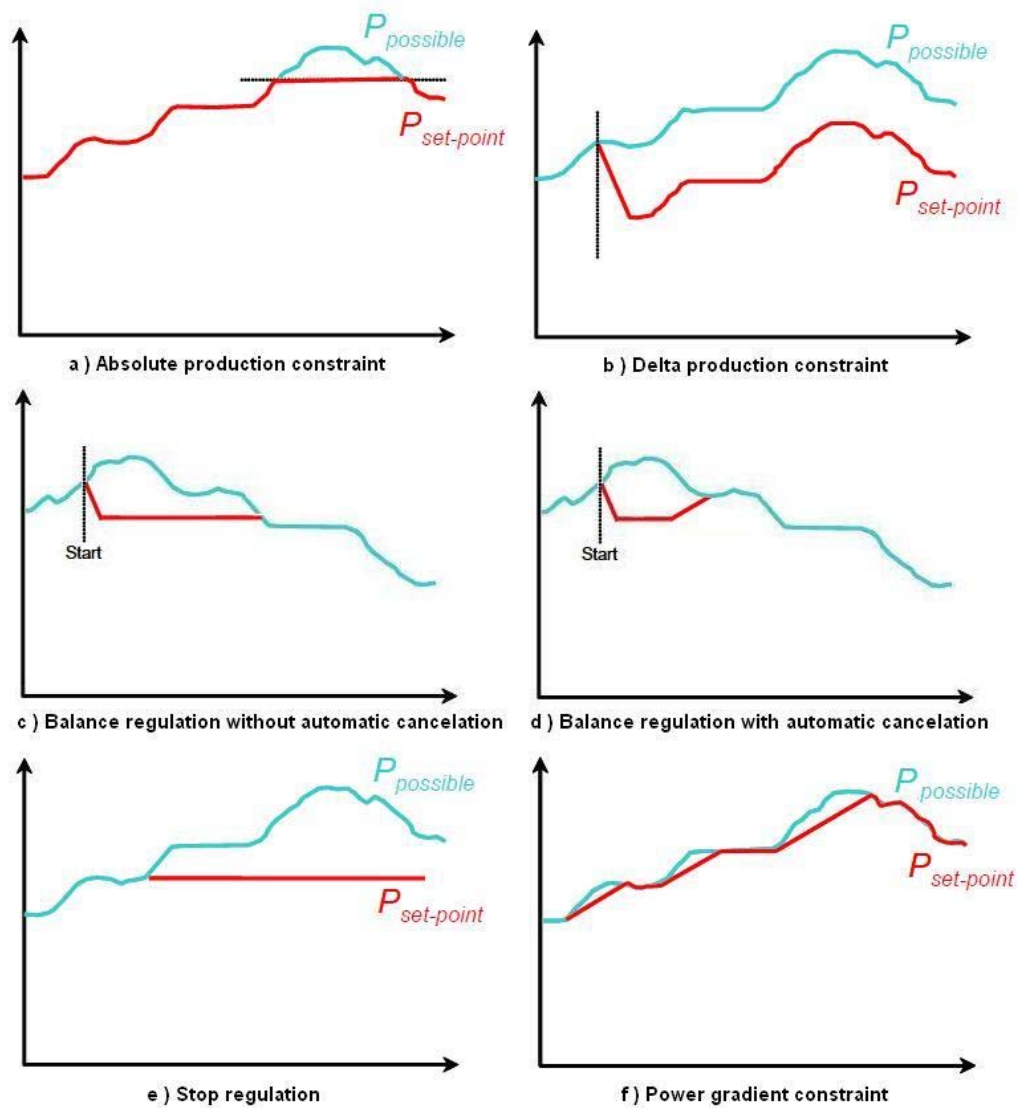


Figure 3.1 Active Power Control Requirements

3.2.2 Reactive Power and Voltage Control

Wind turbines have to regulate their reactive power output in response to the voltage deviations at the grid connection point and reactive power references sent by the

TSOs. The reactive power requirements depend on the grid connection point characteristics, which include short-circuit power of the connection point, X/R ratio, and wind power penetration level. For the grid operation, there are three different possibilities for reactive power references set by the TSO; reactive power, power factor and voltage references. Grid codes state these reactive power operating conditions, such as P/Q and V/Q curves depicted in Figure 3.2 and Figure 3.3 respectively. Additionally, the reactive power ramp rate, reactive power control and measurement accuracy, settling and rise times for reactive power change are specified in the grid codes.

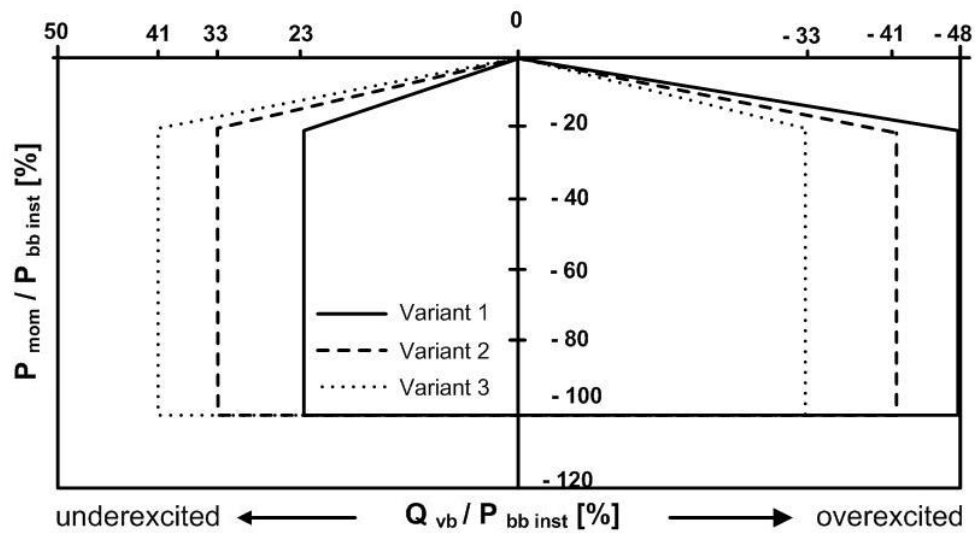


Figure 3.2 P-Q Dependencies of Three Variants [6]

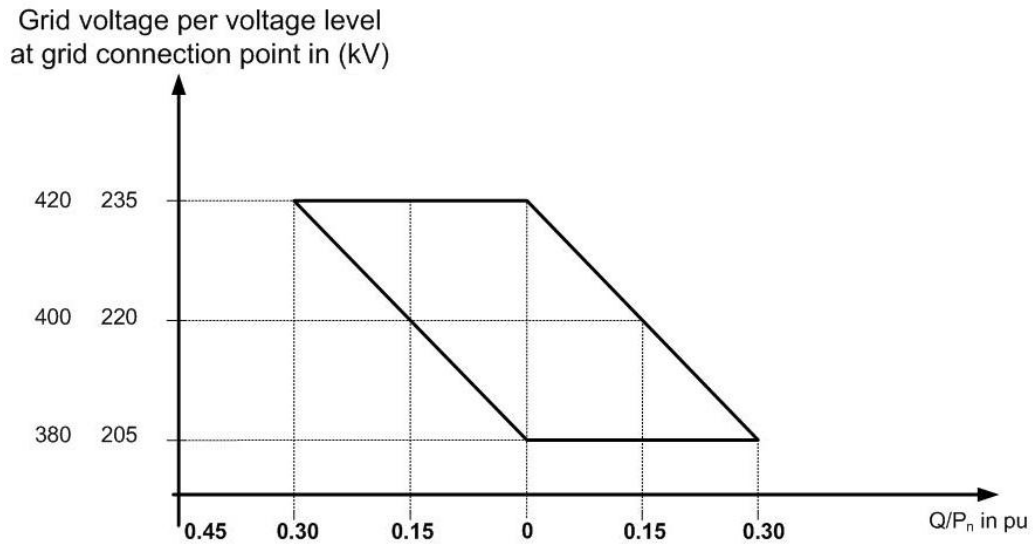


Figure 3.3 V-Q Dependency [9]

3.2.3 Frequency and Voltage Operating Ranges

Wind turbines must have the capability to operate within a range around the rated voltage and frequency values of the point of common coupling (PCC) to avoid instabilities due to the grid disturbances. Typically, this requirement can be described as the following frequency/voltage operation zones:

- Continuous operation in a limited range below and above the nominal point.
- Time limited operation with possible reduced output in extended ranges.
- Immediate disconnection.

In grid codes, the voltage-frequency operational range window is graphically represented in Figure 3.4. These ranges are relied on the characteristics of the transmission system. Figure 3.5 provides a comparison of the operating frequency limits in countries using 50 Hz.

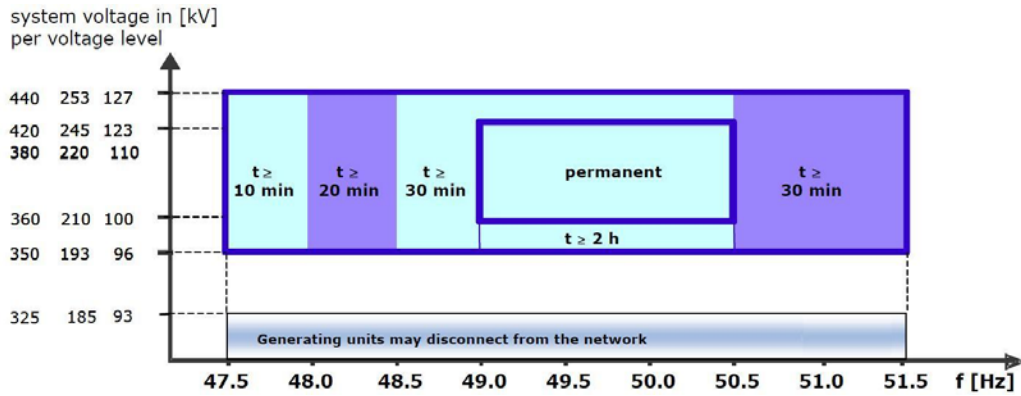


Figure 3.4 Voltage/Frequency Operating Ranges

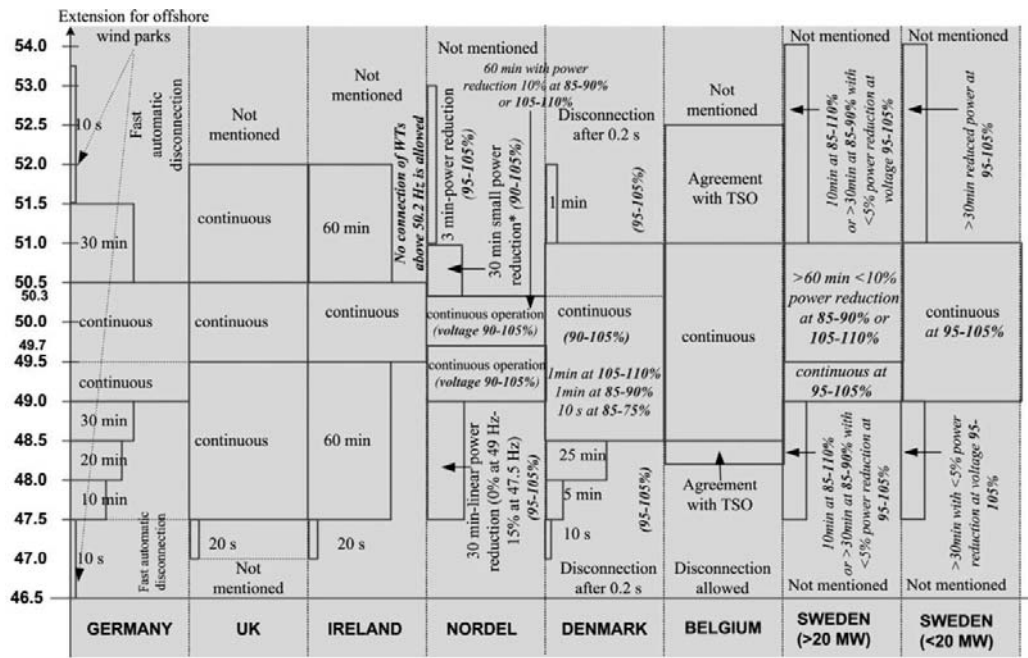


Figure 3.5 Comparison of the Operating Frequency Limits in European Countries

3.2.4 FRT Capability

During grid disturbances, voltage dips typically lead to WPP disconnections that will create even worse system conditions which can cause instability and even yield to blackouts. To avoid these problems, the grid codes require WPPs to continue operation even if the voltage dip reaches very low levels, support the voltage recovery by injecting reactive current and restore active power after the fault clearance with limited ramp values. All these features are defined as FRT capability of the wind turbine in the following way:

- FRT in terms of minimum and maximum voltage ride through (low and high VRT) and recovery slope for symmetrical and asymmetrical faults that WPPs must be able to withstand without disconnection from the grid,
- Active power and reactive power limitation during faults and recovery,
- Reactive current injection for voltage support during fault and recovery,
- Restoration of active power with limited ramp after fault clearance.

Generally in grid codes, Figure 3.6 describes the FRT as the limiting voltage curve at the grid connection point. The explanation of the shaded areas can be made as follows:

- In zone 1, 3-phase short circuits or symmetrical voltage drops because of the disturbances must not lead to instability or to a disconnection of the wind turbines from the power system.
- In zone 2, there are two options. The first option is that wind turbines have to stay connected to the grid during the fault. If wind turbines are not capable of satisfying the requirement, it is admitted to change the borderline by agreement with the TSO. In the second option, a short-time disconnection of the wind turbines from the power system is permitted by agreement with the

TSO, if the turbines become instable when passing through the fault or the generator protection becomes activated.

- In zone 3, a short-time interruption of the wind turbines from the grid is accepted. Moreover, the disconnection of the wind turbines through protection systems is admissible.

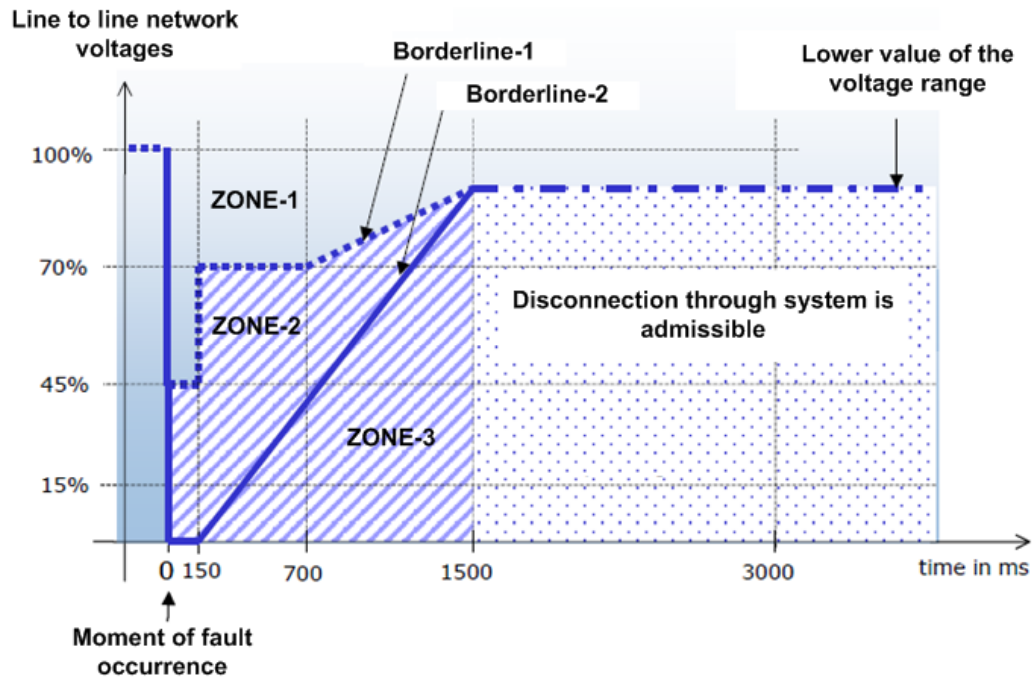


Figure 3.6 Limiting Voltage Curves at PCC

During a voltage drop, the wind turbines must support the grid voltage by means of injecting additional reactive current as defined in Figure 3.7. In addition to these figures, reactive current injection dead, rise, and settling time together with the post fault support time are specified correspondingly in the grid codes.

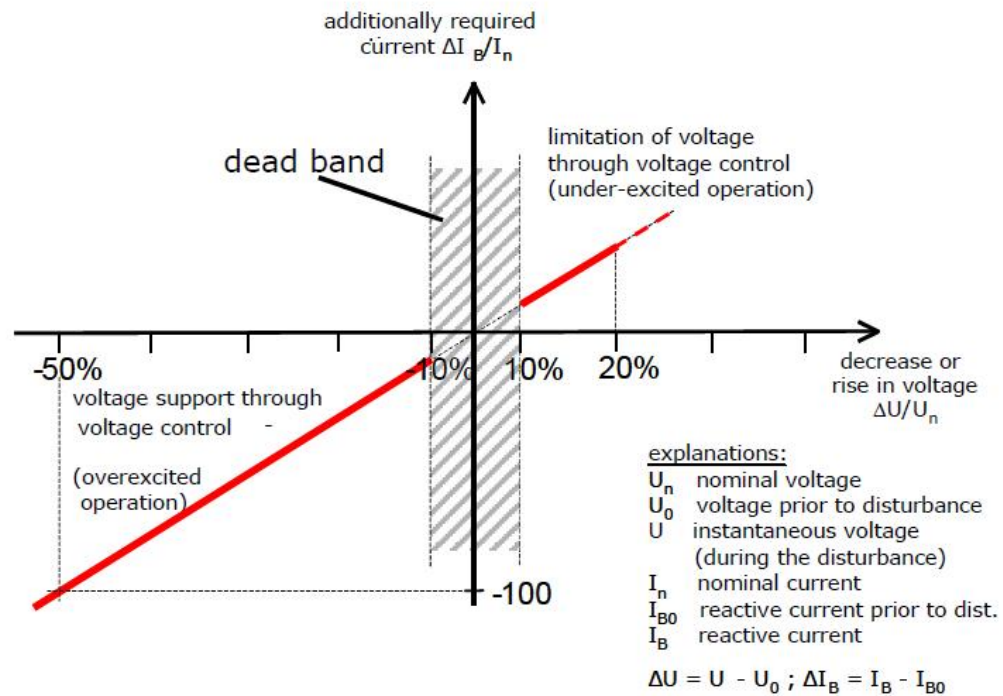


Figure 3.7 Principle of Voltage Support During a Grid Fault [6]

3.3 Turkish Grid Code Review

In Turkey, the technical requirements that wind power plants should meet are published on 24.09.2008 by EMRA. Up to that time the only criterion for wind power plants is about the capacity that can be connected to the grid from any point. That criterion was limiting the wind power plants' installed power to be connected to the grid from any point up to 5 % of the short circuit MVA of the related access point. The new part of the grid code about wind power plants published on 24.09.2008 is an annex [42] of the main grid code. It covers the three main characteristics of wind power plant to be met: FRT capability, voltage/reactive power response and frequency/active power response. Generally Annex 18, the annex of Turkish Grid Code about wind power plants, is very rigid in terms of the technical

specifications. It completely eliminates the first generation wind turbines, i.e. fixed speed wind turbines. In order to provide the requirements of Annex 18, any synchronous/asynchronous machine may be used with complicated power electronic systems. DFIG or PMSG typed wind turbines are the alternatives used recently. However, Annex 18 does not cover all the issues related to the wind power plants connected to a transmission system. Reactive power response speeds, high voltage ride through capability, power factor range and ramp rate are some of the points that questions arise by the manufacturers in the market. Moreover, the 5% limitation is an important obstacle for the investors in wind energy market. In most of the places where wind is available, the transmission grid is not strong enough. Even keeping the short circuit power limit same, technical requirements must be revised by the TSO.

3.4 FRT Overview

Not long ago, in case of a grid fault, wind turbines were just disconnected from the grid in order not to affect the grid. However, with the increased penetration of wind energy into power systems, such a disconnection of wind turbines could bring problems in the control of voltage and in a worst case, cause a system collapse. Thus, TSOs must revise and increase the connection requirements of wind turbines in grid codes as described in 3.2. As described in 3.2.4, FRT capability is a measure of whether wind turbine is able to remain grid-connected during grid faults or not [29].

According to literature, there are two major wind turbine categories according to their speed. These are fixed speed wind turbines and variable speed wind turbines. These wind turbines have different methods to provide FRT. Although fixed speed wind turbines are not in the scope of this thesis, their FRT topologies will also be explained briefly in this part of the thesis.

3.4.1 FRT Methods for Fixed Speed Wind Turbines

This type of wind turbines were widely used in the early 1990s and had the highest number of installations, due to their simple solution, where the generator is directly connected to the grid. Since the generator is directly coupled to the grid; the rotor has to rotate at almost same frequency with the grid. This type of wind turbine was attractive because of its advantages like being simple, cost effective, robust, reliable and well-proven. However it is not preferred nowadays, since direct coupling of generator with grid results in high interference, even it has been improved by soft-starters or other solutions. Synchronous Static Compensator (STATCOM), Pitch Control System, Braking Resistor (BR), and Superconducting Magnetic Energy Storage have recently been reported as stabilization (FRT) methods for fixed-speed wind generator systems [30].

1. STATCOM

The STATCOM is one of the FACTS devices that is connected to the system and is able to independently control the capacitive or inductive current from the AC bus voltage. The WPPs can be equipped with a STATCOM as seen in Figure 3.8, to deliver the reactive power required to accelerate the voltage restoration. The STATCOM can provide dynamic reactive power compensating and it leads to an increase in bus voltage during and after fault. This raises the electric torque generated by the fixed speed induction generator, prevents accelerating of the rotor, and finally extends the FRT capability and improves the system stability [31].

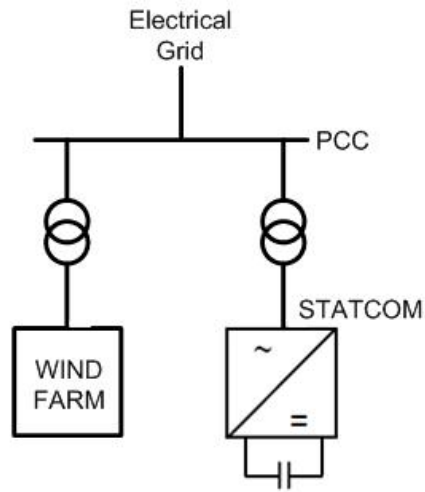


Figure 3.8 Connection of STATCOM at PCC

2. Pitch control system

Although the main purpose of the pitch control system is maintaining the output power of turbine at the rated value when the wind blows above the rated wind speed, it can also increase the transient stability of wind turbines by controlling the generator rotor speed. Fixed speed wind turbines, which are usually stall controlled [27], can be equipped with pitch drives that quickly increase the pitch angle when acceleration of the rotor is detected. This reduces the mechanical power and thus limits the reactive power consumption and the generator speed after the fault.

3. Dynamic Braking Resistor

Braking resistor has been known and used as a cost-effective measure for transient stability control of synchronous generators for a long time. For the fixed speed wind turbines, the braking resistor aims to provide the active power balance of the turbine during a fault. This is achieved by dynamically inserting a

resistor serially to the turbine connection as in Figure 3.9. By doing this, the voltage at the terminals of the generator is increased and therefore destabilization of electrical torque and power at the terminals during the fault period is quickly recovered. The switch of the braking resistor is in closed position under normal conditions, i.e., it is bypassed. Voltage dip below a selected set-point should trigger the switch and it is opened. Thus current can flow over the resistor during the fault period. When voltage recovers to above reference value, the switch would close and the circuit would be restored to its normal operating state. During the short insertion period, the energy would be dissipated in the resistor and this would raise resistors temperature. The resistor would be selected according to the limiting temperature of its resistive elements and the maximum energy dissipated during the insertion period [32].

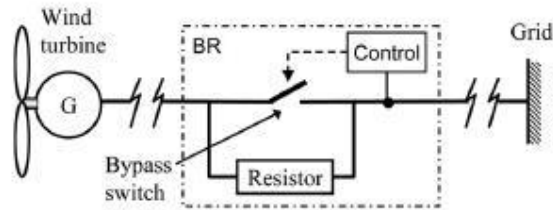


Figure 3.9 Schematic Arrangement of Braking Resistor [32]

4. Superconducting Magnetic Energy Storage

Superconducting magnetic energy storage is a large superconducting coil which has the capability of storing energy in the magnetic field generated by the current flowing in it. The real power can be absorbed by charging or released by discharging from the superconducting magnetic energy storage coil according to system power requirements. Since the losses in superconducting coil are negligible, the transfer of energy into the coil and out of the coil is very efficient and rapid. However, to remain superconducting, the coil must be cooled to cryogenic temperatures, which requires a fairly sophisticated refrigeration

subsystem [33]. A superconducting magnetic energy storage system can be interfaced with a power distribution system, as shown in Figure 3.10 and can provide reactive power to the bus voltage during and after the fault to accelerate the voltage restoration as in the case of STATCOM.

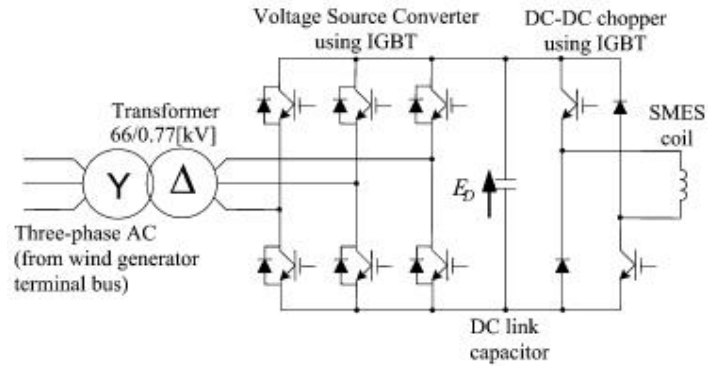


Figure 3.10 Basic Configuration of Superconducting Magnetic Energy Storage System [30]

Overall comparison of the fixed speed wind turbines FRT methods are listed in Figure 3.11. It can be inferred from this figure that, although the pitch control system is the cheapest solution, its response in transient stability enhancement as well as power fluctuation minimization is slow. As a consequence, the pitch control system cannot be considered as an effective solution. The braking resistor can be considered as a very simple and cost-effective solution from the viewpoint of transient stability enhancement of wind generator system. From the perspective of transient stability enhancement as well as voltage fluctuations minimization, STATCOM provides a cost-effective solution. Superconducting magnetic energy storage is the most expensive device; however, from the viewpoint of transient stability enhancement and minimization of power and voltage fluctuations, this system is the most effective solution [30].

Criteria	Stabilization methods			
	Pitch control	BR	STATCOM	SMES
Ability to control active and reactive powers	Can control only active power	Can consume only active power	Can control only reactive power	Can control both active and reactive powers
Transient stability enhancement during successful reclosing	Can stabilize the overall system, but its response is slower compared to BR, STATCOM, and SMES	Can stabilize the overall system and effective	Can stabilize the overall system and effective	Can stabilize the overall system and the most effective
Transient stability enhancement during unsuccessful reclosing	Can stabilize the wind generator but cannot stabilize the synchronous generator, that is, cannot stabilize the overall system	Can stabilize the overall system and effective	Can stabilize the overall system and effective	Can stabilize the overall system and the most effective
Minimization of power and voltage fluctuations	Able to minimize only power fluctuations	Not able to minimize power and voltage fluctuations	Able to minimize only voltage fluctuations	Able to minimize both power and voltage fluctuations
Controller complexity	More complex than BR	Simplest	More complex than pitch system	Most complex
Manufacturing cost	Cheapest	Costlier than pitch control	Costlier than BR	Most expensive

Figure 3.11 Overall Comparison of Fixed Speed Wind Turbines FRT Methods [30]

3.4.2 FRT Methods for Variable Speed Wind Turbines

VSWT has become the common installed wind turbine type among others in recent years. They were built up to increase the aerodynamic efficiency in various ranges of wind speeds. Their electrical system is more complicated with respect to the fixed-speed turbines. They are typically equipped with an induction or synchronous generator and connected to the grid through back-to-back converters. Generator speed was controlled by back-to-back converters; that is, the fluctuations in the output power caused by wind variations are absorbed mainly by changes in the generator speed. Higher amount of energy capture, better power quality and less mechanical stress on the wind turbines are considered as the major advantages of VSWTs. On the other hand, losses in semi-conductors, use of more components and increased cost of equipment are major disadvantages of these types of wind turbines [18]. There are two VSWTs types which are DFIG and PMSG type wind turbines.

3.4.2.1 FRT Methods for DFIG Wind Turbines

In the DFIG type wind turbines, the rotor of induction generator is wound and has a slip ring. The rotor is connected to the grid through two back-to-back converters via slip ring, where stator is directly coupled to the grid. Power is controlled by using the pitch system and also by control of the back-to-back converters. This type is widely used today since; it provides high efficiency with its variable speed operation, interference with grid is reduced as the turbine is decoupled from the grid, and it is more cost-effective, since its back-to-back converter has partial rating of wind turbine rated power.

In response to grid faults, a sharp voltage dip at the generator terminals is detected and may sustain longer than the fault duration. The DFIG stator currents will dramatically increase and exceed their rated values. Consequently, larger rotor currents will be observed pushing the dc link voltage to higher values and might lead to converter damage. Furthermore, the electromagnetic torque will fluctuate which may cause a mechanical stress on the drive train system of the wind turbine. As a result, the DFIG protection will disconnect the wind generator from the grid.

The implemented FRT methods for DFIG should ensure the following tasks [34]:

- Protect the switches of the converters against over-current and over-voltage stress and the DC-link capacitor against over-voltage.
- Satisfy the grid code requirements which are reactive current injection during grid fault and active power support after clearing the fault.
- Optimize the control techniques and the hardware added to the generator.

There are several methods which will be described below to fulfill these tasks.

1. Active Crowbar

Crowbar is a device which is placed between rotor-side converter and generator rotor terminals to protect the converter system as shown in Figure 3.12. When there is high voltage in the DC-link, the rotor circuit is short circuited by the crowbar in order to prevent damaging of the converter system. While the crowbar is active, the rotor side converter is disconnected and there is no control on the generator. The crowbar thyristors are substituted with controllable semiconductor switches to deactivate the crowbar as fast as possible to regain control on the machine. When the crowbar is deactivated and the converter regains control, high current transients may take place and sometimes the crowbar is reactivated [35].

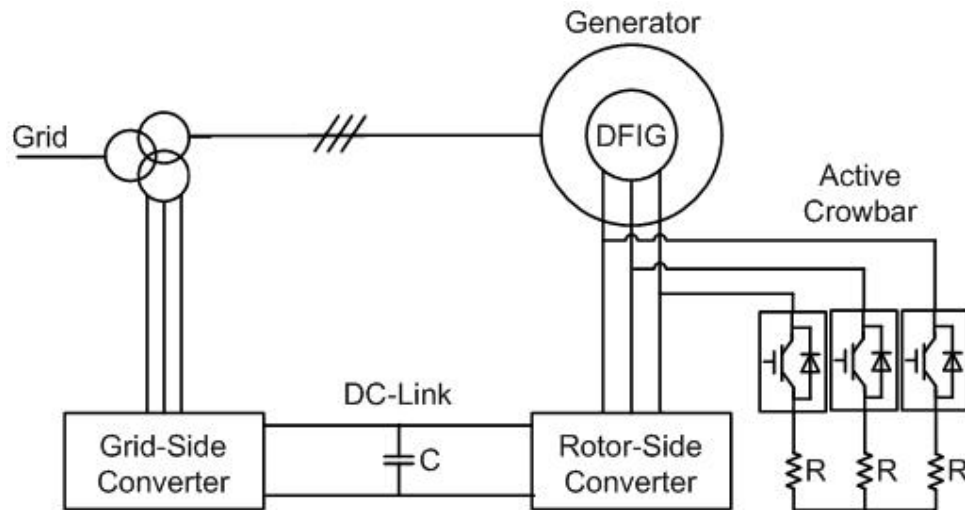


Figure 3.12 Schematic of a Crowbar System

2. Series Anti-parallel Thyristors

In order to provide a quick disconnection of the generator from the grid during a grid disturbance, anti-parallel thyristors can be inserted in series with the stator

terminals of the generator as shown in Figure 3.13. By decoupling the stator from the grid, the flux oscillation will also be interrupted; hence it is possible to re-magnetize the DFIG quickly through the converter system. When the grid voltage recovers, high transient currents occur in the stator terminals. Anti-parallel thyristors are used to control these high transient currents by increasing the stator voltage in a controlled manner. Since the thyristors are closed during normal operation of the wind turbine, the efficiency decreases due to the conduction losses of the thyristors. This issue could be avoided by bypassing the thyristors with commutators. However, the switching time of the commutators may be too slow to respond fast enough to a voltage dip during the grid disturbances [36].

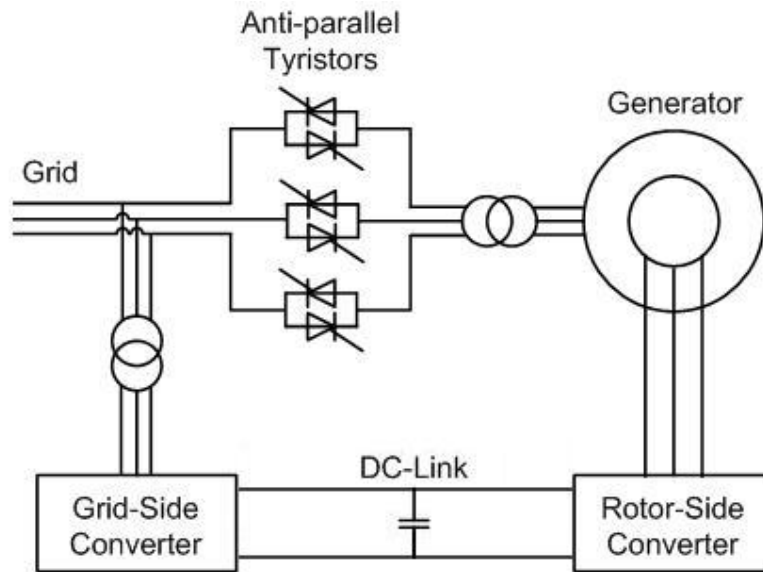


Figure 3.13 Schematic of Anti-parallel Thyristor System

3. Transient Control Mode

In this method, reconfiguration of rotor side converter and switching of crowbar circuit simultaneously with appropriate transient control mode are main

procedures. Transient control mode protects the DC-link capacitor and power converters against high voltages, limits the rotor short-circuits currents and supports the voltage recovery at PCC during the fault. Once the fault is detected, the bypass crowbar is shunted by closing switch S_1 in Figure 3.14. By the crowbar connection, the current peaks will be reduced and rapidly damped. The rotor-side converter will be separated from the rotor terminals by the action of the static transfer switch S_2 and connected in parallel to the grid-side converter. Thus, it is completely isolated from the generator rotor terminals. By changing the connection scheme to be on parallel with the grid-side converter gives a credit rating, employed for injecting reactive current during the fault and guarantee healthy operation [34].

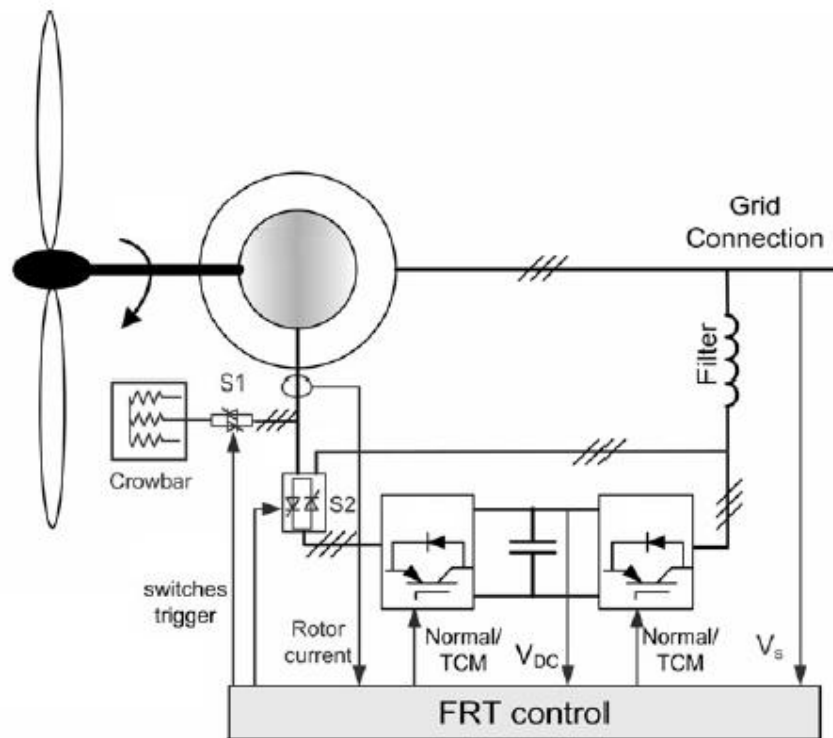


Figure 3.14 Schematic of Transient Control Mode System [34]

4. Active Crowbar and Pitch Control

In this FRT method, crowbar protection and pitch control techniques operate simultaneously to contribute the recovery of the PCC voltage without any wind turbine disconnection after a grid fault. After occurrence of a grid fault in the power system, the following control steps are performed [19]:

- The excess of either the rotor current limit or the DC-link voltage limit will activate the protection to short-circuit the generator rotor and deactivate the rotor-side converter, while the induction generator and the grid-side converter are kept in connection with the grid.
- Regulating the pitch angle reduces the aerodynamic power output of the turbine. This helps to decrease the generator speed and re-establish the voltage at connection point of the turbine.
- When the voltage at the connection point of the turbine is recovered after the clearance of the fault, the rotor-side converter is return its work and the DFIG restores its normal operation.

3.4.2.2 FRT Methods for Full Scale Wind Turbines

FSWTs are the state-of-the-art type wind turbines, since the generator is completely decoupled from the grid with two back-to-back converters and whole power is transferred through those controlled converters. One converter is used on the generator side and the other side is on the grid side. FSWTs can employ both induction (asynchronous) and synchronous type generators, where synchronous generators can be separately excited (conventional) or permanent magnet type. Generally multi-pole permanent magnet synchronous generators are employed, which remove the need for a gearbox between rotor and generator. Since this type of wind turbine has many advantages like mechanical reliability, better efficiency, reduced risk of possible drive-train oscillations, this thesis will deal with PMSG type FSWTs.

The full converter type wind turbines have the most flexible technology from an FRT point of view, as the reactive and active power output can be controlled using the converters. When a disturbance happens in the power system, a resulting voltage dip arises at the connection terminals of the wind turbine. The maximum active power that the turbine can deliver is reduced in proportion to the terminal voltage reduction. The output power of the inverting converter is quickly reduced by its controller. However, the input power to the generator which is extracted from the turbine blades cannot be reduced quickly. Therefore there is an energy imbalance in the wind turbine compared to its operation at pre-fault terminal voltage. The excess power from the generator that cannot be delivered to the grid must flow into the dc capacitor. This causes the dc link voltage to rise uncontrollably. An excessive dc link voltage will damage both the rectifying and inverting converters, so a protective action must be taken.

The wind turbine shows some promising FRT behavior, but the dc-link voltage rise is unacceptable [37]. Hence, some of the several methods that enhance the FRT capability of FSWT will be explained below.

1. Pitch Control

The most obvious attempt to mitigate the energy imbalance is to pitch the turbine blades to reduce the captured wind power. This will mean that the energy imbalance decreases during the voltage dip. Therefore when abnormal voltage is measured at the ac terminal of the inverting converter, the pitch controller is requested to increase the pitch angle of the blades to reduce the energy imbalance. The speed at which the blades can be pitched is important in this emergency operation state. The pitch controller is ordered to increase the pitch angle to the value that restores the energy balance in the system. As the blade pitch angle increases, the active power reference value for the generator-side converter is decreased in accordance with the decrease in wind power. This is an

attempt to maintain the torque balance in the drive train. As a result, the dc link voltage rise problem is reduced but not satisfactorily eliminated. Therefore including emergency pitching action alone will not solve the FRT problem totally [37].

2. Capacitor Sizing

Another way of dealing with the excess energy during a voltage dip is to store it in a larger capacitance, thus reducing the dc-link voltage rise. The excess energy stored in the capacitor can be expressed as a power integral as in (3.1) where P_C is the power of capacitor, C is the capacitance and V is the DC-link voltage. The required capacitor size will increase if the voltage dip duration increases, therefore this idea is obviously not practical [37].

$$\int P_C dt = \frac{1}{2} C (V^2 - V_0^2) \quad (3.1)$$

3. Changing Control Mechanism

In the general control strategy of FSWT, the generator-side converter controls the active power and the stator voltage, whereas the grid-side converter regulates the DC-link voltage and the reactive power output of the turbine as shown in Figure 3.15-a. By changing this control strategy as in Figure 3.15-b, the task of the generator-side converter is to control the DC-link voltage and to control the stator voltage around its rated value. The grid-side converter controls the active and reactive power output of the turbine in the grid voltage reference frame independently. Note that in this control strategy, the control functions of the converter are slightly reversed when compared with those in the general strategy. Because of the constant stator voltage, the risk of converter overvoltage at high speeds is eliminated. The generator and the power converter can thus always operate at the rated voltage they are designed and optimized. A disadvantage of

this strategy is that it demands variable reactive power from the generator, and thus an increased converter rating is needed. In other words, besides the reactive power necessary for the grid support, the converter also has to provide reactive power to the generator [38].

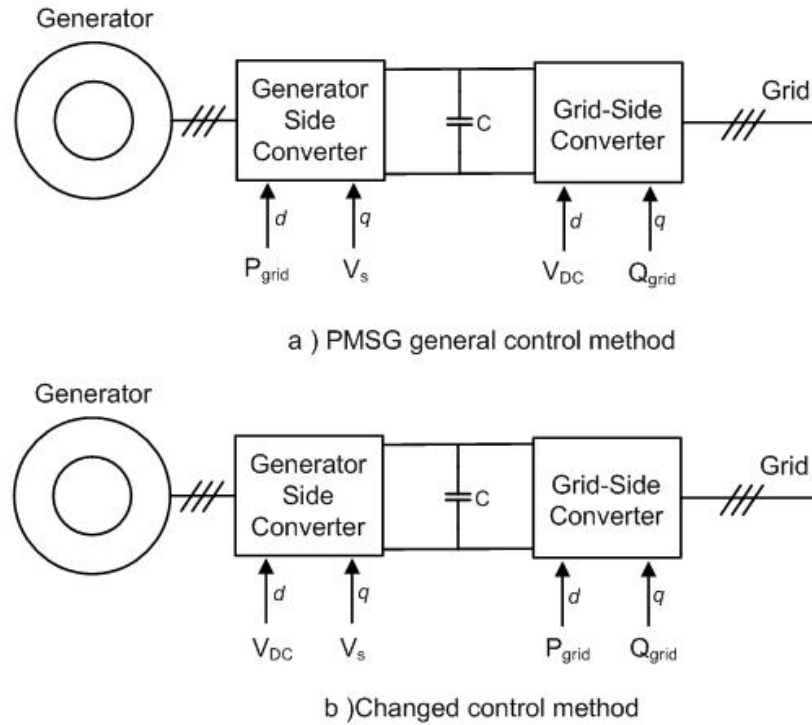


Figure 3.15 Control Strategies for PMSG Type Wind Turbines [38]

4. Braking Resistor

Instead of storing the excess energy in the dc-link circuit, the idea of dissipating this energy is investigated. This means that a resistor is inserted in the dc circuit to dissipate the excess energy and restore the balance. In variable speed drives, this braking resistor balances output torque variations and prevents the dc-link voltage from rising excessively. This resistor is typically controlled using a

power electronic switch. In Figure 3.16, the position of braking resistor and the controlling switch are shown. The switch is triggered when the DC-link voltage increases over a critical threshold. The power imbalance is thus reduced by burning the surplus power in the resistance. The power dissipation of the resistor is controlled by controlling the duty cycle of the switch S . As a result, the capacitor discharges, the DC-link voltage decreases below the threshold and the resistance is switched off. The control scheme for the braking resistor in a wind turbine must be carefully designed to avoid large transients and resistor/switch overheating [37].

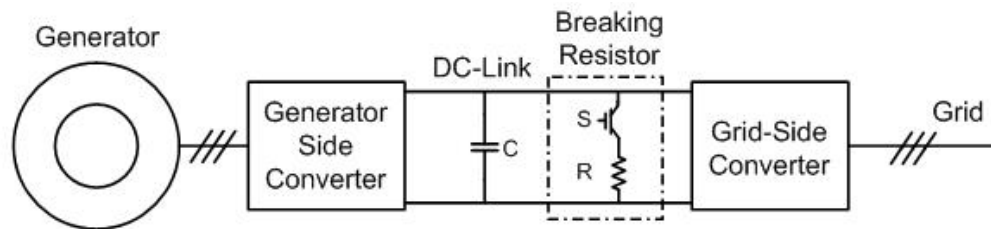


Figure 3.16 Positioning of Braking Resistor in PMSG Type Wind Turbines

CHAPTER 4

SIMULATION RESULTS

4.1 Introduction

In this chapter, the FRT capability of wind farms with variable speed wind turbines connected to the grid is studied. First, model aggregation technique and power system model are prepared. Then, using the mathematical models explained in Chapter 2, a 30 MW wind power plant consisting of VSWTs with DFIG and a 30 MW wind power plant consisting of VSWTs with PMSG are implemented in PSCAD/EMTDC simulation program as described in Appendix B and Appendix C, respectively. Then, by integrating these turbine models into the 4-bus power system model, performances of the turbines and interaction with the grid under 3-phase short circuit faults are investigated. After that, the comparisons of variable speed wind turbines according to simulation results are done. Finally, an additional assessment for the integration of WPPs connected to the grid is done.

4.2 Model Aggregation

Grid connected wind farms consist of large number of small size wind turbines as opposed to conventional power plants. Hence, calculation time of simulations increases significantly if every wind turbine is represented in detail individually. To overcome this, model aggregation can be used which reduces the complexity and simulation time without compromising the accuracy of the simulation results with respect to related analysis. In [44], [45] and [46], the model aggregation techniques of wind turbines are explained in detail. In [45], it is proposed to use one equivalent model for converters, controllers and electrical part of the generators. The generator

inertia, aerodynamics and pitch controllers are not parts of the aggregation. Moreover, since the simulation time is short in transient stability investigations, wind speed at each wind turbine is assumed constant and one equivalent wind speed model is used. Rotor model can be used without any change since aerodynamics is not a part of the aggregation. Besides, one-equivalent pitch angle controller is sufficient to represent pitch control in the aggregated model and this is same with the not-aggregated case. Generators and the back-to-back converters are scaled to the size of the WPP by multiplying their rated powers by the number of wind turbines in the plant. The generator parameters do not change since they are given in per unit values. The filter parameters are divided by the number of wind turbines to supply new rated output current of the converter with the same voltage ratings. Finally, the control parameters, PI parameters, are arranged to new settings to provide new rated current output of the controllers. Moreover, the limits of the PI control blocks must be increased by multiplying the number of aggregated wind turbine numbers.

4.3 Power System Modeling

The scope of the study focuses on the FRT capabilities of wind turbines and wind farms; hence it is not necessary to model the entire transmission system. The equivalent system model in terms of Thevenin equivalent circuit (short circuit power of the bus) is used in this study. As the National Power Quality (NPQ) real time monitoring devices had been installed to obtain real data, the equivalent model is focused on Bares substation as seen in studied region in Figure 4.1. While building the system equivalent diagram, three neighbor 154 kV substations located near Bares Substation; namely Göbel, Bandırma2, Bandırma3, are used. This 4-bus equivalent system includes Bares Substation at one end and, Göbel and Bandırma2 Substations at the other ends. Modeling the grid beyond these two substations will not make the fault simulation results deviate much from the base 4-bus equivalent model.

As seen from Table 4.1, since the line lengths are shorter than 80 km, series R-L model is used for transmission lines. Considering the typical 154 kV tower-line design of TEIAS, the line parameters are as follows;

Table 4.1 154 kV Line Parameters of the Equivalent Circuit

From-To	Line Length& Cross Section	Line Resistance (Ω /phase)	Line Inductance (H/phase)
Bares-Bandırma3	8 km-477 MCM	1.06816	0.010924
Bandırma3-Bandırma2	28 km-477 MCM	3.7384	0.03822
Bandırma3-Göbel	38 km-477 MCM	5.0738	0.05188

The grid is represented at two substations; Göbel and Bandırma2. The short circuit MVAs (SCMVA) of these substations are calculated and published in [50] and used for determination of equivalent resistances and reactance of the Thevenin equivalent circuit behind Göbel and Bandırma2. The system loads at these substations are modeled after the 154/34.5 kV transformers. Values representing the loads and transformers are based on the TEIAS standards and records.

In simulations, three different types of disturbances are performed. First, at point “Fault at PCC” in Figure 4.2 which is the PCC of the WPP, a 3-phase to ground fault is created for duration of 150 milliseconds for zero voltage ride-through (ZVRT) simulations of the WPP. Then, at point “Fault Position-1” and “Fault Position-2” in Figure 4.2, a 3-phase to ground fault is created for duration of 150 milliseconds for low voltage ride-through (LVRT) simulations of the WPP. Finally at point “Fault Position-1” and “Fault Position-2” in Figure 4.2, a 3-phase to ground fault is created for duration of 150 milliseconds and the faulted line is opened for duration of 1 second.

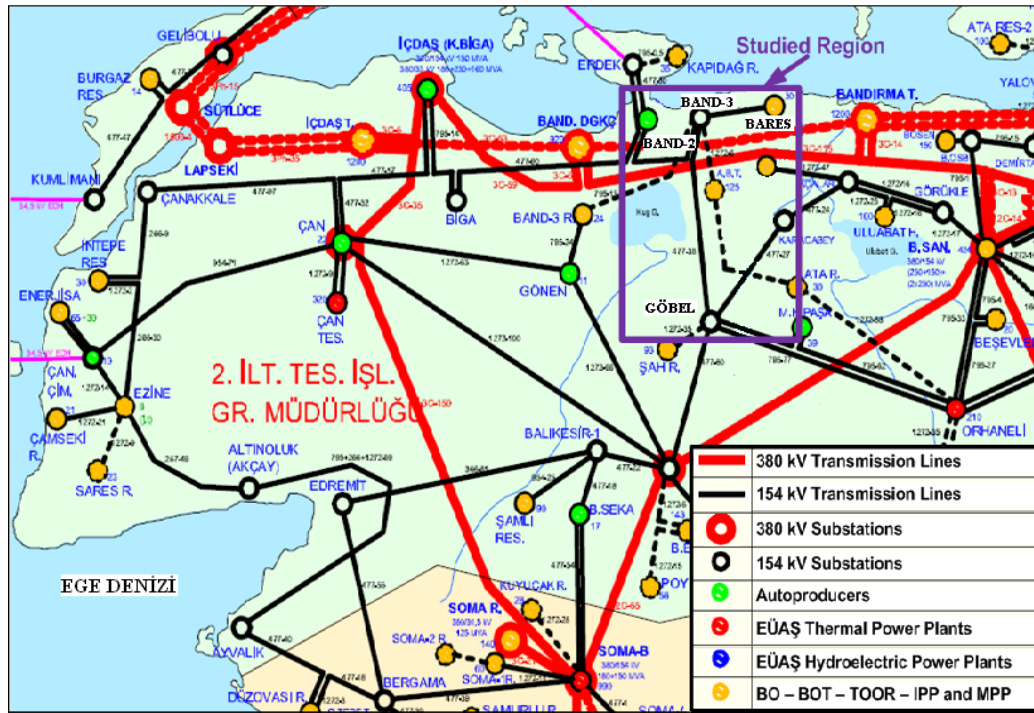


Figure 4.1 Single Line Diagram of the Studied Region

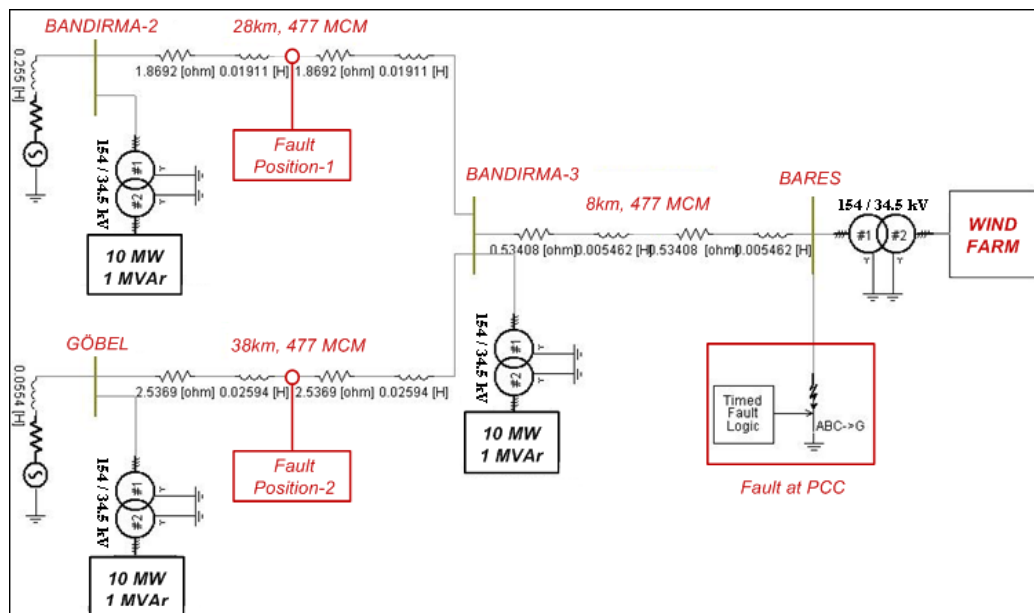


Figure 4.2 Power System Model

4.4 Wind Farm Model based on Wind Turbines with DFIG

The computer simulation model has been constructed using the library of PSCAD/EMTDC and implemented blocks based on theoretical background and operating principles introduced in Chapter 2 in PSCAD/EMTDC software. To validate the implemented model and benchmark the simulation results afterward, wind turbine used in [19] is modeled. The generator parameters used in the model are given in Table 4.2.

Table 4.2 DFIG parameters used in PSCAD/EMTDC model

Rated power	2 [MVA]
Rated voltage(L-L)	0.69 [kV]
Base angular frequency	314.16 [rad/s]
Stator/Rotor turns ratio	0.4333
Angular moment of inertia	1.99 [s]
Mechanical damping	0.02 [pu]
Stator resistance	0.0175 [pu]
Rotor resistance	0.019 [pu]
Stator leakage inductance	0.2571 [pu]
Rotor leakage inductance	0.295 [pu]
Mutual inductance	6.921 [pu]

Moreover, other parameters used in this model are given in Table 4.3;

Table 4.3 Other Parameters Used in Wind turbine with DFIG Model

Capacitor in the DC-Link	0.03 [F]
DC-Link Voltage	0.8 [kV]
Filter resistance	0.0084 [Ω]
Filter inductance	0.0004 [H]
Gearbox ratio of the turbine	100

Considering the parameters given in Table 4.2 and Table 4.3, a 2 MVA wind turbine with DFIG which consists of a wind speed block, a pitch system block, a turbine block, a generator block, rotor side and grid side converter controllers and a converter block is modeled in PSCAD/EMTDC. The simulation time step is chosen as 20 μ sec, which is a feasible value since it is smaller than electrical time constants of the model and the control time constants. Smaller time steps are not required, since the converters are modeled as controlled voltage sources and power electronic switches are not implemented. In addition to time step, duration of the simulation runtime is set to 15 seconds, which is enough for models to establish their steady state conditions. Larger settings will take longer simulation times which are not desired. Furthermore, a number of simulations have been run in order to set control parameters (PI parameters) using Ziggler-Nichols Method [47] in various grid and wind conditions. However, the control parameters found from the result of simulations are different for each condition. Thus, the control parameters have been optimized to obtain a satisfactory result for all grid and wind conditions. After completing 2 MVA wind turbine modeling, it is aggregated to 30 MVA based on the assumptions and technique mentioned in Section 4.2. The complete DFIG based wind turbine model including wind turbine block, turbine block, generator block, rotor side and grid side converter controllers and converters block are described in detail in Appendix B.

The steady state and transient performances of the model are investigated via the simulations and validation of this model is performed by comparing the consistency of simulation results with the references [18], [19] and [48].

The rest of this section, firstly, the performance of DFIG type wind turbine under normal operating conditions is investigated. Then, FRT capability of the turbine under grid disturbances before and after the suggested FRT method is discussed.

4.4.1 Performance of DFIG type Wind Turbines under Normal Operating Conditions

Before implementing the FRT analysis, a set of simulations is performed in order to show the performance of modeled DFIG type wind turbine under normal operating conditions. By varying the wind speed including gust and ramp components, the response of the pitch system, generator speed, and active/reactive power output of the converters are observed in Figure 4.3. As seen from Figure 4.3, the mean value of the wind speed is approximately 12 *m/s* and has a small turbulence, the gust component of wind speed is started at 40th second and continues for 20 seconds and the ramp component is started at 80th second and continues for 20 seconds.

As described in pitch model section, below the rated wind speed (about 12 *m/s*), the converter seeks to maximize the turbine output power and the pitch system does not respond as shown in blade angle in Figure 4.3. However, if wind speed exceeds this rated wind speed, pitch system turn the blades to limit the output power to the rated power of the turbine. Since whole power output of the turbine is delivered to the grid in normal operating condition, the DC-link voltage is almost stable with the varying wind speed. As illustrated in Figure 4.3, when the generator speed is greater than synchronous speed (super-synchronous mode), some of the air-gap power which is proportional to slip flows from the rotor to the grid through the converters. On the contrary, when the generator speed is slower than synchronous speed (sub-synchronous mode), some of the air-gap power is drawn from the grid to the rotor by the converter system. Also, generator speed change with varying wind speed but the pitch system limits it in the case of high wind speeds. Since the output power of the turbine is proportional to the cube of the wind speed, it dramatically decreases at low wind speeds. On the other hand, at high wind speeds, pitch system limits the output power to its rated power as seen in Figure 4.3. Moreover, both stator and rotor side reactive power output of the turbine are kept almost zero by the converters whose set points are sent by the converter controllers.

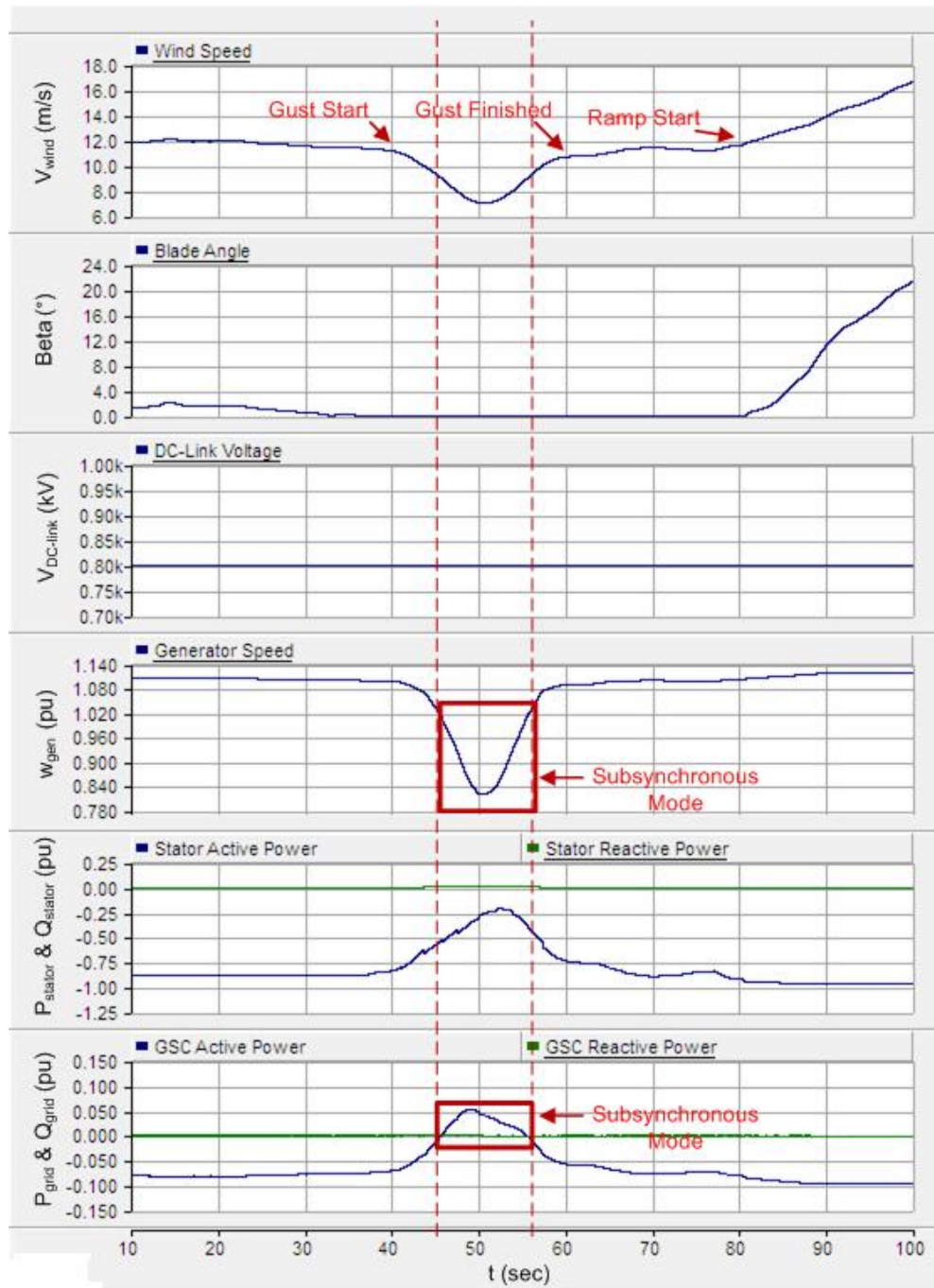


Figure 4.3 Performance of DFIG type Wind Turbine under Normal Operating Condition with Varying Wind Speed

4.4.2 Performance of DFIG type Wind Turbines under Grid Disturbances

In this section, the performance of DFIG type wind turbine under grid disturbances without a necessary FRT method is discussed. To represent the worst case scenario simulations, DFIG is assumed to operate at rated power and a three-phase fault is performed at the PCC, i.e., “Fault at PCC” position in Figure 4.2 . Due to this grid fault, a voltage drop occurs at the stator terminals of the DFIG, while stator and rotor fluxes also decrease. This in turn leads to corresponding reductions of the electromagnetic torque and active power of the generator as seen in Figure 4.4. As the stator flux decreases, the magnetization, stored in the magnetic field, has to be released over the stator. Due to these changing fluxes and voltages in the generator, high transient currents pass over the stator and rotor windings. In order to prevent these high currents, the rotor-side converter controller increases the rotor voltage. Thus, the power flow increase from the rotor to the DC-link. The grid-side converter however cannot deliver this power to the grid because of the low stator voltage and this surplus power goes into the DC-link capacitor. So, the DC-link voltage immediately exceeds the limits, approximately 25 % above its rated value. As a result, both the rotor current and the DC-link voltage reach very high transient values, which may damage the power electronics in the converter or the DC-link capacitor. Thus, the converter protection is activated which leads the tripping of turbine. Moreover, because of the difference between the aero-dynamical power and electrical power of the turbine, the generator can reach high speeds which will lead to tripping of the turbine. When the fault is cleared, the stator voltage is restored which leads to an increase in the electromagnetic torque and active power. Since the grid voltage and the flux increase, the demagnetized stator and rotor are against this change in flux which again leads to the rotor and the stator current transients. Thus, a turbine without any FRT method will trip under grid disturbance and cannot satisfy the grid code requirements determined by the TSOs.

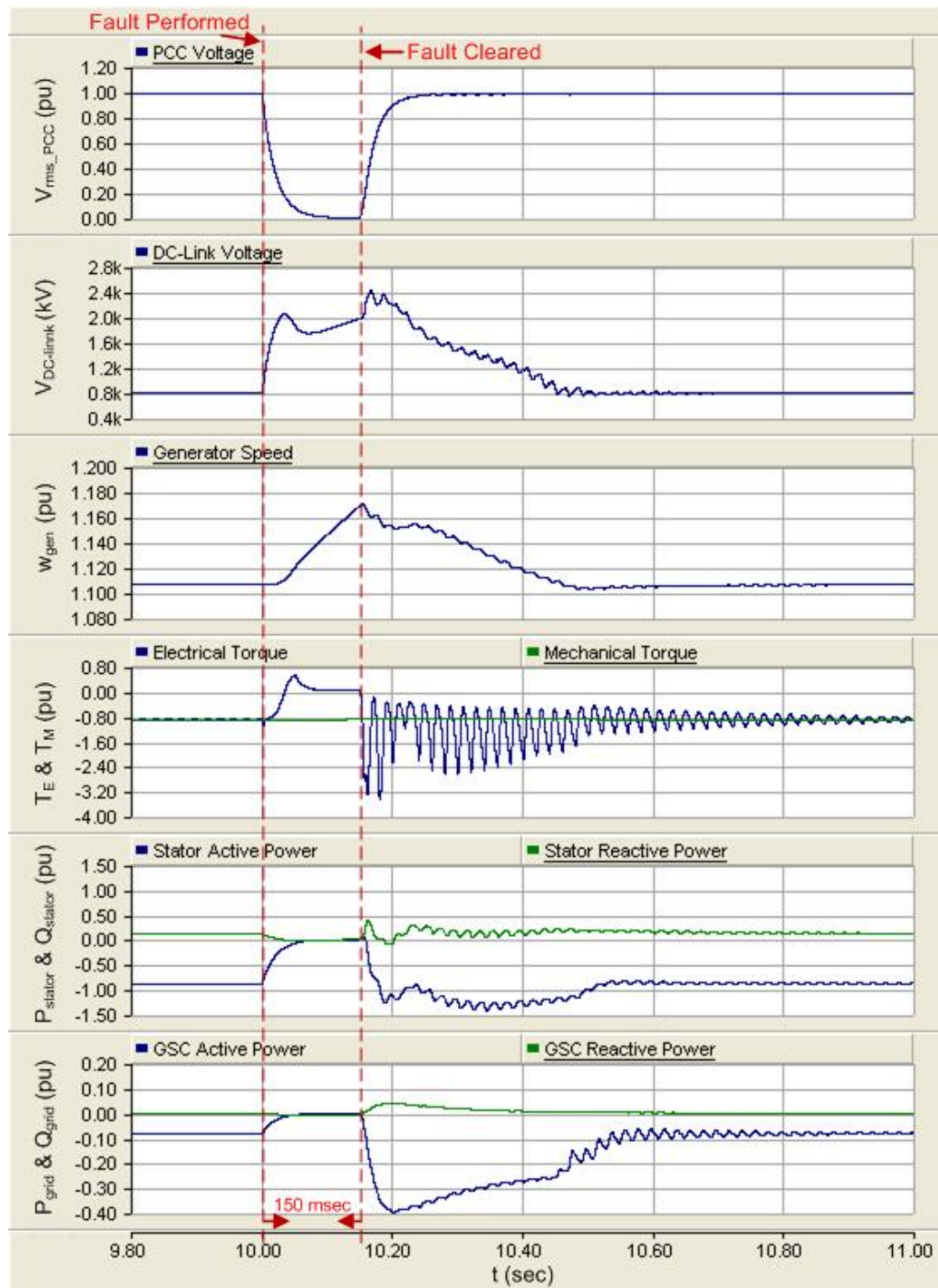


Figure 4.4 Simulation Results of DFIG Type Wind Turbine for a 3-Phase to Ground Fault at PCC for Duration of 150 ms

4.4.3 Suggested Method to Improve FRT Capability of DFIG type Wind Turbine

In this section, implementation of a control method, which enables the DFIG wind turbine for FRT and provides reactive power supply for voltage recovery during grid faults are presented. The method is implemented by a combined control mechanism of the crowbar, the pitch system and the grid-side converter.

As described in Section 4.4.2, high rotor currents and DC-link voltages arise during grid faults which constitute damaging risks for the rotor side converter. Additionally, generator can reach unacceptable speeds. To overcome these problems, the active crowbar method described in Section 3.4.2.1 is used. By the active crowbar method, the rotor of the generator is short circuited via external resistances (crowbars) by power electronic switches when there are high rotor currents or when the DC-link voltage exceeds the pre-specified limit. The crowbar protects the converter system and supports FRT capability of the turbine, however during crowbar coupling, the rotor-side converter is disabled and the generator's controllability is temporarily lost. In other words, DFIG behaves as a conventional SCIG with an increased rotor resistance. This crowbar resistance improves FRT capability by reducing the reactive power demand of the DFIG during the grid fault as seen in Figure 4.5. However this resistance value must carefully be selected, because the small resistance values cause higher current and torque transient peaks in the fault incident. On the other hand, the high crowbar resistance can however imply a risk of excessive rotor current, reactive power and torque transients when the crowbar is removed.

The crowbar coupling time is another important aspect during the active crowbar design, since the crowbar must be decoupled as fast as possible in order to regain the generator's controllability. If the crowbar is decoupled at the fault clearing time, it can be retriggered because of the high transient currents during the fault clearing

moment. Moreover, the rotor-side converter controller needs some time to restart power electronics switches in converter. In order to avoid transient currents and voltages to retrigger the crowbar, in these simulations, the crowbar is decoupled from the rotor for 150 milliseconds after the fault cleared which is seen on Figure 4.5.

In addition to crowbar protection, the grid-side converter injects reactive current to the grid to support the voltage recovery. As explained in Section 2.3.1.7, the q-component of the grid-side converter controller controls the reactive power output of the grid-side converter. During grid fault, reference of the q-component is set to its limit (1.0 p.u.), so that the converter always contributes with its maximum reactive power to voltage reestablishment. However, since the voltage level is significantly reduced during the fault, the grid side converter's reactive power production capability is also reduced.

Moreover, pitch system is used to limit the generator speed by decreasing the output power of the turbine. Since grid fault causes a voltage drop at the generator terminal, electrical output torque of the turbine is significantly reduced. On the other hand, since mechanical system response is slower than the electrical one, generator starts to accelerate. As the DFIG behaves like a SCIG when the crowbar is activated, the acceleration of the generator causes an increased reactive power consumption of it. Both increased speed and increased reactive power consumption have a negative impact on power system stability and over-speeding of the generator could lead to a tripping of the whole turbine. As a consequence, pitch system should immediately respond to the grid faults and limits the acceleration of the generator by reducing the aerodynamic power.

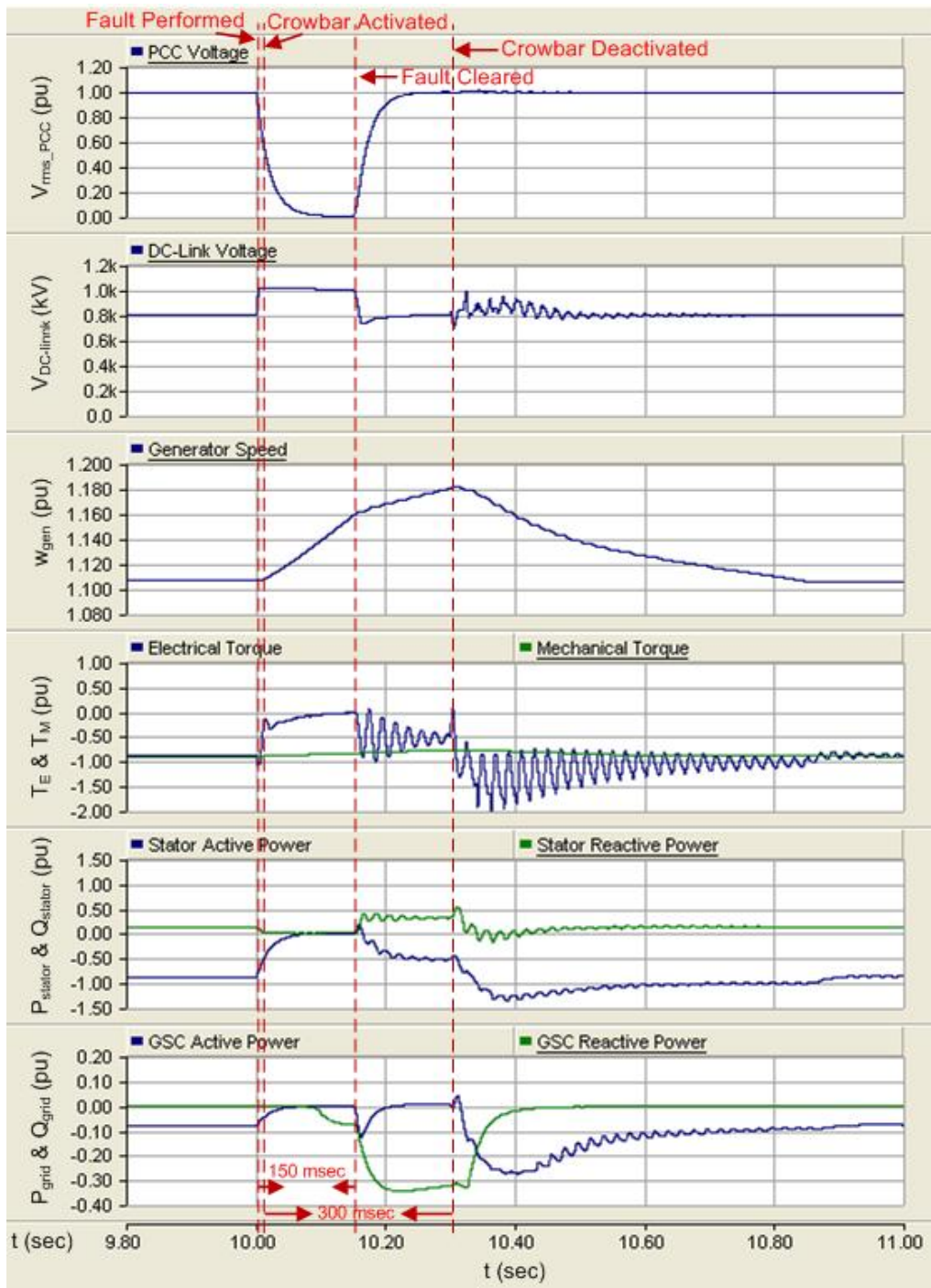


Figure 4.5 Simulation Results of DFIG Type Wind Turbine with Suggested FRT Method for a 3-Phase to Ground Fault at PCC for Duration of 150 ms

Similar to ZVRT simulations, LVRT simulations of DFIG type wind turbine also performed. In this case, a three-phase to ground fault is considered to occur for duration of 150 milliseconds at the middle of the lines, “Fault Position-1” and “Fault Position-2” in Figure 4.2. During these disturbances, the grid side converter can provide more reactive power to the grid with respect to ZVRT condition. In other words, since the PCC voltage is not zero and is greater than ZVRT condition, converter can deliver more reactive power during the fault and the terminal voltage can return to its pre-fault level quickly as seen in Figure 4.6 and Figure 4.7. As seen from the figures, wind turbine in the “Fault position-1” condition turns its steady state condition quickly. The reason for this is the higher PCC voltage because of the line parameters.

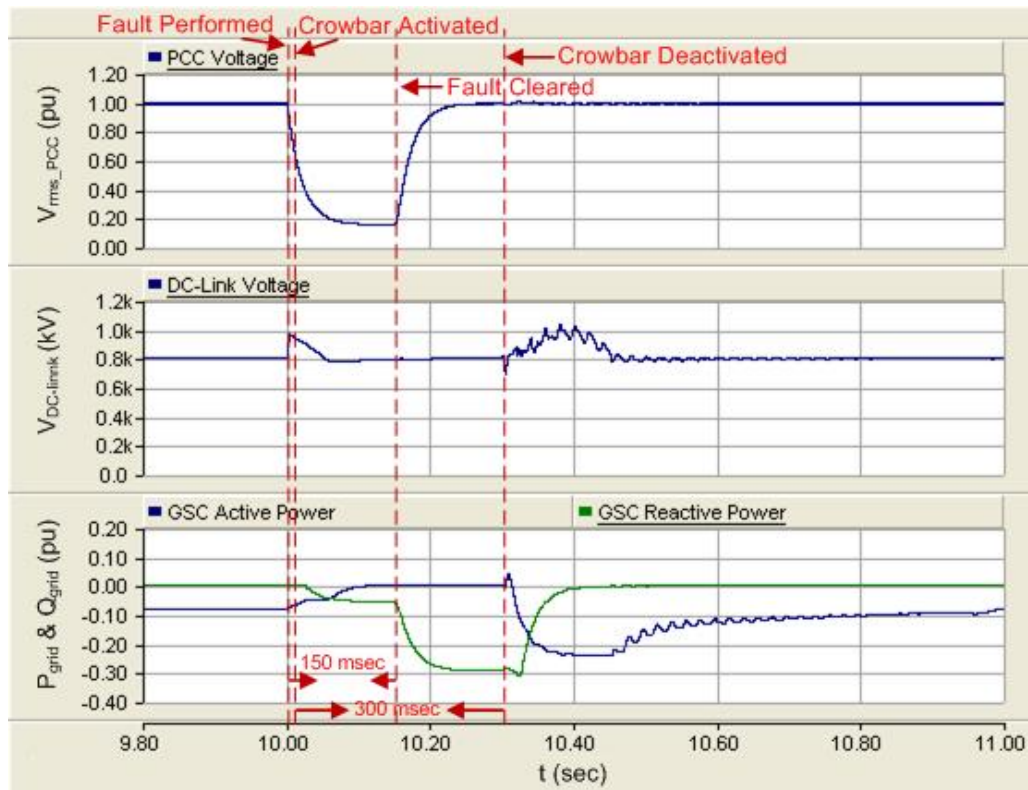


Figure 4.6 Simulation Results of DFIG Type Wind Turbine with Suggested FRT Method for a 3-Phase to Ground Fault at Fault Position-1 for Duration of 150 ms

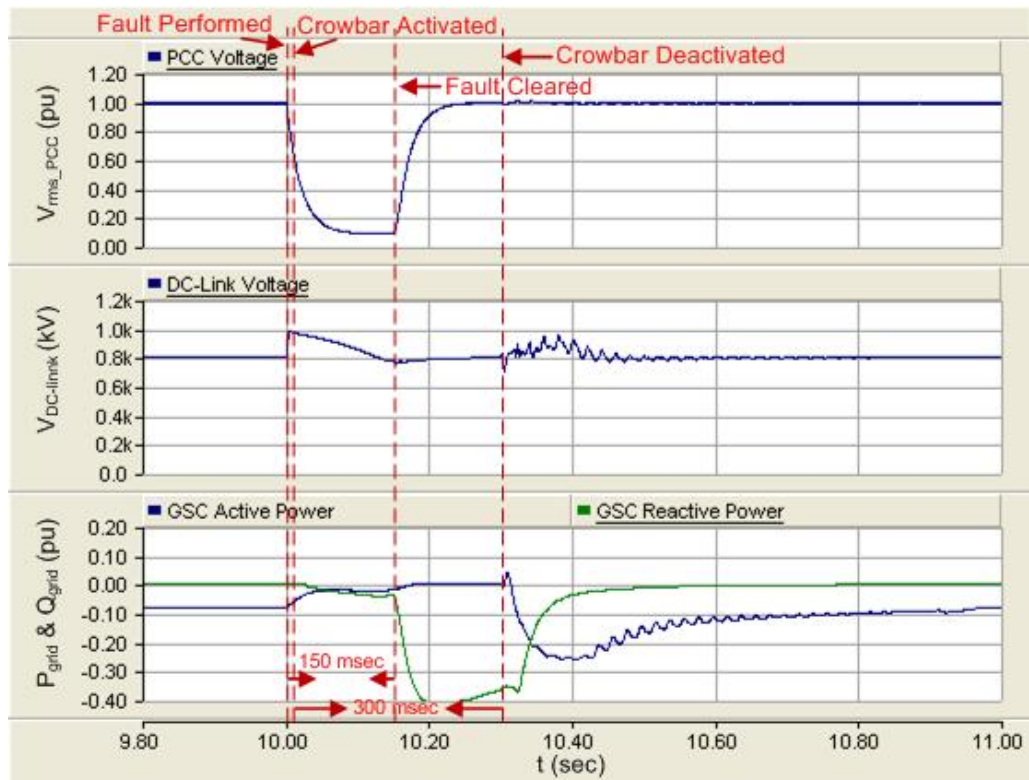


Figure 4.7 Simulation Results of DFIG Type Wind Turbine with Suggested FRT Method for a 3-Phase to Ground Fault at Fault Position-2 for Duration of 150 ms

In this case, a 3-phase to ground fault is created at point “Fault Position-2” for duration of 150 milliseconds and the faulted line is opened for duration of 1 second. The simulation results are almost same with the previous case as seen from Figure 4.7 and Figure 4.8. The only difference is the small decrease of PCC voltage during 1 second period while line is opened. This is because of the line parameters as the voltage drop is higher on the line.

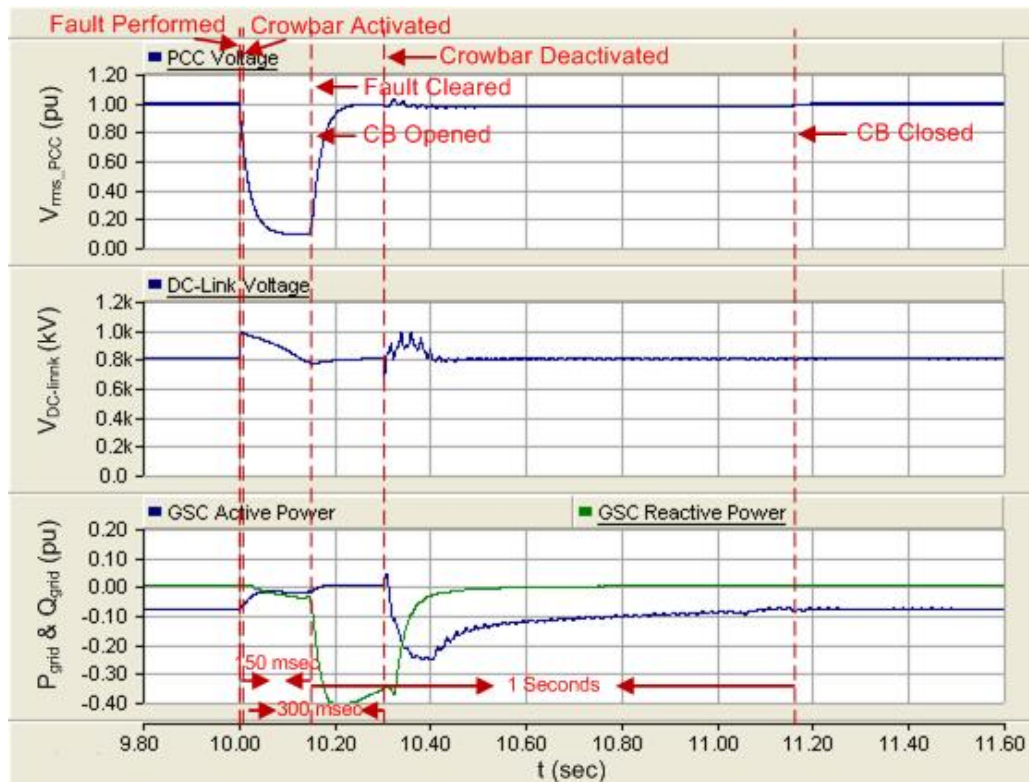


Figure 4.8 Simulation Results of DFIG Type Wind Turbine for a 3-Phase to Ground Fault at Fault Position-2 for Duration of 150 ms and the Faulted Line is opened

4.5 Wind Farm Model based on PMSG Wind Turbines

Similar to Section 4.4, the computer simulation model of the wind farm consisting of wind turbines with PMSG has been constructed using library blocks of PSCAD/EMTDC and implemented blocks based on theoretical background and operating principles introduced in Chapter 2 in PSCAD/EMTDC medium.

To validate the implemented model and benchmark the simulation results afterward, wind turbine used in [49] is modeled. The generator parameters used in the model are given in Table 4.4.

Table 4.4 PMSG parameters used in PSCAD/EMTDC model

Rated power	5 [MVA]
Rated voltage(L-L)	1 [kV]
Frequency	20 [Hz]
Number of poles	150
Angular moment of inertia	3 [s]
Stator resistance	0.01 [pu]
Stator leakage inductance	0.019 [pu]
d-axis reactance	1.0 [pu]
q-axis reactance	0.7 [pu]

Moreover, other parameters are given in Table 4.5;

Table 4.5 Other Parameters Used in Wind turbine with PMSG Model

Capacitor in the DC-Link	0.01[mF]
DC-Link Voltage	2.3 [kV]
Filter resistance	0.0084 [Ω]
Filter inductance	0.0004 [H]

Considering the given parameters in Table 4.4 and Table 4.5, a 5 MVA wind turbine with PMSG which consist of a wind speed block, a turbine block, a pitch system block, a generator block, rotor-side and grid-side converter controllers and a converter block is modeled in PSCAD/EMTDC. The simulation time step, duration of the simulation and control parameters are determined in the same manner with Section 4.4. After completing 5 MVA wind turbine modeling, it is aggregated to 30 MVA based on the assumptions mentioned in Section 4.2. The complete PMSG based wind turbine model including wind turbine block, turbine block, generator block, rotor side and grid side converter controllers and converters block are described in detail in Appendix C.

The steady state and transient performances of the model are investigated via the simulations and validation of this model is made by comparing the consistency of simulation results with the references [37], [38] and [49].

The rest of this section, firstly, the performance of PMSG type wind turbine under normal operating conditions is investigated. Then, FRT capability of the turbine under grid disturbances before and after the suggested FRT method is discussed.

4.5.1 Performance of PMSG type Wind Turbines under Normal Operating Conditions

Before considering the fault ride through analysis, a set of simulations is performed in order to show the performance of modeled PMSG type wind turbine under normal operating conditions. By varying the wind speed including gust and ramp components, the response of the pitch system, generator speed, and active/reactive power output of the converters are observed in Figure 4.9. As in DFIG type wind turbine simulations, the mean value of the wind speed is approximately 12 *m/s* and has a small turbulence, the gust component of wind speed is started at 40th second and continues for 20 seconds and the ramp component is started at 80th second and continues for 20 seconds. As described in pitch model section, below the rated wind speed (about 12 *m/s*), the converter seeks to maximize the turbine output power and the pitch system does not respond as shown in blade angle in Figure 4.9. However, if wind speed exceeds this rated wind speed, pitch system limits the aerodynamic torque input to the generator. Since whole power output of the turbine is delivered to the grid through the converter system in normal operating condition, DC-link voltage does not change with varying wind speed. Generator speed is changed with varying wind speed, but pitch system limits it in the high wind speeds. Output power of the farm is varying with changing wind speed, because it is dependent on the wind speed.

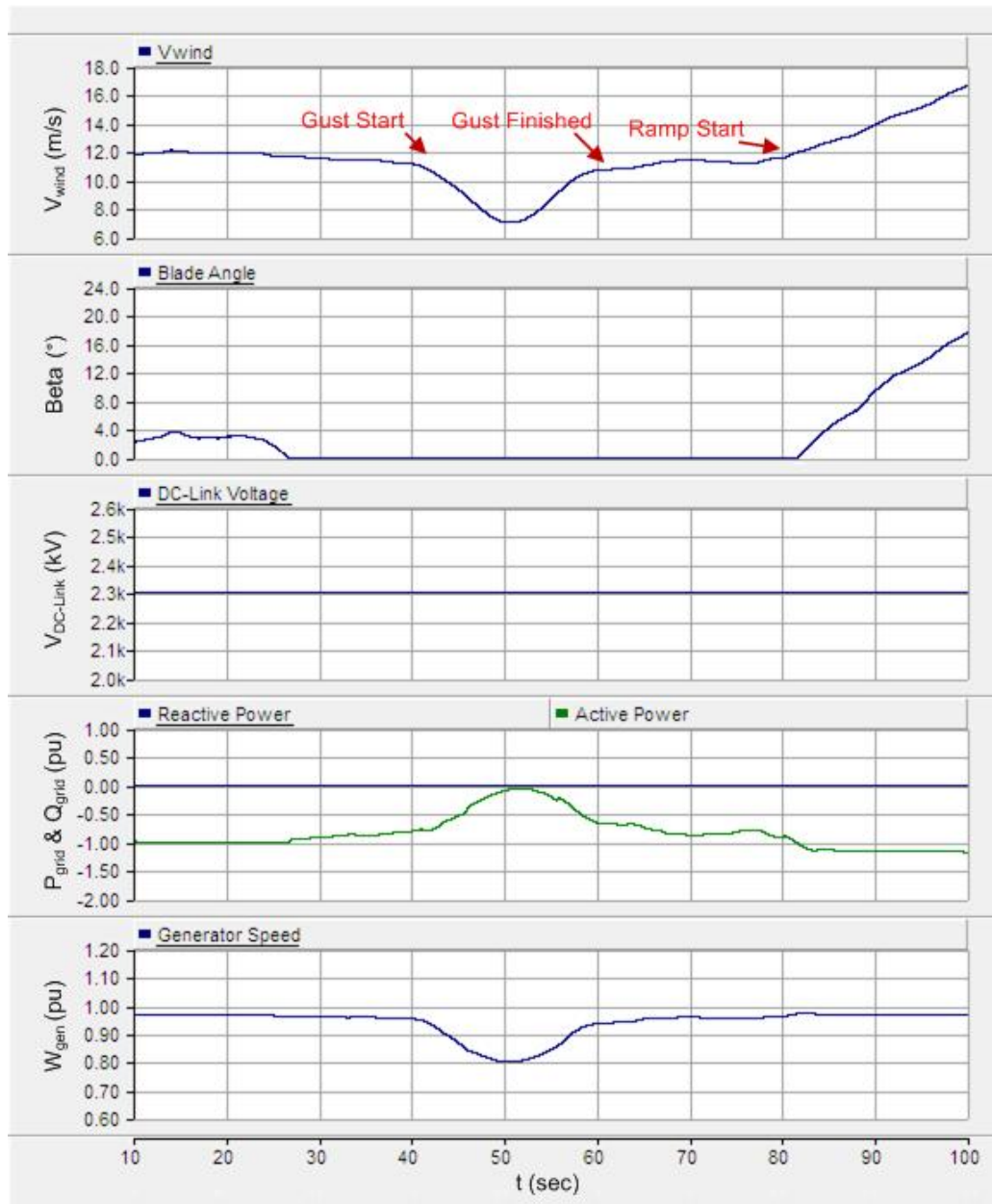


Figure 4.9 Performance of PMSG Type Wind Turbine under Normal Operating Condition with Varying Wind Speed

4.5.2 Performance of PMSG type Wind Turbines under Grid Disturbances

In this section, the performance of PMSG type wind turbine under grid disturbances is discussed. To represent the worst case scenario simulations as in DFIG type turbine, PMSG is assumed to operate at rated power and a three-phase to ground fault is performed for duration of 150 milliseconds at the PCC, i.e., “Fault at PCC” position in Figure 4.2 . Due to this grid fault, a voltage drop occurs at the grid side of the converters. Hence, the grid-side converter cannot deliver the active power output of the turbine to the grid. On the other hand, the wind turbine continues its power production which will result in a power imbalance in the converter system. As the generator side converter continues to deliver the power from the generator-side to the DC-link, the surplus power which cannot be transferred to the grid will cause charging of the DC-link capacitor. As seen in Figure 4.10, this charging of DC-link capacitor increases the voltage of the DC-link to high values in fault condition which is not tolerable for the converters and the capacitor. Thus, the converter protection is activated which leads the tripping of turbine. Thus, a PMSG type wind turbine without necessary FRT method will trip under grid disturbance and cannot satisfy the grid code requirements determined by the TSOs.

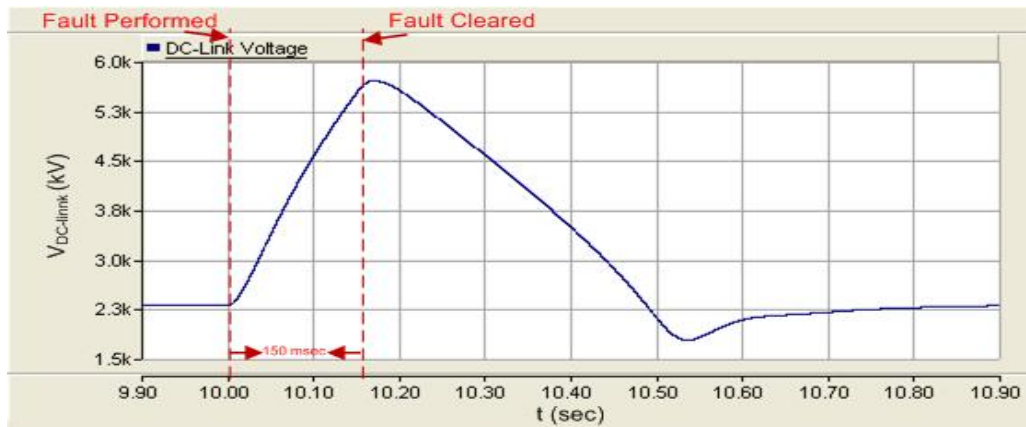


Figure 4.10 DC-link Voltage of PMSG Type Wind Turbine under Grid Fault for Duration of 150 ms

4.5.3 Suggested Method to Improve FRT Capability of PMSG type Wind Turbine

In this section, implementation of a control method, which enables the PMSG wind turbine for FRT and provides reactive power supply for voltage recovery during grid faults are presented. As described in Section 4.5.2, high DC-link voltages arise during grid faults which constitute damaging risks for the converters and capacitor. To overcome this problem, the braking resistor method described in Section 3.4.2.2 is used.

A three-phase to ground fault is considered to occur at the PCC of the wind farm, “Fault at PCC” position in Figure 4.2. This fault is applied exactly at 10th second of the simulation for duration of 150 milliseconds which causes a voltage drop down to zero at the PCC. It is assumed that at the fault incident, the wind turbine is operating at rated power and the power imbalance is triggered since the grid side converter active power output is decreased dramatically down to zero. However, in order not to damage the converters and the capacitor, the DC-link voltage must be kept between the limits of the converters and capacitor, $\pm 25\%$ around their rated value. To avoid the charging of the DC-link capacitor, a braking resistor can be applied to the DC link as described in Section 3.4.2.2. A braking resistor represents a resistor with semi-conductor switch, which is added parallel to the capacitor in the DC-link and is switched on if the DC link voltage exceeds the critical level. When the switch is on, the surplus power is burned in the resistance until the DC-link discharges to lower critical voltage level. At this point, the braking resistor switch is off and again DC-link voltage start to increase. When it reaches the upper limit again, the switch of the resistor is made on again, and this repetition goes on until the DC-link voltage returns to its steady state condition as in Figure 4.11.

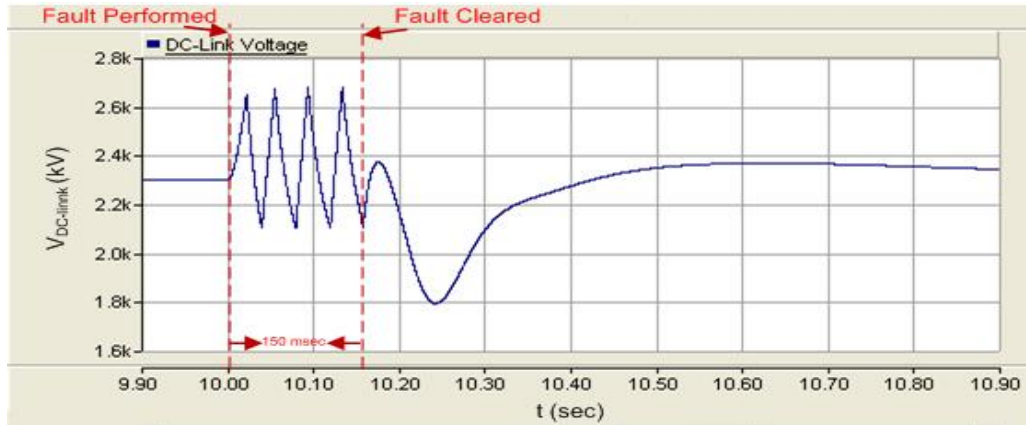


Figure 4.11 DC-link Voltage of PMSG Type Wind Turbine under Grid Fault for Duration of 150 ms with Suggested FRT Method

In addition to this DC-link regulation, during the network disturbance, the grid side converter can provide the necessary reactive power to the grid to support the terminal voltage as seen in Figure 4.12. By adjusting the q-component of the grid side converter controller with respect to voltage level, converter can provide the necessary reactive power to the grid to recover the terminal voltage to its pre-fault level quickly. Moreover to these, since the generator is decoupled from the grid by back-to-back converters, the generator side is hardly affected from the network disturbances.

In Appendix C, the modified DC-Link block is seen where the trip signal, $Trip$, and the braking resistor, R_b , are the new inputs to the block. Trip signal is sent by protection system and it is set to “1” whenever DC-Link voltage exceeds 1.2 pu and set to “0” whenever DC-Link voltage is under 0.9 pu. R_b is calculated to dissipate rated power of the turbine which is 0.176Ω in our case. As seen in Figure 4.13, when trip signal is “0”, the normal DC-Link equation is used. However, if the signal is “1”, surplus power must be dissipated which means subtracting the braking resistor current from ordinary DC-link block equation. As a result, the capacitor discharges,

the DC-link voltage decreases below the threshold value and the braking resistor is off which means that the block returns to its normal operating condition.

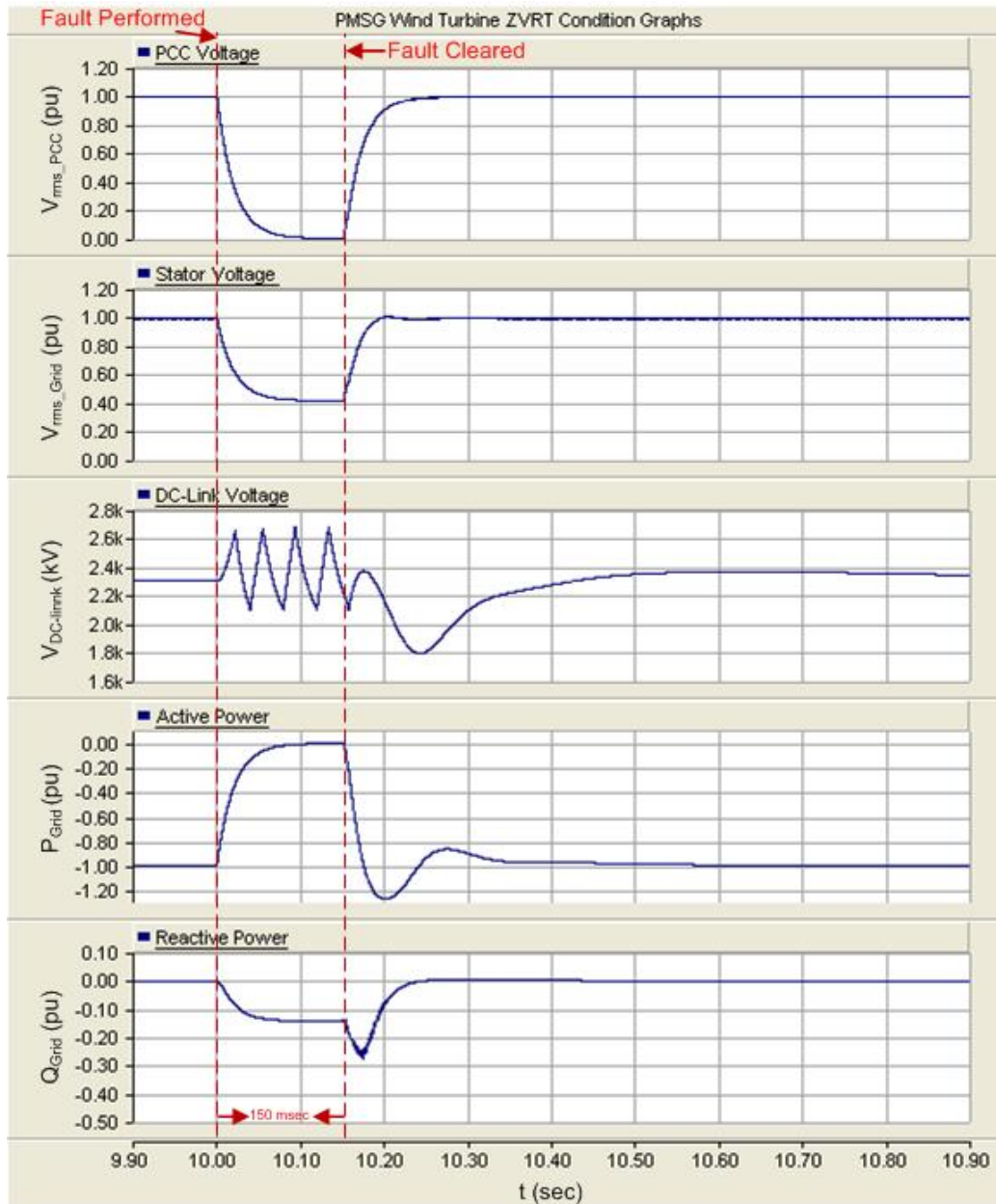


Figure 4.12 Simulation Results of PMSG Type Wind Turbine with Suggested FRT Method for a 3-Phase to Ground Fault at PCC for Duration of 150 ms

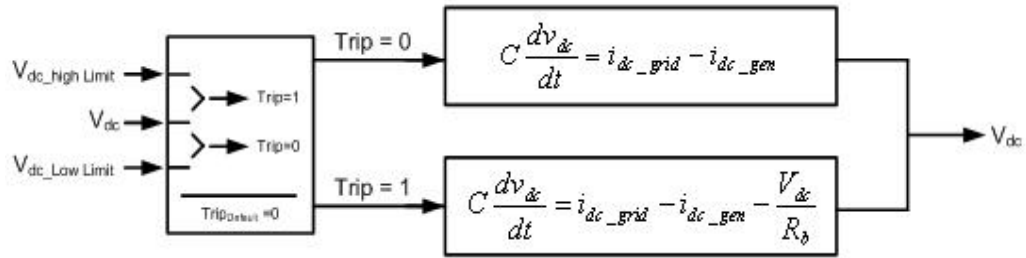


Figure 4.13 Function Diagram of DC-Link Block with Protection Signal

Similar to ZVRT simulations, LVRT simulations of PMSG type wind turbine also performed. In this case, a three-phase to ground fault is considered to occur for duration of 150 milliseconds at the middle of the lines, “Fault Position-1” and “Fault Position-2” in Figure 4.2. Since the PCC voltage is decreased to low values but not zero during the grid fault, the grid-side converter can provide the necessary reactive power to the grid. Since the PCC voltage is greater than ZVRT condition, converter can deliver more reactive power during the fault and the terminal voltage can return to its pre-fault level quickly as seen in Figure 4.14. The general response of the turbine except the PCC voltage level and reactive power is approximately same with ZVRT condition as seen in Figure 4.14. Moreover to this grid fault, a 3-phase to ground fault is created at point “Fault Position-1” for duration of 150 milliseconds and the faulted line is opened for duration of 1 second. The simulation results are almost same with the previous case as seen from Figure 4.14 and Figure 4.15. The only difference is the small decrease of PCC voltage during 1 second period while line is opened.

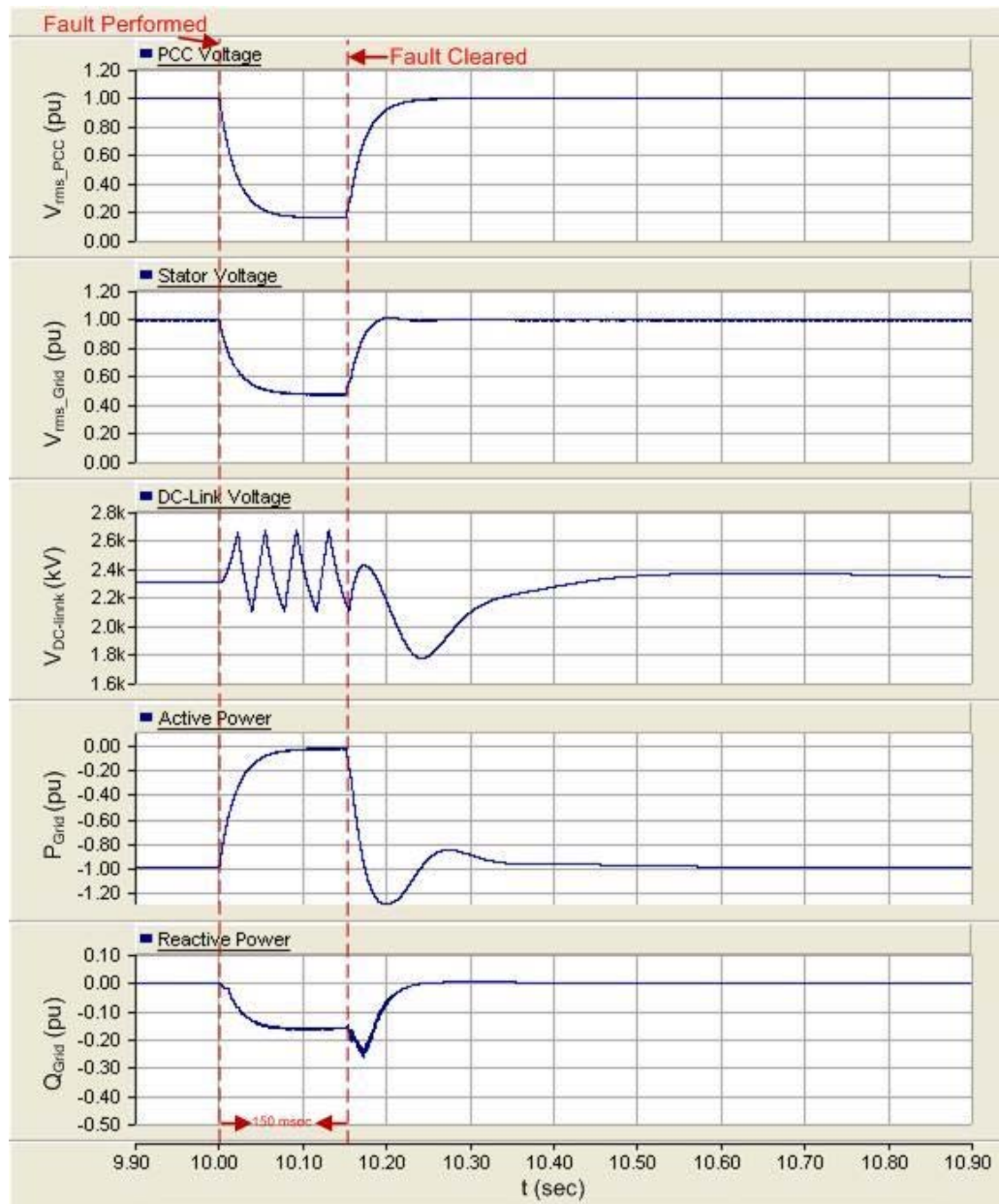


Figure 4.14 Simulation Results of PMSG Type Wind Turbine with Suggested FRT Method for a 3-Phase to Ground Fault at Fault Position-1 for Duration of 150 ms

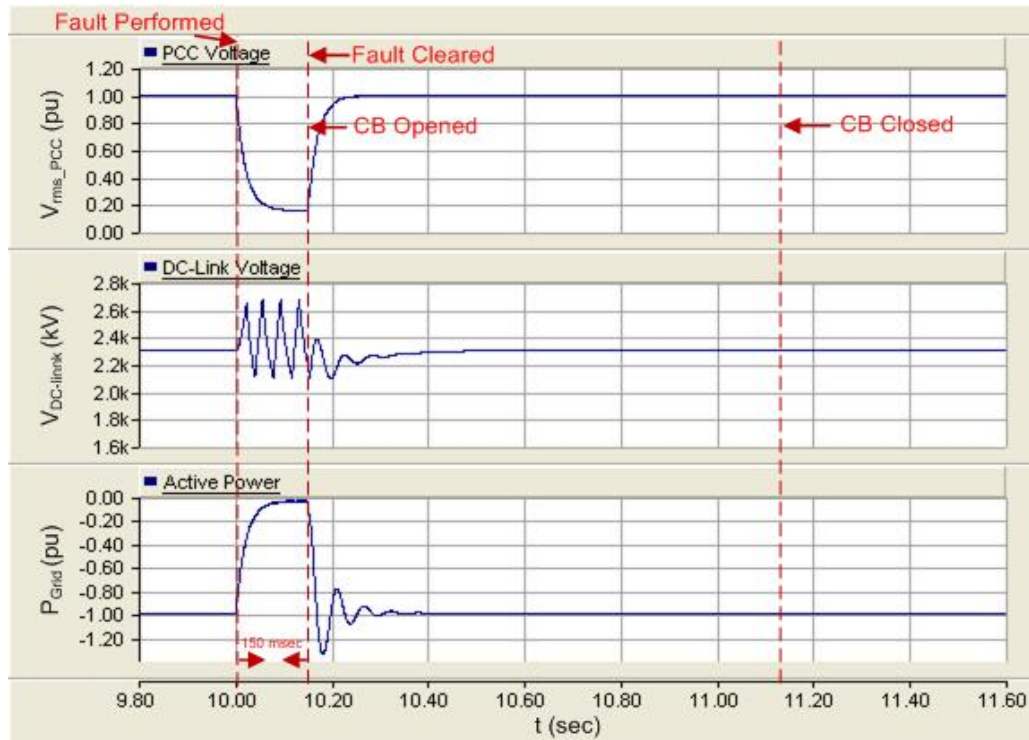


Figure 4.15 Simulation Results of PMSG Type Wind Turbine for a 3-Phase to Ground Fault at Fault Position-1 for Duration of 150 ms and the Faulted Line is opened

4.6 Comparison of the DFIG and PMSG Type Wind Turbines

As mentioned before in DFIG, the stator terminal of the DFIG is directly connected to the grid whereas the rotor circuit is connected to the rotor-side converter. By using such a connection, back-to-back converter has to handle only a fraction (about 30%) of the generator's rated power. This smaller size converter means reduced power losses and cost efficient wind turbine. Despite these advantages, because of the smaller size converter, the reactive power supply capability of DFIG wind turbines is smaller compared to PMSG type wind turbines. Moreover, reactive power supply even further reduces since the rotor-side converter is deactivated by the crowbar during grid faults. In addition to these disadvantages, due to direct coupling to the

grid, generator, converter and turbine system are directly exposed to the grid fault impacts. Hence, oscillations may occur in generator speed and torque, which are immediately transferred to the grid voltage.

Since the back-to-back converter system decouples the PMSG type wind turbines from the grid, they are less sensitive to the grid fault impacts than direct connected DFIG type turbines. Because PMSG type turbines are being capable of injecting the rated reactive current, they can fully meet the grid code requirement of the voltage support. Moreover, a sufficient active power ramp-up rate is also easily achieved and because of the braking resistor installed to dissipate the excess energy from the generator to the DC-link, this type of turbine has excellent voltage dip ride through performance. Another advantage is that, PMSG type turbines do not require any gearbox which reduces the installation and maintenance costs.

4.7 An Additional Assessment for Integration of WPPs Connected to the Grid

While performing the connection process of WPPs to the grid, TEIAS's preferences are mainly focused on:

- Short Circuit MVA (SCMVA) of the PCC: Transmission System Supply Reliability and Quality Regulation clarify this as "Connection of generation facility based on wind energy is permitted for a capacity up to 5% of the system short circuit power at the connection point".
- Distance between the planned WPP and the PCC: TEIAS is in charge of the transmission investments; hence the shorter connection option for WPP is more desirable in terms of economic and technical aspects.
- Power transfer capacity of the substation containing PCC: The transmission capacity of the substation at PCC is defined by load flow study results considering the transfer capacities of transmission lines and autotransformers.

As mentioned above, these three essential criteria are considered when WPPs are connected to the grid. Based on these three main criteria, there may appear more than one proper connection point. At this condition, TEIAS decides on the connection point by considering the technical and non-technical (environmental, social, feeder availability of substation) issues.

During this progress, TEIAS does not consider the wind turbine structure and the existing plants at the substation. However the licensed projects up to year 2007 are mainly fixed speed and DFIG type wind turbines; and both these type of WPPs are exempted from Annex 18. This means that there still exists around 2000 MW of valid WPP license containing DFIG and fixed speed wind turbines which may not support the grid during disturbances. Moreover, 8000 MW additional WPP projects are approved which will satisfy the requirements of [42]. Once the WPP project is evaluated according to the three main criteria and if the result has more than one reasonable connection point, the planned WPP topology can be considered as an assessment for integration of WPP connection to the grid. The positive effects of connecting planned WPPs to the installed WPPs are arising in two ways:

- Disconnection of existing wind farms: When the applied grid fault causes a voltage drop at the PCC down to approximately 10% of its rated value, the delivered active power significantly reduces which results in large speed and torque oscillations, and rotor acceleration of the installed wind turbines. Due to these reasons, the old type turbines generally trips since they do not have FRT capability. At this point, if the planned WPP will connect to the type WPPs' PCC, the significant power deficit due to disconnection of old type turbines during grid faults can be avoided by the active and reactive power support of new turbines. The simulation results illustrate how the new type turbines support the voltage, active power and reactive power of the PCC.
- Increase in the FRT capacity of old type WPPs: When the nearby connected new WPP with PMSG or DFIG support the power system stability by

reactive power injection during a grid fault, the installed old type WPPs are maybe no longer necessary to be disconnected from the grid. As the PCC voltage drops, the grid-side converter controllers provoke an increase of reactive power supply due to the new connected WPP which increases the voltage level at the PCC. The reactive current injection of the grid-side converter increases after the fault is cleared due to the increased voltage level. The reactive power supply is reduced to zero when the voltage at the PCC reaches its rated value. Thus, the PCC voltage support of new type WPPs has furthermore a positive impact on the FRT capability and behavior of the installed old type WPPs by increasing the PCC voltage. Moreover, keeping old type WPPs connected to the grid during a disturbance by supporting the PCC voltage helps to regain the system stability much faster. In addition to this, having not disconnected the old farm from the grid, a significant loss of active power production can also be avoided.

The concluding statements about connecting the planned wind farms (DFIG or PMSG type WPPs) to the vicinity of old wind farms are;

- Voltage and system stability can much faster be regained,
- The FRT performance of a nearby connected wind farm during the grid faults is improved,
- Significant loss of active power production can also be avoided, if old wind farm is disconnected after a grid fault.

Thus, if the planned WPP project is evaluated according to the three main criteria resulting in more than one reasonable connection point; the planned WPP topology can be considered as an assessment for integration of WPP connection to the grid.

CHAPTER 5

CONCLUSION

The installation of the large amount of wind turbines at both onshore and offshore are rapidly increasing by virtue of the recent developments in wind turbine technology and the incentives provided by the governments. According to the wind integration studies performed by the TSOs and organizations from academy and industry, the grid code requirements have been revised, wind turbine manufacturers have been implementing new developments to the market, and the wind power plant developers have been conducting the connection studies considering grid codes and wind turbine technology. FRT capability of the wind turbine, which is the much studied grid code requirement, have been investigated and analyzed with the promising wind turbine technologies in this study.

To investigate the FRT capability of the wind turbine, detailed wind turbine models are described and implemented. The modeling chapter is presented as a tutorial for the future power system analyses of the wind turbines. After giving the details of the wind turbine models, the grid code chapter summarizes the latest requirements from the TSOs. In Turkey, integration studies together with the grid code revisions have been carried out by TEIAS and EMRA, however there are still open issues related to the performance of the wind turbines. Reactive power response speeds, high voltage ride through capability and maximum high voltage level, power factor range are some of the points that questions arise by the manufacturers in the market. At this point, this study gives an idea about the FRT capability of the DFIG and PMSG wind turbines in a comparative way.

In the simulation part, implemented models are simulated for the three phase short circuit faults in the grid. Different FRT control algorithms are evaluated with respect to the response time and transient voltage support performance. The important consideration is the implemented controllers might change according to the manufacturer and grid connection point. From this point of view, the parameters are chosen from the generic values available in the literature, and the grid characteristics are modeled from the real values of the small area of the transmission system.

The following results are determined from the simulation studies:

- Since the stator of DFIG is directly connected to the grid and rotor is connected to the back-to-back converters, converters have to handle only a fraction of the generator's rated power. Reduced power losses and cost efficiency are the advantages of DFIG type wind turbines because of the smaller size converters. However, as seen from the simulation results, this type of wind turbines requires additional power electronic circuits and components such as a crowbar to establish the over-voltage and over-current protection. Moreover, since the DFIG is a partial scale wind turbine, its reactive power support capability during grid faults for the voltage recovery is smaller with respect to PMSG as seen in simulation results. Additionally, since the stator is directly connected to the grid, turbine and generator are easily affected from the faults and torque, power, generator speed and voltage oscillations are more compared to PMSG type wind turbines. Furthermore, since the generator consume reactive power when the crowbar activated, this also negatively effects the voltage stability.
- With the help of full scale converters, PMSG type wind turbines can fully meet the FRT grid code requirements and voltage support by being capable of injecting the rated reactive current. In addition to reactive power support, a sufficient active power ramp-up rate is also easily achieved with the flexible control systems as seen in simulation results. Furthermore, the converter

system decouples generator and turbine from the grid so that both are less subjected to the grid fault impact than turbines with direct grid connected DFIGs.

- If the planned WPP project is evaluated according to the main criteria resulting in more than one reasonable connection point; the planned WPP topology can be considered as an assessment for integration of WPP connection to the grid to increase the voltage and system stability and FRT performance of the nearby connected WPP.

Proposed further works can also be done in the future:

- The transient behaviors of the DFIG and PMSG wind turbines under the disturbances of other grid failures should be studied.
- A detailed PWM voltage source converter model with high-frequency switches should be implemented to provide more accurate transient responses for grid-connected wind turbines.
- Other grid code requirements analysis can be investigated by using these models and new grid code requirements can be proposed.
- If possible, field tests should be carried out to verify the simulation results shown in this thesis.
- The interactions between the wind turbines in the wind farm can be investigated by not aggregating the models.

REFERENCES

- [1] A.Pullen, L. Qiao and S. Sawyer, “Global Wind Report 2009”, Global Wind Energy Council GWEC, Brussels, Belgium, March 2010.
- [2] I. Martinez de Alegria, J. Andreu, J.L. Martin, P. Ibanez, J.L.Villate and H. Camblong, “Connection requirements for wind farms: a survey on technical requirements and regulation”, *ScienceDirect Renewable and Sustainable Energy Reviews 11*, pp.1858-1872, January 2006.
- [3] “*Türkiye Rüzgar Potansiyeli Atlası*”, <http://www.eie.gov.tr/>, last accessed date: 23/08/2010.
- [4] T. Ackermann, Ed.,“*Wind Power in Power Systems*”, Chichester: John Wiley & Sons Ltd, 2005.
- [5] O. A. Lara, N. Jenkins, J. Ekanayake, P. Cartwright and M. Hughes, “Wind Energy Generation, Modelling and Control”, Chichester: John Wiley & Sons, 2009.
- [6] Transmission Code 2007. Networks and System Rules of the German Transmission System Operators, VDN-e.v. beim VDEW, August 2007
- [7] Grid connection of wind turbines to networks with voltages above 100 kV, Regulation TF 3.2.5, Eltra and Elkraft System, December 2004.
- [8] NGET, “The Grid Code”, Issue 4, National Grid Electricity Transmission Plc, June 2009.
- [9] Red Electrica, “Resolution-P.O.12.3-Response requirements against voltage dip in wind installations”, March 2006.
- [10] “*Inside of a Wind Turbine*”, <http://www.starshipzoom.com/>, last accessed date: 23/08/2010.

- [11] S.Mathew, “*Wind Energy Fundamentals, Resource Analysis and Economics*”, Verlag Berlin: Springer, 2006.
- [12] P.M. Anderson and A. Bose, “Stability simulation of wind turbine systems”, *IEEE Trans. on Power Apparatus and Systems*, Vol. PAS-102, No. 12, pp. 3791-3795, December 1983.
- [13] G. L. Johnson, “*Wind Energy Systems*”, Manhattan, Kansas, October 2006. [E-book] Available: <http://eece.ksu.edu>.
- [14] J.G. Slootweg, H. Polinder and W.L. Kling, “Representing wind turbine electrical generating systems in fundamental frequency simulations”, *IEEE Trans. On Energy Conversion*, Vol. 18, No. 4, pp. 516-524, December 2003.
- [15] S. Heier, ”*Grid Integration of Wind Energy Conversion Systems*”, England: John Wiley & Sons, 1998.
- [16] A. Petersson, “Analysis, Modeling and Control of Doubly-Fed Induction Generators for Wind Turbines”, Ph.D. dissertation, Chalmers University of Technology, Göteborg, Sweden, 2005.
- [17] Z. Chen and E.Sponner, “Grid power quality with variable speed wind turbines”, *IEEE Trans. On Energy Conversion*, Vol. 16, No. 2, pp. 148-154, June 2001.
- [18] M.G. Simoes and F.A. Farret, “*Alternative Energy Systems; Design and Analysis with Induction Generator*”, Boca Raton: CRC Press, 2008.
- [19] T. Sun, “Power Quality of Grid-Connected Wind Turbines with DFIG and Their Interaction with the Grid”, Ph.D. Dissertation, Aalborg University, Denmark, May 2004.
- [20] P. Kundur, “*Power System Stability and Control*”, Toronto: McGraw-Hill Inc, 1994.
- [21] H. Shuju, L. Jianlin and X. Honghua, “Modeling on converter of direct-driven WECS and its characteristic during voltage sags”, *IEEE International conference on Industrial Technology*, pp. 1-5, 2008.

- [22] S. Achilles and M. Poller, "Direct drive synchronous machine models for stability assessment of wind farms", *4th International Workshop on Large Scale Integration of Wind Power and Transmission Networks for Offshore Wind-Farms*, Billund, Denmark, 2003.
- [23] A.E Fitzgerald, C. Kingsley Jr and S. D. Umans, "*Electric Machinery*", London: McGraw-Hill, 1992.
- [24] J.C. Smith, M.R. Milligan, E.A. DeMeo and B. Parsons, "Utility wind integration and operating impact state of the art", *IEEE Transactions on Power Systems*, Vol. 22, No. 3, pp. 900-908, August 2007.
- [25] EWEA, "Generic grid code format for wind power plants", The European Wind Energy Association EWEA, Brussels, Belgium, November 2009.
- [26] M. Tsili and S. Papathanassiou, "A review of grid code technical requirements for wind farms", *IET Renewable Power Generation*, Vol. 3, Iss. 3, pp. 308-332, September 2009.
- [27] E. Hau, "*Wind Turbines; Fundamentals, Technologies, Application, Economics*", Berlin: Springer, 2006.
- [28] V. Akhmatov, "Analysis of Dynamic Behaviour of Electric Power Systems with Large Amount of Wind Power", Ph.D. Dissertation, Technical University of Denmark, Denmark, April 2003.
- [29] A.D. Hansen, N.A. Cutululis, P. Sorensen and F. Iow, "Grid fault and design-basis for wind turbines - Final report", Riso DTU National Laboratory for Sustainable Energy, Roskilde, Denmark, Riso-R-1714, January 2010.
- [30] M.H. Ali and Bin Wu, "Comparison of stabilization methods for fixed speed wind generator systems", *IEEE Transaction on Power Delivery*, Vol. 25, No. 1, pp. 323-331, January 2010.
- [31] M. Sedighizadeh, A. Rezaadeh and M. Parayandeh, "Comparison of SVC and STATCOM impacts on wind farm stability connected to power system",

International Journal of Engineering and Applied Sciences, Vol. 2, Issue 2, pp. 13-22, September 2009.

- [32] A. Causebrook, D.J. Atkinson and A.G. Jack, "Fault ride-through of large wind farms using series dynamic braking resistors", *IEEE Transactions on Power Systems*, Vol. 22, No. 3, pp. 966-975, August 2007.
- [33] S. M. Schoenung, J. M. Eyer, J. J. Iannucci, and S. A. Horgan, "Energy storage for a competitive power market", *Annual Review of Energy and the Environment*, Vol. 21, pp. 347-370, November 1996.
- [34] A.H. Kasem, E.F. El Saadany, H.H. El-Tamaly and M.A.A. Wahab, "An improved fault ride-through strategy for doubly fed induction generator-based wind turbines", *IET Renewable Power Generation*, Vol. 2, No. 4, pp. 201-214, March 2008.
- [35] M. De Alegria, J.L. Villate, J. Andreu, I. Gabiola and P. Ibanez, "Grid connection of doubly fed induction generator wind turbines: A survey", *European Wind Energy Conference*, London, UK, 2004.
- [36] A. Petersson, S. Lundberg and T. Thiringer "A DFIG wind turbine ride through system influence on energy production", *Nordic Wind Power Conference*, March 1-2, 2004.
- [37] J.F Conroy and R.Watson, "Low-voltage ride-through of a full converter wind turbine with permanent magnet generator", *IET Renewable Power Generation*, Vol. 1, No. 3, pp. 182-189, September 2007.
- [38] A.D Hansen and G. Michalke, "Multi-pole permanent magnet synchronous generator wind turbines' grid support capability in uninterrupted operation during grid faults", *IET Renewable Power Generation*, Vol. 3, Iss. 3, pp. 333-348, 2009.
- [39] J. F. Manwell, J. G. McGowan and A. L. Rogers, "*Wind energy explained: theory, design and application*", Chichester: John Wiley & Sons Ltd, 2002.
- [40] K. Salman and A.L. J. Teo, "Windmill modeling consideration and factors influencing the stability of a grid-connected wind power-based embedded

- generator”, *IEEE Trans. On Power Systems*, Vol. 18, No. 2, pp. 793-802, May 2003.
- [41] Anca D. Hansen and G. Michalke, “Modeling and control of variable speed multi-pole permanent magnet synchronous generator wind turbine”, *Wind Energy Wiley Interscience*, pp. 537-554, May 2008.
- [42] EMRA, “*Wind Interconnection Rule Annex 18*”, Turkish Energy Market Regulatory Authority, Ankara, Nov. 2008
- [43] *PSCAD User’s Guide*, Manitoba HVDC Research Centre Inc., Manitoba, Canada, 2003.
- [44] J.G Slootweg, “Wind Power Modeling and Impact on Power System Dynamics”, Phd. Thesis, Delft University of Technology, Netherland, 2003.
- [45] M. Poller and S. Achilles, “Aggregated wind park models for analyzing power system dynamics”, *4th International Workshop on Large Scale Integration of Wind Power and Transmission Networks for Offshore Wind-Farms*, Billund, Denmark, 2003.
- [46] E. Muljadi and B. Parsons, “Comparing single and multiple turbine representations in a wind farm simulation”, *European Wind Energy Conference*, Athens, Greece, 2006.
- [47] “*PID Tuning via Classical Methods*”, <http://controls.engin.umich.edu/>, last accessed date: 24/08/2010.
- [48] R. Pena, J.C. Clare and G.M. Asher, “Doubly fed induction generator using back-to-back PWM converters and its application to variable speed wind-energy generation”, *IEE Proc.-Electr. Power Appl.*, Vol. 143, No. 3, pp. 231-241, May 1996
- [49] S.M.Muyeen, J. Tamura and T.Murata, “*Stability Augmentation of a Grid-connected Wind Farm*”, Verlag London: Springer, 2009
- [50] “*Short circuit MVAs of Turkish Electricity Transmission System*”, <http://www.teias.gov.tr/yukdagitim/kisadevre.xls>, last accessed date: 26/08/10

APPENDIX A

CLARKE AND PARK TRANSFORMATION

Let the axis a and axis α be in the same direction as in Figure A.1, then a transformation from the three-phase stationary coordinate system (a-b-c) to the two-phase stationary coordinate system (α - β) is called Clarke transformation. The Clarke transformation and inverse Clarke transformation are given respectively in (A.1) and (A.2).

$$\begin{bmatrix} \alpha \\ \beta \\ 0 \end{bmatrix} = \frac{2}{3} \begin{bmatrix} 1 & -\frac{1}{2} & -\frac{1}{2} \\ 0 & \frac{\sqrt{3}}{2} & -\frac{\sqrt{3}}{2} \\ \frac{1}{2} & \frac{1}{2} & \frac{1}{2} \end{bmatrix} \begin{bmatrix} a \\ b \\ c \end{bmatrix} \quad (\text{A.1})$$

$$\begin{bmatrix} a \\ b \\ c \end{bmatrix} = \begin{bmatrix} 1 & 0 & 1 \\ -\frac{1}{2} & \frac{\sqrt{3}}{2} & 1 \\ -\frac{1}{2} & -\frac{\sqrt{3}}{2} & 1 \end{bmatrix} \begin{bmatrix} \alpha \\ \beta \\ 0 \end{bmatrix} \quad (\text{A.2})$$

Let the axis orientation be as in Figure A.1, and then a transformation from the two-phase stationary coordinate system (α - β) to the two-phase rotating coordinate system (d-q) is called Park transformation. The Park transformation and inverse Park transformation are given respectively in (A.3) and (A.4).

$$\begin{bmatrix} d \\ q \end{bmatrix} = \begin{bmatrix} \cos(\theta) & \sin(\theta) \\ -\sin(\theta) & \cos(\theta) \end{bmatrix} \begin{bmatrix} \alpha \\ \beta \end{bmatrix} \quad (\text{A.3})$$

$$\begin{bmatrix} \alpha \\ \beta \end{bmatrix} = \begin{bmatrix} \cos(\theta) & -\sin(\theta) \\ \sin(\theta) & \cos(\theta) \end{bmatrix} \begin{bmatrix} d \\ q \end{bmatrix} \quad (\text{A.4})$$

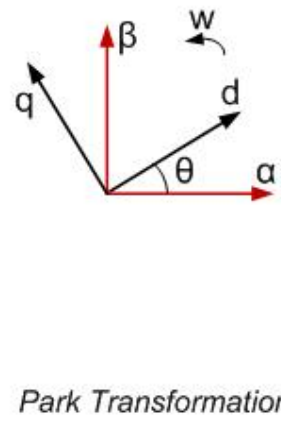
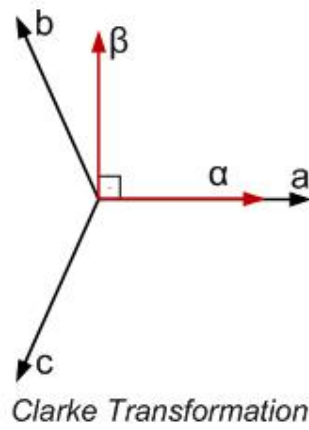


Figure A.1 Phasor Diagrams Used in Deriving Transformation Matrices

APPENDIX B

PSCAD/EMTDC MODEL FOR DFIG

In Figure B.1, general block diagram of a 30 MW WPP implemented in PSCAD/EMTDC according to the mathematical models explained in Chapter 2 can be seen. The block diagram consists of a wind speed block, a turbine block, an induction generator block, a converter block and a controller block.

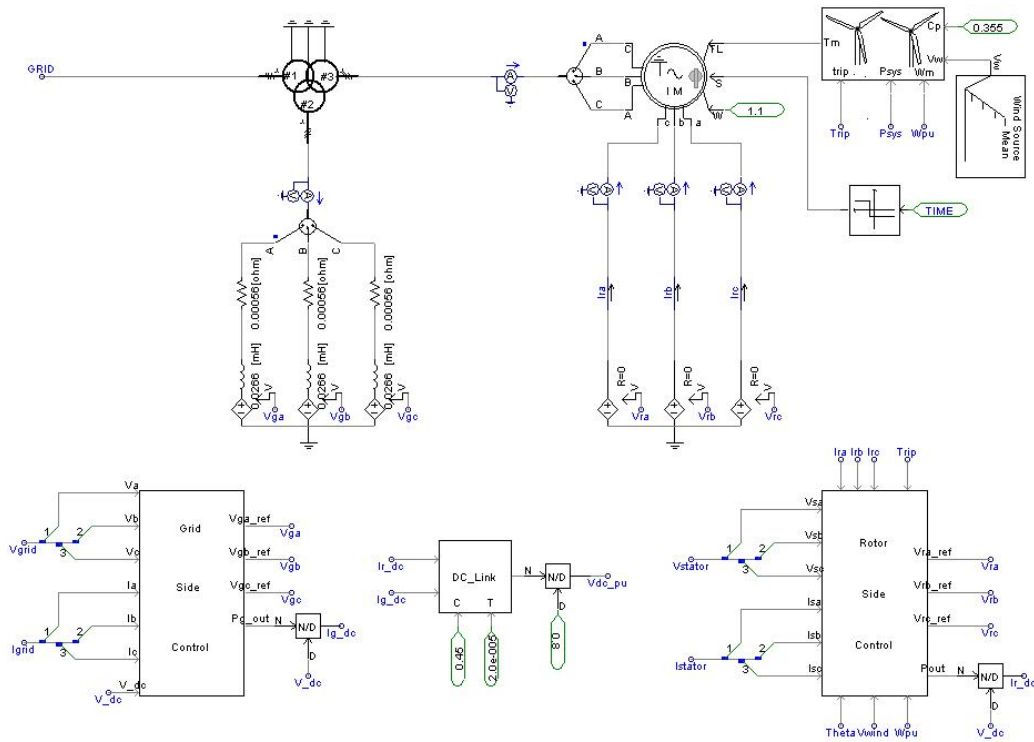


Figure B.1 General Block Diagram of DFIG Type WPP Model

B.1 Turbine and Wind Speed Blocks

The wind speed block is built with default components in PSCAD/EMTDC library as seen in Figure B.2, and is comprised of a mean wind component, a gust wind component, a ramp wind component and a noise wind component. Since the thesis especially investigates the transient conditions, the mean wind component is the main input to the turbine block. The turbine block which consists of a rotor model, a shaft model and a pitch system are implemented according to formulas in sections 2.3.1.2, 2.3.1.3 and 2.3.1.4. According to calculations with respect to these formulas, the output of this block is the torque and it is directly input to the generator block. The trip signal seen in Figure B.2 is used in emergency conditions and sent by protection system of the turbine. Pitch System turns the blades in required angles to decrease the power output of the turbine whenever this signal is received.

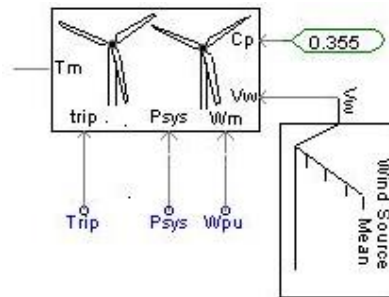


Figure B.2 Block Diagram of Turbine and Wind Speed Model

B.2 Generator Block

The wound rotor induction generator available in PSCAD/EMTDC main library is used to represent DFIG block as seen in Figure B.3. The generator block is modeled in the state variable form using generalized machine theory as described the formulas in Section 2.3.1.5. The generator can be operated in either 'speed control' or 'torque control' modes. Generally, the machine is started in speed control mode with the W

input set to rated per-unit speed and then switched over to torque control via the selection input, S , after the initial transients of the generator die out [43]. The block provides 3-phase terminals for stator connection to the grid and 3-phase terminals to rotor windings for rotor side converter connection. The block can internally provide rotor position, mechanical and electrical torques and the shaft speed as output signals.

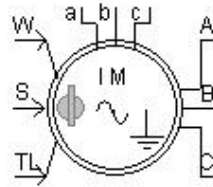


Figure B.3 Diagram of the DFIG

The generator parameters used in the 30 MW PSCAD/EMTDC DFIG Model is given in Table B.1

Table B.1 DFIG Type WPP Parameters

Rated power	30 [MVA]
Rated voltage(L-L)	0.69 [kV]
Base angular frequency	314.16 [rad/s]
Stator/Rotor turns ratio	0.4333
Angular moment of inertia	1.99 [s]
Stator resistance	0.0175 [pu]
Rotor resistance	0.019 [pu]
Stator leakage inductance	0.2571 [pu]
Rotor leakage inductance	0.295 [pu]
Mutual inductance	6.921 [pu]

B.3 Converter Blocks

In Figure B.4, block diagrams of both grid-side and rotor-side converters are seen. Since the scope of this thesis is not switches or switching's of the power electronic devices and to improve the simulation speeds, converters are modeled as controlled voltage sources. V_{ga} , V_{gb} , V_{gc} are the reference inputs to the grid-side controlled voltage sources sent by grid-side controller and V_{ra} , V_{rb} , V_{rc} are the reference inputs to the rotor-side controlled voltage sources sent by rotor-side controller. Moreover, the grid-side converter is connected to the grid through a filter circuit as in Figure B.4 to reduce the output harmonic content of the converter.

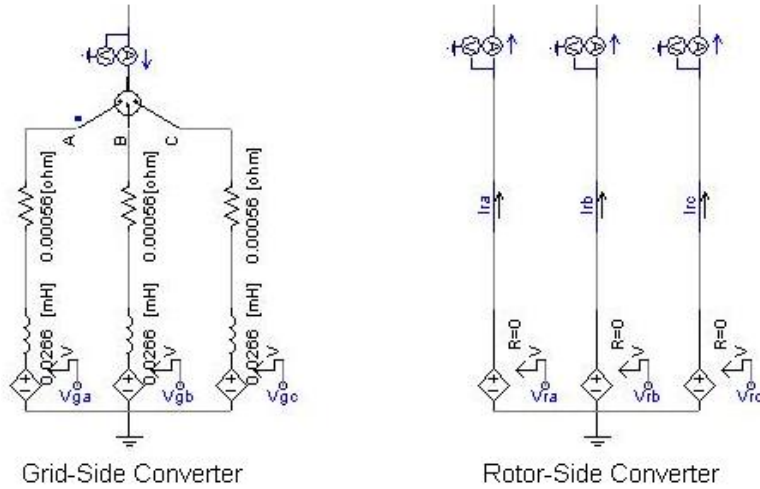


Figure B.4 Block Diagram of Converters

B.4 Converter Controller Blocks

The controller blocks seen in Figure B.5 are implemented according to the formulas and control schemes of sections 2.3.1.7 and 2.3.1.8. The grid-side converter is providing unity power factor at grid side and is controlling the DC-link voltage. To provide this, grid-side converter controller block takes grid voltage, V_{grid} , and current

of converters AC side, I_{grid} , as input signals and send V_{ga} , V_{gb} and V_{gc} to the converter as reference voltage signals. Besides, DC-side current of the converter, I_{g_dc} , is send to DC-Link Block. This block also takes DC-side current of the rotor-side converter and according to formulas in Section 2.3.1.7, calculates the DC-link voltage to send to the protection system. On the other hand, rotor-side converter is controlling the generator active and reactive power and work in slip frequency. The rotor-side converter controller block takes stator voltage, V_{stator} , and stator current, I_{stator} , and rotor current I_{rotor} , as input signals and send V_{ra} , V_{rb} and V_{rc} to the converter as reference voltage signals. Besides, *trip* signal which is send by protection system is used for activating the crowbar in order to protect converters and DC-link capacitor.

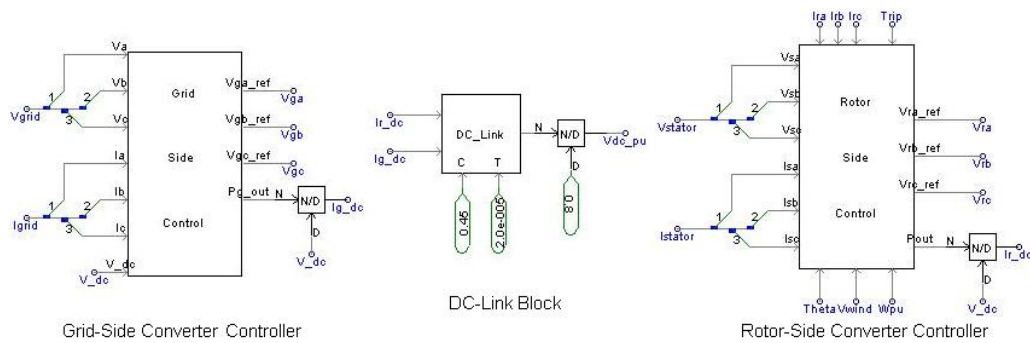


Figure B.5 Block Diagram of the Converter Controllers

APPENDIX C

PSCAD/EMTDC MODEL FOR PMSG

In Figure C.1, general block diagram of a 30 MW WPP implemented in PSCAD/EMTDC according to the mathematical models explained in Chapter 2 can be seen. In this WPP, VSWTs with PMSG are used. The block diagram consists of a wind speed block, a turbine block, a generator block, a converter block and a controller block as in DFIG Model.

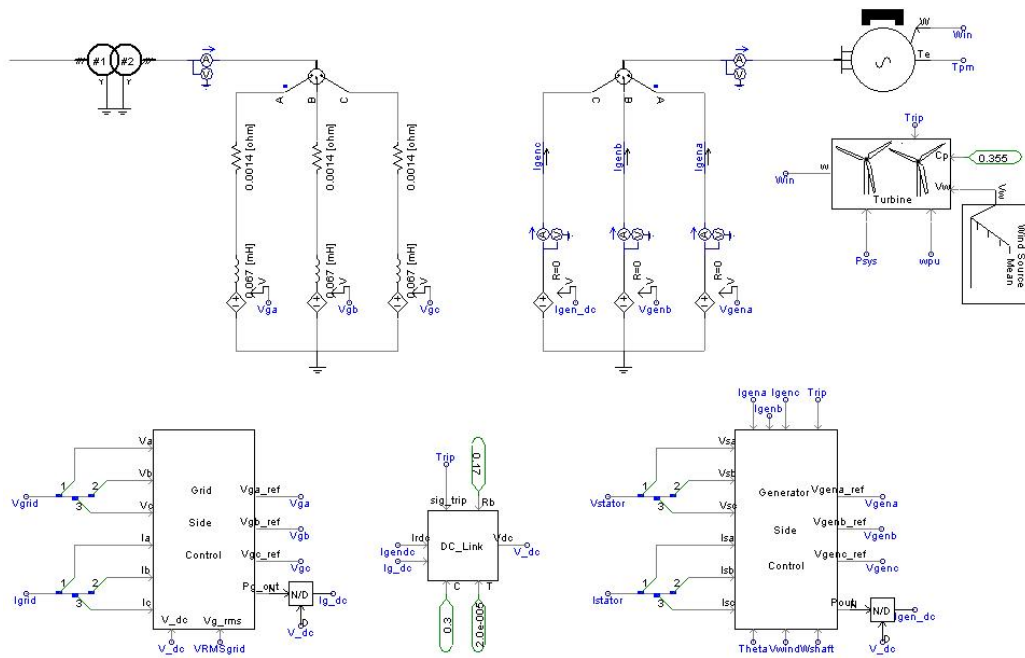


Figure C.1 General Block Diagram of the PMSG Type WPP Model

C.1 Turbine and Wind Speed Blocks

The wind speed block and turbine block including rotor model and pitch system seen in Figure C.2 are same as the turbine block and the wind speed block used in DFIG given in Appendix B.

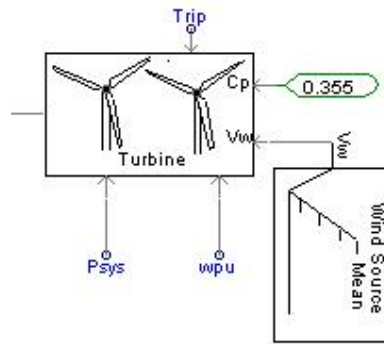


Figure C.2 Block Diagram of the Turbine Model

C.2 Generator Block

The permanent magnet synchronous generator present in PSCAD/EMTDC Main Library is used to represent PMSG block as seen in Figure C.3. The generator block is modeled as described the formulas in Section 2.3.1.5. In addition to the three stator windings, two additional, short-circuited windings are included to model the effect of electromagnetic damping. The speed of the machine may be controlled directly by entering a positive value into the W input of the machine, and T_e is the output electrical torque [43]. The block can also internally provide rotor position, as an output signal.

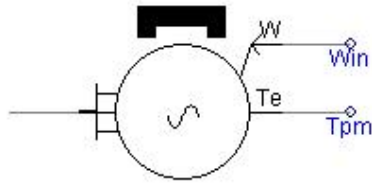


Figure C.3 Diagram of the PMSG

The generator parameters used in the 30 MW PSCAD/EMTDC PMSG Model is given in Table C.1.

Table C.1 PMSG Type Wind WPP Parameters

Rated power	30 [MVA]
Rated voltage(L-L)	1 [kV]
Rated frequency	20 [Hz]
Magnetic Strength	1.0
Stator resistance	0.017 [pu]
Stator leakage reactance	0.064 [pu]
D: Unsaturated reactance [Xd]	0.55 [pu]
Q:Unsaturated reactance [Xq]	0.11[pu]

C.3 Converter Blocks

In Figure C.4, block diagrams of both grid-side and generator-side converters are seen. Due to similar reasons in DFIG Model, to improve the simulation speed, the converter is modeled as controlled voltage sources. V_{ga} , V_{gb} , V_{gc} are the reference inputs to the grid-side controlled voltage sources sent by grid-side controller and V_{gena} , V_{genb} , V_{genc} are the reference inputs to the generator-side controlled voltage sources sent by generator-side controller. Moreover, the grid-side converter is connected to the grid through a filter circuit as in Figure C.4 to reduce the output harmonic content of the converter.

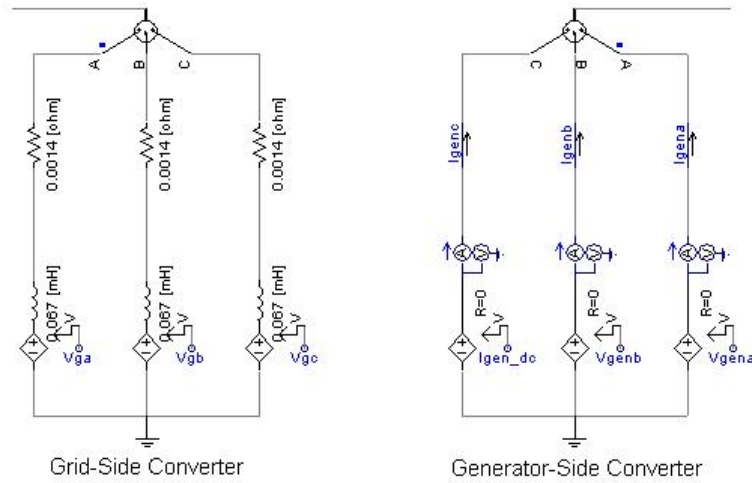


Figure C.4 Block Diagram of Converters

C.4 Converter Controller Blocks

The controller blocks seen in Figure C.5 are implemented according to the formulas and control schemes of sections 2.3.2.4 and 2.3.2.5. The grid-side converter controller is providing unity power factor at grid side and is controlling the dc-link voltage. To provide these, grid-side converter controller block takes grid voltage, V_{grid} , and current of converters on the AC-side, I_{grid} , as input signals and send V_{ga} , V_{gb} and V_{gc} to the converter as reference voltage signals. Besides, DC-side current of the converter, I_{g_dc} , is send to DC-Link block. This block calculates the DC-link voltage and sends it to protection system according to signals coming from controllers. Furthermore, generator-side converter is controlling the generator active and reactive power. The generator-side converter controller block takes stator voltage, V_{stator} , and stator current, I_{stator} , as input signals and sends V_{gena} , V_{genb} and V_{gen_c} to the converter as reference voltage signals. Besides, *trip* signal in DC-Link Block which is sent by protection system is used for protecting the converters and DC-link capacitor from over-voltages.

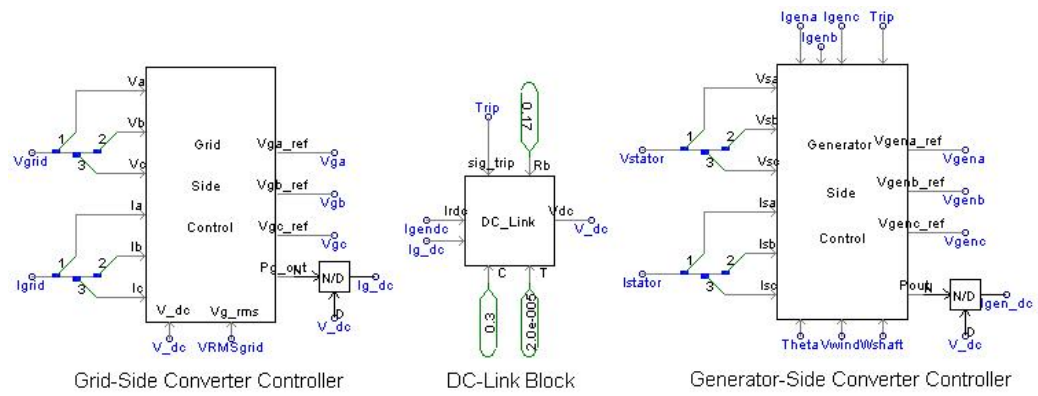


Figure C.5 Block Diagram of Converter Controllers